NOTICE

The quality of this microform is heavily dependent upon the quality of the original thesis submitted for microfilming. Every effort has been made to ensure the highest quality of reproduction possible.

If pages are missing, contact the university which granted the degree.

Some pages may have indistinct print especially if the original pages were typed with a poor typewriter ribbon or if the university sent us an inferior photocopy.

Reproduction in full or in part of this microform is governed by the Canadian Copyright Act, R.S.C. 1970, c. C-30, and subsequent amendments.

AVIS

La qualité de cette microforme dépend grandement de la qualité de la thèse soumise au microfilmage. Nous avons tout fait pour assurer une qualité supérieure de reproduction.

S'il manque des pages, veuillez communiquer avec l'université qui a conféré le grade.

La qualité d'impression de certaines pages peut laisser à désirer, surtout si les pages originales ont été dactylographiées à l'aide d'un ruban usé ou si l'université nous a fait parvenir une photocopie de qualité inférieure.

La reproduction, même partielle, de cette microforme est soumise à la Loi canadienne sur le droit d'auteur, SRC 1970, c. C-30, et ses amendements subséquents.

ISBN 0-315-53209-2

GEOLOGY AND GEOCHEMISTRY OF THE CHENAUX GABBRO, NEAR RENFREW, ONTARIO

By

Zuber Abdurahman

A thesis submitted to the School of Graduate Studies in partial fulfillment of the requirements for the degree of Master of Science in Geology

UNIVERSITY OF OTTAWA
OTTAWA - CARLETON GEOSCIENCE CENTRE
OTTAWA, CANADA, 1989

UNIVERSITÉ D'OTTAWA
UNIVERSITY OF OTTAWA

ABSTRACT

The Chenaux gabbro pluton (3 km diameter) of proterozoic age occurs in the western margin of the Central Metasedimentary Belt of the Grenville Structural Province (Canadian Shield). The gabbro consists mainly of plagioclase (anorthite 0.59 to 0.70), Ca pyroxene ($X = Mg/Mg + Fe^{2+} = 0.65 - 0.85$), orthopyroxene ($X = 0.64 - 0.80$), and Ca amphibole ($X = 0.51 - 0.80$; dominantly aluminous), magnetite and ilmenite, with local olivine ($X = 0.75 - 0.78$), spinel, biotite, almandine-rich garnet, scapolite, epidote, titanite, rutile, apatite and pyrite. Rock composition is variable ($SiO_2 = 45 - 51$ wt. %, $X = 0.42 - 0.79$), and four rock types are recognized: olivine gabbro, leuco-gabbro, pyroxene gabbro, and hornblende gabbro. Olivine gabbro appears to dominate in the central part of the pluton; layering is only locally visible.

The country rocks consist mainly of marble (calcite, dolomite, diopside, tremolite, local forsterite), with smaller proportion of amphibolite, metagabbro, biotite-muscovite gneiss, biotite-hornblende-garnet gneiss, tonalite gneiss, and granite gneiss (with local sillimanite). These rocks were evidently deformed prior to emplacement of the gabbro. Pronounced shear zones occur in the gabbro and adjacent marble, especially at the east contact of the pluton.

A gravity anomaly of some 24 milligals occurs over the gabbro pluton. Modelling of the gravity data produces, as one possibility, a three-dimensional mushroom-shaped body, with a steeply-inclined cylindrical 'stem' extending to a depth of 2.7 km.

The microstructure of the gabbro is highly variable, including sub-ophitic (igneous), mosaic (metamorphic) and reaction-zone (corona) microstructures. Reaction microstructures include zones of orthopyroxene and amphibole-spinel between olivine and plagioclase, zones of amphibole between Ca pyroxene and plagioclase, and rims of biotite around ilmenite. Some of the abundant amphibole in the rock is obviously metamorphic; some may be of igneous origin. With regard to the reaction,

olivine + plagioclase = orthopyroxene + hornblende + spinel,

at one locality, a calculation shows that mass balance was realized except for K, Ti and H (possibly as H_2O) which were transported to the reaction site.

Geothermomenters (2-pyroxene, plagioclase-scapolite) give temperatures of about 800°C, which may indicate incomplete metamorphic adjustment to the regional metamorphic temperature (mid-amphibolite facies) of about 600°C.

A record is preserved in the Chenaux gabbro, of a complex igneous and metamorphic history. Variation in rock composition is interpreted as a result of magmatic differentiation during emplacement, promoted by crystal settling of olivine and pyroxene. Later, during regional metamorphism, various often incomplete metamorphic changes occurred, the progress of these being controlled largely by influx of H_2O. Evidence for deformation occurs in the form of shear zones, which were possibly related to the late Grenville Orogeny, and in the form of faults, related to the development of the Ottawa Rift System.

ACKNOWLEDGEMENTS

I would like to thank sincerely Dr. Ralph Kretz, my thesis supervisor, for his suggestion of the topic, for his generous help in the field, for many valuable discussions all the way through the project, and for reading this and all the earlier versions of the manuscript patiently. I would also like to thank Dr. John Moore, Dr. Tony Fowler and Tomas Feininger for their critical appraisals.

I am greatly indebted to the the Geological Survey of Canada, Geophysics Division for lending gravity survey equipment and also providing an access to gravity modelling computer program. Help provided by Dr. Alan K. Goodacre is highly appreciated.

Special thanks are due to the technical staff at the University of Ottawa: Edward Hearn for photography and drafting guidance, Ron Hartree and John Loop for their aid in the Geochemistry Laboratory, George Mrazek and Jean-Francois Tardif for making thin sections. My thanks also go to Sandy Boal who typed the manuscript very patiently and efficiently.

The World Bank scholarship for the last three and a half years is greatly acknowledged.

CONTENTS

LIST OF FIGURES

LIST OF TABLES

Table

Chapter I

INTRODUCTION

The study area is located in the southwestern part of the Grenville Province, within the Central Metasedimentary Belt. It lies adjacent to the Ottawa River, eight kilometres north of Renfrew.

The principal rocks of the study area include calcite and dolomite marbles, interlayered intermediate to mafic gneisses, and a gabbroic pluton all regionally metamorphosed to middle-to-upper amphibolite facies. The marbles and the associated gneisses are assigned to the Grenville Supergroup (Wynne-Edwards, 1972).

A determination of the stratigraphy and extent of the basin of deposition of the Grenville Supergroup is difficult because of the absence in continuity of exposure, extreme deformation and metamorphic recrystallization. Volcanism and sedimentation of the Grenville Supergroup took place between 1280 and 1250 Ma, followed by an episode of plutonism and probably metamorphism that lasted at most 30 Ma, ceasing about 1220 Ma (Easton, 1986).

Work by Moore and Thompson (1980) indicated, that at least part of these supracrustal successions, that are close and continuous to the type locality (Flinton Group) to have been deposited close in time (1.3 to 1.1 Ga) to the Grenvillian Orogeny. This orogenic cycle in the Central Metasedimentary Belt includes a

succession of events, spanning some 250 Ma, representing the entire orogenic history of the belt; culminating around 1.1 Ga during Ottawan Orogeny.

There is systematic variation in the temporal relations among volcanism (1250 ± 90 Ma), mafic intrusions (1240 Ma) and syenitic suites (1220-1250 Ma) in the Central Metasedimentary Belt of Ontario (Easton, 1986).

Several late to post metamorphic gabbro, diorite, granodiorite, granite and syenite plutons are wide spread throughout most of the Central Metasedimentary Belt (Britton, 1979), and only a few of these intrusions predate the Grenvillian Orogeny. It is not also clear whether these mafic plutons are generated independently as roots of volcanic centers or to have a genetic link with the associated plutons.

The gabbroic plutons have recently attracted much attention; one of the medium sized plutons (the Chenaux gabbro) is here described in some detail.

Location and Geological Setting

The Chenaux body of gabbro lies within the Grenville Structural Province of the Canadian Shield, 100 km west of Ottawa and 8 km north of Renfrew (Fig. 1). The body was mapped by Lumbers (1982) who presented preliminary information on the gabbro and the surrounding marble, gneiss, amphibolite and other rock types.

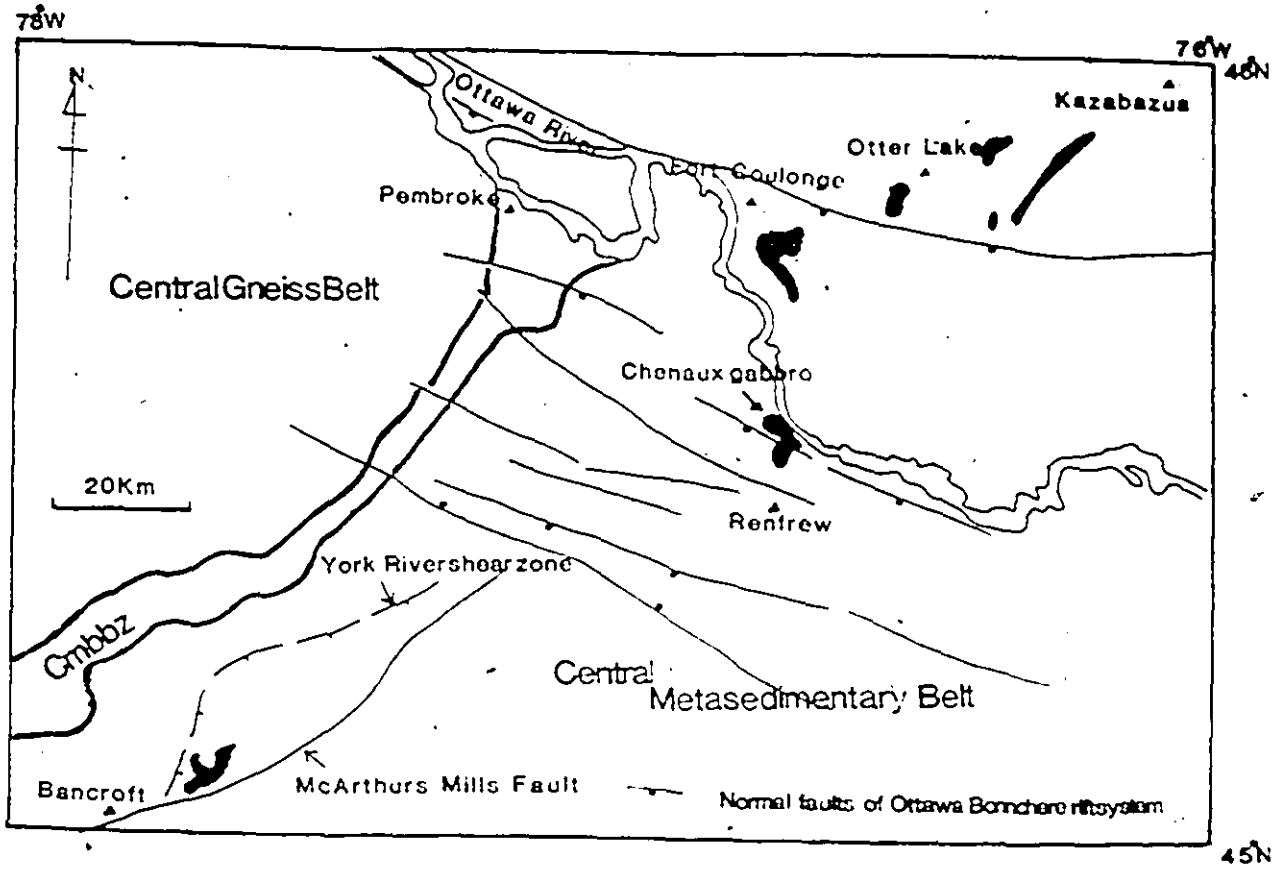

Fig. 1. Regional setting and location of the Chenaux gabbro, showing (in black) some other gabbro and metagabbro plutons. Cmbbz denotes Central Metasedimentary Belt Boundary Zone.

The southwestern Grenville Province has been divided into the Central Gneiss Belt to the northwest, which consists predominantly of gneisses and migmatites of high metamorphic grade, and the Central Metasedimentary Belt to the southeast, which dominantly consist of marble, gneisses, amphibolite, and granitic to syenitic rocks of medium-to-high grade (Wynne-Edwards, 1972).

The structure of both belts is highly complex, and both were affected by the Grenvillian Orogeny which culminated at about 1.1 Ga (Easton, 1986). The

Chenaux pluton lies at the western margin of the Central Metasedimentary Belt, and forms one of many gabbro and metagabbro bodies that are scattered within this belt and the adjacent Central Gneiss Belt (Quinn, 1951; Britton, 1979; Davidson and Grant, 1986; Kretz, 1989).

Purpose of Study

The present study was undertaken to increase our understanding of the emplacement, crystallization, and metamorphism of the Chenaux gabbro. Building on the field data reported by Katz (1969) and Lumbers (1982) additional field observations were recorded, and numerous microscopic and geochemical data (rock and mineral analyses) were obtained. Some data on the enclosing rocks were also collected, particularly on the amphibolite to the south of the pluton and the tonalite to the north, to determine if these are related to the gabbro. A gravity study was carried out to provide information on the shape and extent of the pluton at depth.

Methods Employed

Forty-five days were devoted to field study, paying special attention to the lithology and structure of the gabbro and the immediately surrounding rocks. Three hundred samples were collected and 70 were examined microscopically. The resulting geological map, which agrees with that of Lumbers (1982) but contains additional structural data, is shown in Fig. 2. Thirty-four rock samples were

analyzed by X-ray fluorescence in the University of Ottawa Geochemistry Laboratory; FeO was determined by titration. The minerals of the gabbro and garnet and biotite from the enclosing gneisses were analyzed by microprobe in the McGill University Microprobe Laboratory. Gravity data were obtained along two traverses across the gabbro pluton; details are presented below.

Chapter II

THE COUNTRY ROCKS

General Statement

The Chenaux gabbro was intruded into a terrain consisting predominantly of marble, with smaller porportions of amphibolite and gneiss (Fig. 2). It is well exposed (50% exposure) but much of the surrounding terrain is covered by a veneer of Pleistocene till, gravel, sand, clay and recent alluvium. The gabbro and adjacent marble are best exposed in road cuts (Highways 17 and feeder roads) and in the bed of the Ottawa River at the Chenaux dam site (Fig. 2).

A stratigraphic sequence for the country rocks could not be determined, and the sequence in which the rock units are here described is arbitrary.

Marble and Skarn

Marble is the prominent supracrustal component throughout the study area and is the immediate host rock to the gabbro. The two principal varieties (dolomite-rich and calcite-rich marbles) are commonly intercalated at various scales. In typical exposures, calcite-rich and dolomite-rich marbles show a wide range of textural and deformational features. Generally the rocks are medium to coarse grained, and vary in color from white to dark grey; white marble is predominant. Thin layers rich in silicates are present; these evidently reflect the

National Library
of Canada

Canadian Theses Service

Bibliothèque nationale
du Canada

Service des thèses canadiennes

NOTICE

AVIS

THE QUALITY OF THIS MICROFICHE IS HEAVILY DEPENDENT UPON THE QUALITY OF THE THESIS SUBMITTED FOR MICROFILMING.

UNFORTUNATELY THE COLOURED ILLUSTRATIONS OF THIS THESIS CAN ONLY YIELD DIFFERENT TONES OF GREY.

LA QUALITE DE CETTE MICROFICHE DEPEND GRANDEMENT DE LA QUALITE DE LA THESE SOUMISE AU MICROFILMAGE.

MALHEUREUSEMENT, LES DIFFERENTES ILLUSTRATIONS EN COULEURS DE CETTE THESE NE PEUVENT DONNER QUE DES TEINTES DE GRIS.

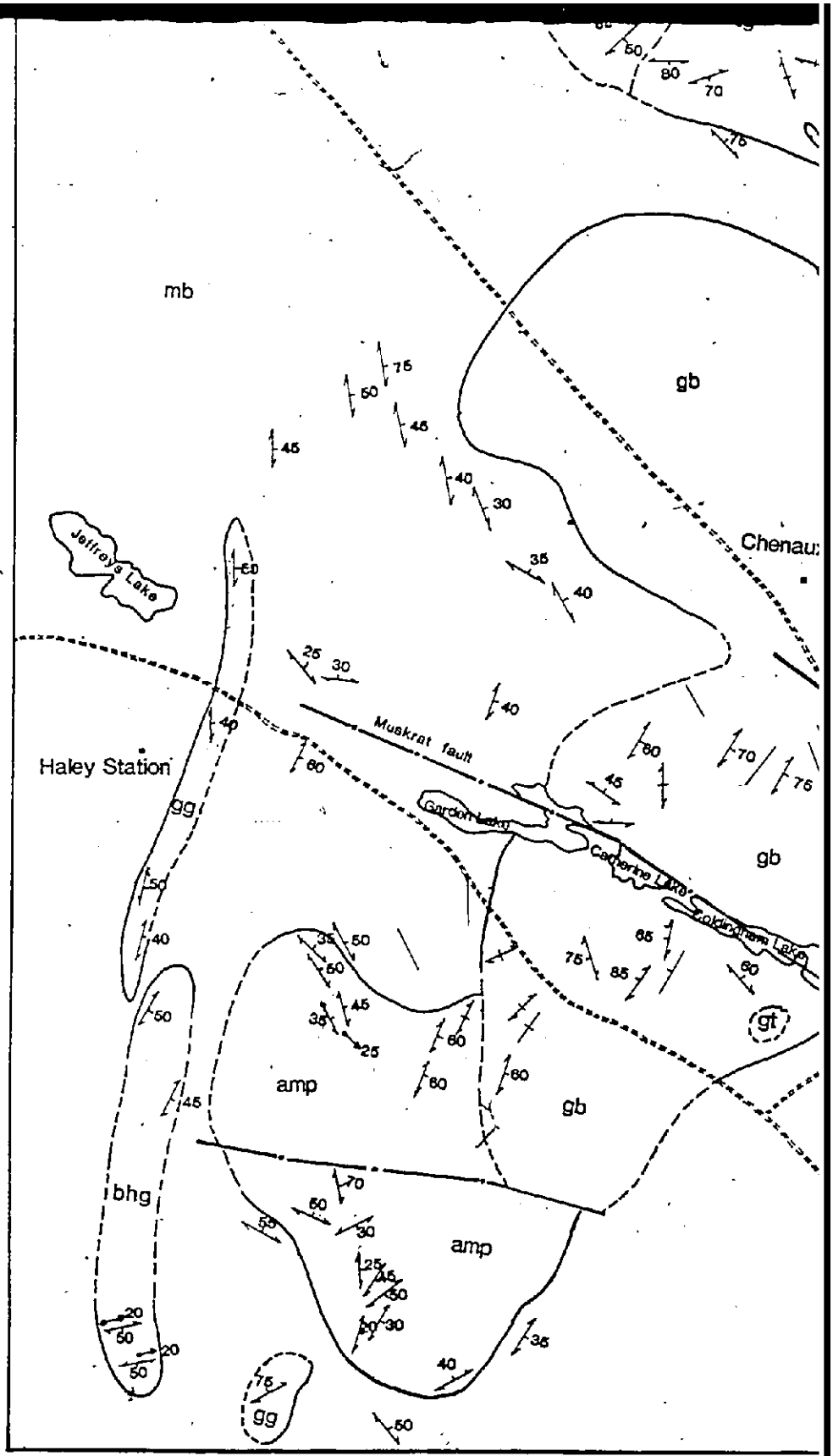

Fig.2. Geological map of the Chenaux gabbro

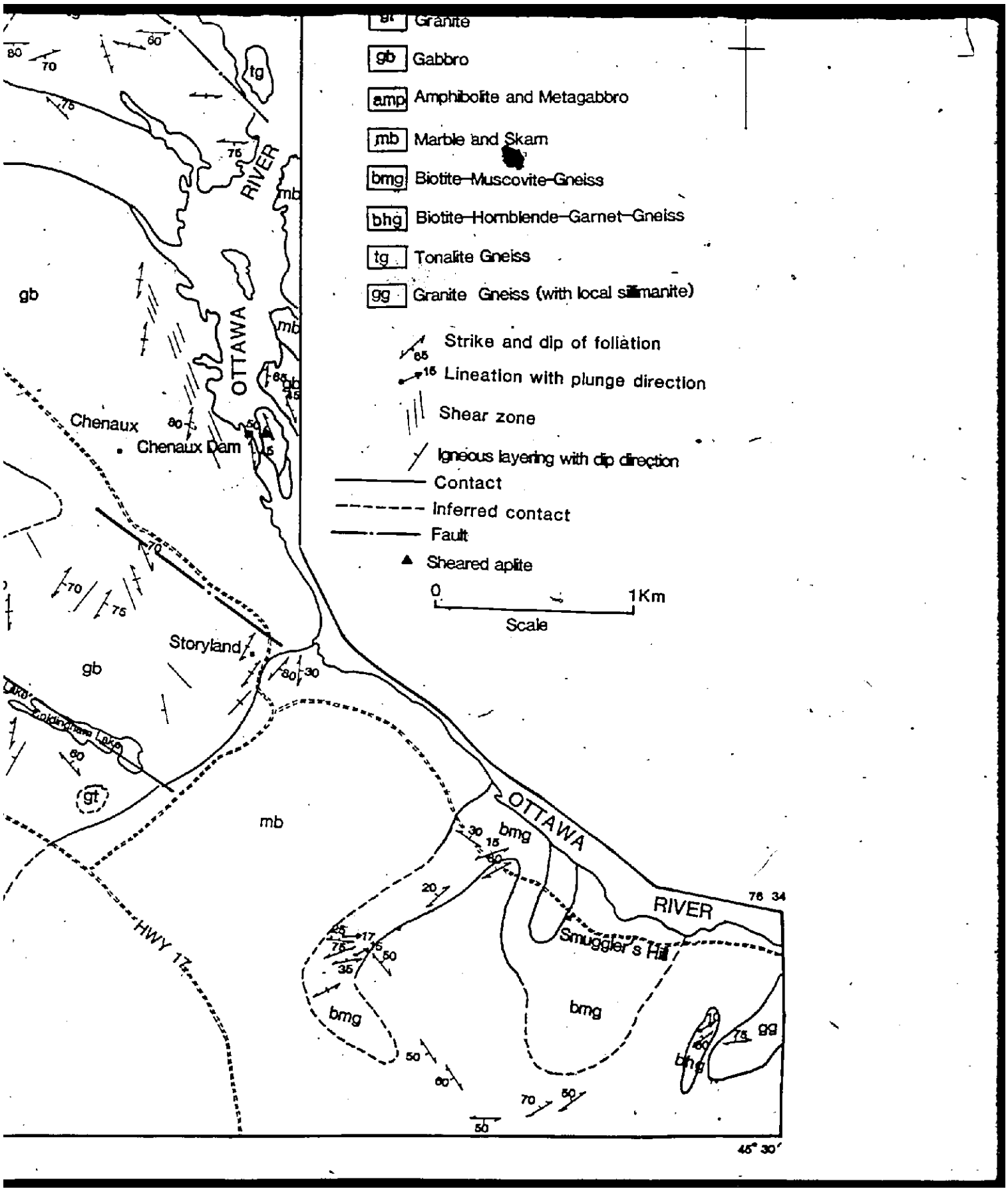
gr Granite
gb Gabbro
amp Amphibolite and Metagabbro
mb Marble and Skarn
bmg Biotite–Muscovite–Gneiss
bhg Biotite–Hornblende–Garnet–Gneiss
tg Tonalite Gneiss
gg Granite Gneiss (with local sillimanite)
Strike and dip of foliation
Lineation with plunge direction
Shear zone
Igneous layering with dip direction
Contact
Inferred contact
Fault
Sheared aplite
0
1Km
Scale
OTTAWA RIVER
Chenaux
Chenaux Dam
Storyland
Smuggler's Hill
HWY 17
gb
mb
bmg
bhg
gg
gt
tg
45° 30'

original bedding. Layering and mineral-aggregate foliation trend northwesterly on the western side of the Chenaux pluton; toward the east, the layering swings to the northeast (Fig. 2). South of the pluton, layering mainly dips to the southeast. This trend indicates the presence of a major south-plunging fold; the nose of the fold is occupied by the gabbroic pluton.

Near contacts with the gabbro and also elsewhere, there are numerous localized highly strained zones roughly parallel to the foliation, marked by highly attenuated and mylonitized marble. Kinematic indications, given by detached folds and thin sigmoidal graphitic and calc-silicate layers indicate a sense of transport similar to that recorded in the sheared gabbroic rocks, to be described below.

Small scale disharmonic folds are very common, particularly near the gabbro. Here the calcite-rich layers are very coarsely recrystallized compared to the associated darker layers that contain some graphite.

The main constituents east of the pluton are calcite, dolomite, tremolite, diopside, and phlogopite with varying and minor proportions of chlorite, sulfide, graphite, quartz, titanite and scapolite. Dolomite exsolution lamellae are common along calcite twinning planes. Forsterite and serpentine are found close to the western contact zones and also to the north, at Chenaux Dam. Wollastonite and brucite were not identified. South of the area mapped, along Highway 17, calcite marble with some quartz is present. Representative mineral assemblages are listed in Table 1.

Table 1 - Mineral Assemblage, Marble and Skarn

	Marble			Skarn
	1	2	3	4
Calcite	50	40	25	<5
Dolomite	-	10	20	-
Tremolite	10	20	15	-
Phlogopite	<5	5	trace	-
Forsterite	20	-	-	-
Scapolite	10	-	-	<5
Serpentine	-	-	30	-
Epidote	trace	trace	-	-
Diopside	-	15	10	70
Iron Oxides	trace	trace	-	10
Hornblende	-	-	-	<5
Garnet	-	-	-	<5
Quartz	-	trace	-	-

A serpentine-rich marble, near Haley Station, contains 'concretions' with a dolomite core rimmed by pale yellow serpentine; tremolite here is extremely coarse and the crystals are oriented randomly. The 'concretions' range from about 2 cm up to 0.3 m in diameter.

Gabbroic dikes that have been folded together with the enclosing marbles are found near the Chenaux Dam. Here the marbles adjacent to the gabbro contact are coarsely recrystallized.

Skarn is commonly developed in the marbles near contacts with the gabbroic

pluton and as aureoles around pegmatite dikes. The rock is medium to coarse grained, light to dark green, and very rich in diopside and an undetermined amphibole. Most of the skarns are massive and in places contain a network of thin K-feldspar-rich pegmatite veins. In addition to diopside and amphibole, the other major minerals present are scapolite, calcite, magnetite and garnet. The mineralogical distribution and field relationships of these rocks indicate that most of them are metasomatic rocks, formed by the introduction to the marbles of Si, Al, Fe and other elements.

Biotite-Muscovite Gneiss

Biotite-muscovite gneisses are found in the eastern part of the map-area and good exposures are restricted to the road cuts near Smugglers Hill (Fig. 2). The gneisses which are mostly grey, but weather rusty-yellowish, are foliated, folded, sheared and faulted. Layering is well developed ranging in thickness from 1 mm to 2 cm. It is marked by alternating biotite-and quartz-feldspar-rich layers. Transition from this layered type to a more homogeneous variety is commonly observed.

These gneisses have been folded and refolded into tight isoclinal folds. The first foliation (S_1) is parallel to the compositional layering. The F_1 folds are mainly upright; axes have northwest to northeast trends with plunges ranging from

horizontal to about 5°. The folding is non-coaxial and the axial planes (S_2) dip toward the northwest. F_2 folds developed as recumbent folds with horizontal axial planes. Small scale sinistral shear zones present on the axial plane of some F_2 folds. These minor shears strike northeast and dip steeply northwesterly.

Metamorphism accompanying the deformation did not exceed the amphibolite facies. Metamorphic minerals in these gneisses consist mainly of quartz, plagioclase and microcline, with lesser muscovite, biotite, garnet, and epidote. Representative mineral assemblages are listed in Table 2.

Table 2 Mineral Assemblages in the Gneisses

	1	2	3	4	5	6	7	8
Quartz	20	30	15	20	30	35	25	30
Plagioclase	25	20	35	30	30	35	40	35
Microcline	20	15	---	---	25	15	---	---
Biotite	15	25	10	20	5	10	15	5
Muscovite	10	10	---	---	<5	5	<5	<5
Hornblende	---	---	15	10	tr	tr	---	---
Garnet	<5	---	10	15	---	---	<5	10
Sillimanite	---	---	---	---	5	---	---	---
Epidote	tr	tr	tr	tr	tr	tr	tr	tr
Titanite	---	---	<5	<5	---	---	---	---
Apatite	---	---	tr	tr	tr	tr	tr	tr
Sericite	---	---	---	---	---	tr	10	15
Calcite	---	---	tr	tr	---	---	---	---
Opaque Oxides	<5	tr	10	<5	5	tr	<5	tr

1-2 (Biotite-Muscovite Gneiss)

3-4 (Biotite-Hornblende-Garnet Gneiss)

5-6 (Granite Gneiss)

7-8 (Tonalite Gneiss)

Layering is defined by alternating concentrations of inequigranular quartz, plagioclase and microcline, and lepidoblastic biotite and muscovite. Poikiloblastic garnet and cordierite and some iron oxides are also present. Aluminosilicates have not been identified in these rocks. In places, garnet grew as subhedral to euhedral crystals with few inclusions; elsewhere it forms coarse and anhedral poikiloblastic grains with fine quartz and biotite inclusions. Microprobe analyses of biotite and garnet are given in Table 3.

Table 3 - Microprobe Analyses of a Pair of Biotite and Garnet in Biotite-Muscovite Gneisses

	Biotite				Garnet			
	(S17)	(S92)	(S150)	(S148)	(S17)	(S92)	(S150)	(S148)
SiO_2	36.7	36.4	35.0	36.4	38.2	37.9	36.9	37.5
FeO	18.9*	15.8*	20.9*	16.3*	21.2	31.6	37.0	26.9
Fe_2O_3	nd	nd	nd	nd	1.1	1.5	0.8	0.6
Al_2O_3	16.8	18.7	16.8	19.2	20.7	20.2	20.6	20.8
CaO	0.05	0.008	0.08	0.01	13.1	4.7	1.5	2.5
MgO	9.7	12.1	10.0	11.8	1.4	2.7	2.5	3.9
MnO	0.27	0.13	0.07	0.15	4.3	1.5	1.7	7.7
Na_2O	nd	0.14	0.03	0.23				
F	0.27	0.4	0.94	0.41				
K_2O	9.3	10.4	8.5	10.3				
TiO_2	3.1	2.3	2.4	2.1				
TOTAL	95.09	96.38	94.72	96.90	100.00	100.10	101.00	99.90
				ALM	47.20	71.70	82.2	60.0
				PYR	5.70	10.80	9.9	15.7
				SPS	9.70	3.50	3.7	17.3
				GRS	34.00	9.40	1.9	5.2
				AND	3.40	4.60	2.3	1.8

*All Fe expressed as FeO.

nd = not determined

(S17) = Biotite-Muscovite Gneiss

(S92) = Biotite-Hornblende-Garnet Gneiss

(S148) = Tonalite Gneiss

(S150) = Tonalite Gneiss

Biotite-Hornblende-Garnet Gneiss

This map unit consists of fine to medium grained, well foliated mafic gneisses of unknown origin. They form thin northsouth trending belts which are confined to the western and eastern parts of the map-area (Fig. 2). The contact of these gneisses with the surrounding marbles is marked by the development of calc-silicates and in places by the presence of skarns. The principal minerals of these rocks are quartz, plagioclase, biotite, hornblende, garnet and local diopside. Very coarse (about 1 cm) poikiloblastic crystals of garnet have developed within biotite-rich layers. These crystals contain inclusions of feldspar, quartz, biotite and iron-oxides. Minor epidote and calcite are locally present. Representative mineral assemblages are listed in Table 2.

The rocks show a well developed foliation defined by the parallel alignment of lepidoblastic biotite and hornblende grains with granular to elongated quartz and plagioclase grains which are commonly strained. Layering in these rocks is formed by a compositional variation of the felsic and mafic components of the rock and also by grain size variations, particularly in the felsic layers. Under the microscope, the felsic bands show fine scale layering defined by grain size variations perhaps indicating a sedimentary origin.

Analyses of biotite and garnet from these rocks are listed in Table 3. Application of the Ferry and Spear (1974) geothermometer produced a temperature estimate of 670°C. This is somewhat high, possibly because of the influence of various extraneous elements upon the Fe^{2+} - Mg exchange equilibrium have not been fully taken into consideration (Kretz, personal communication).

Amphibolite and Metagabbro

The rocks of this group include amphibolite (70%) and a variety of metagabbro (30%) found in the southern portion of the map-area (Fig. 2). A characteristic feature of these rocks is their close mutual association without any distinct contact phenomena. Their field association together with their mineralogical similarity suggest that they may be related meta-basalts and gabbroic sills or dikes.

The amphibolites are dark, fine to medium grained and have well-developed foliation. Weathered surfaces are yellowish or brown. The rocks vary in composition from those with about equal amount of hornblende and plagioclase to more mafic types composed dominantly of amphiboles. Small, ultramafic bodies are also present which are composed of hornblende, plagioclase and some iron oxides.

Generally, the amphibolites have a strong penetrative foliation defined by thin layers composed of elongated green hornblende alternating with layers of granular feldspar. Some quartz-rich layers are also present. The metamorphic mineral assemblages include green hornblende, plagioclase, quartz, epidote, scapolite and

some finely disseminated iron-oxides indicating mid-amphibolite facies metamorphism. The hornblende crystals usually contain disseminated iron-oxides and their cleavage planes are the loci of very small crystals, probably rutile. Some scapolitization and sericitization of the plagioclase occurred. Representative mineral assemblages are listed in Table 4.

Table 4 - Mineral Assemblages in Amphibolite and Metagabbro

	Amphibolite			Metagabbro
	1	2	3	
Plagioclase	30	25	10	45
Hornblende	45	60	85	35
Iron-Oxide	10	10	---	10
Scapolite	10	---	trace	trace
Epidote	trace	trace	trace	trace
Apatite	trace	trace	trace	<5
Titanite	<5	5	5	<5
Calcite	trace	---	---	trace
Quartz	trace	---	---	---

A metagabbro unit occurs in close association with the amphibolites. This unit can be distinguished from the Chenaux gabbro on geochemical evidence, to be presented below.

The rocks are dark green and medium grained with granoblastic texture. Locally, they are massive and medium grained; elsewhere the rock is fine grained and grades to amphibolite. The metagabbro contains plagioclase, hornblende, scapolite, epidote, iron-oxides and traces of calcite. Although the component

minerals are highly deformed, no strong fabric is developed, as in the associated amphibolites. A representative mineral assemblage is listed in Table 4.

Hornblende forms very large anhedral to subhedral, occasionally poikiloblastic crystals. Plagioclase crystals are strongly deformed and show undulose extinction. Plagioclase is locally replaced by scapolite. The scapolized feldspar occasionally encloses smaller biotite flakes, iron-oxides and minor calcite. Opaque crystals are commonly rimmed by epidote. Very fine epidote crystals are also developed within the hornblende.

Granite Gneiss

These gneisses occur as an isolated thin linear belt west and south of the Chenaux gabbro (Fig. 2). Similar rocks are also found in the extreme west of the surveyed area. The rocks are grey to pink, medium grained, well foliated and are invariably gneissic. They exhibit considerable evidence of deformation, particularly in the extreme west of the area, where zones of protomylonite occur containing rotated augen of K-feldspar. The stratigraphic relationship of these rocks with the adjacent biotite-muscovite gneisss is not clear. The granitic gneisses were presumably derived from clastic sediments, possibly shaly arkose evidenced by their sub-rounded grain shapes.

Generally, the rocks have a N-S strike over most of the mapped area, and

structurally they lie beneath the biotite-muscovite gneiss. Compositionally, they range from a leucocratic variety rich in quartz and feldspar to a type rich in biotite. The mesocratic gneisses appear to be in part, a highly strained equivalent of the biotite-muscovite gneiss, but this could not be confirmed in the field. In the highly strained zones, stretched and detached layers are present and the K-feldspar forms elongated and rotated augen structures. The leucocratic gneisses are medium grained and have a remarkable gneissosity and are composed of plagioclase, microcline, quartz, biotite, muscovite and local sillimanite. Representative mineral assemblages are listed in Table 2 (p. 11).

Tonalite Gneiss

These rocks are found in the northern part of the map area and occur in close association with mafic rocks such as gabbro and diorite perhaps equivalent to the metagabbro found in the amphibolite. They show distinct variations in color form light to dark (hornblende-biotite gneiss) as one moves from east to west. Plagioclase, quartz, garnet, biotite and minor muscovite are the major constituents. Fluctuations in the percentage of quartz are common and occasionally the rocks grade into a granodioritic variety. In places, fine grained mafic xenoliths, commonly elongated and oriented parallel to the foliation of the gneisses, are present. These xenoliths range in size from a few centimetres to a half metre. Locally these rocks appear massive; elsewhere the constituent minerals form a

centimetre to a millimetre scale layers. Stretched and elongated quartz grains with alternating lepidoblastic layers of biotite and minor muscovite define the foliation. Garnet forms poikiloblastic grains with abundant inclusions of biotite and quartz. One of these garnets is established as a Mn-rich variety. Grains are altered around their rims either to biotite or green chlorite. Feldspars are comonly altered to sericite and epidote. Some iron-oxides occur, mainly associated with biotite. Representative mineral assemblages are listed in Table 2. Microprobe analyses of garnet and biotite are listed in Table 3.

Chapter III

THE CHENAUX GABBRO

General Statement

Several late to post-metamorphic gabbro, syenite, and granite plutons occur throughout the Central Metasedimentary Belt (Baer et al, 1977). Most of these plutons are relatively small and elongate in outline with textural evidence for syntectonic to late tectonic emplacement (Britton, 1979).

The Chenaux gabbro intrusion is one of these plutons. It is only partly deformed and partly recrystallized and was therefore evidently emplaced during the late stage of the regional metamorphism and deformation which, according to Silver and Lumbers (1966) and Easton (1986) culminated at about 1.1 Ga. The body is transected by the major east west trending Muskrat fault which is one of the faults of the Ottawa Rift structure (Lumbers, 1982).

The pluton, which has an irregular elbow-like shape, was intruded into a highly deformed and regionally metamorphosed terrane of Grenville Supergroup marbles and gneisses, and was itself intruded by felsic and mafic dikes and sills.

Contact relations between the gabbro and the enclosing carbonate rocks have been observed at various places. The contacts are either sheared or intrusive, usually marked by a recrystallized marble or by the development of skarn. No

chilled border rocks or signs of a pronounced contact metamorphic effects are seen, as would be expected between these two rock types. Xenoliths of marbles, a few centimetres to metres wide are frequently encountered near Storyland and along Highway 17; in places, they occur as large roof pendants on the same topographic elevation with the gabbro, implying that the pluton has barely been unroofed by erosion.

Igneous layering is not a major feature of this body. Localized individual layers that are modally graded or grain-size graded were seen in places. Modally graded layers consist of a pyroxene-rich bases which grade upward into more plagioclase-rich zones. Individual modally graded layers range in thickness from a few centimeters to half a meter; contacts are generally sharp. Size-graded layering is present in feldspar rich zones; the layers grade from coarser at the bottom to fine at the top; they wedge out over a short distance. Another type of planar feature is planar foliation produced by parallelism of plagioclase, and in rare cases pyroxene crystals.

Sheared varieties commonly occur throughout the pluton as very thin ultramylonite layers. On the northeastern margin of the body, there is a wide shear zone with conspicuous mylonite zones trending in the north-south direction, almost parallel to the regional foliation. It appears that the sheared varieties have the maximum concentration of quartz veins, formed as tension fillings and this zone is also strongly enriched in pyrite.

In the southern part, the pluton is intimately associated with very fine grained amphibolites and also with highly deformed and metamorphosed gabbro-diorite which apparently are the precursor to the amphibolite. Towards the northwestern end of the intrusion, the gabbro is associated with and grades into granitic and granodioritic masses. This later change is unclear; i.e., whether it is due to differentiation of the mafic magma or is related to separate intrusive events.

No definitive proof as to the age of the ductile deformation or the age of the pluton are known to date. The Chenaux pluton is considered by Lumbers (1982) to be part of the syenite-monzonite suite of plutonic rocks which occurs in this part of the Grenville Province.

Petrography

The principal constituents of the gabbro are plagioclase, olivine, clinopyroxene, orthopyroxene and hornblende, in varying proportions, with lesser amounts of biotite, green spinel and Fe-Ti oxide minerals. Garnet, scapolite, pyrite, titanite, and epidote are also present. Rock types based on the proportions of the major phases include olivine gabbro, leucocratic gabbro, pyroxene gabbro and hornblende gabbro. Information on the distribution of these rock types within the pluton is presented in Fig. 2a. Mineral assemblages of each type are given in Table 5 (p.26).

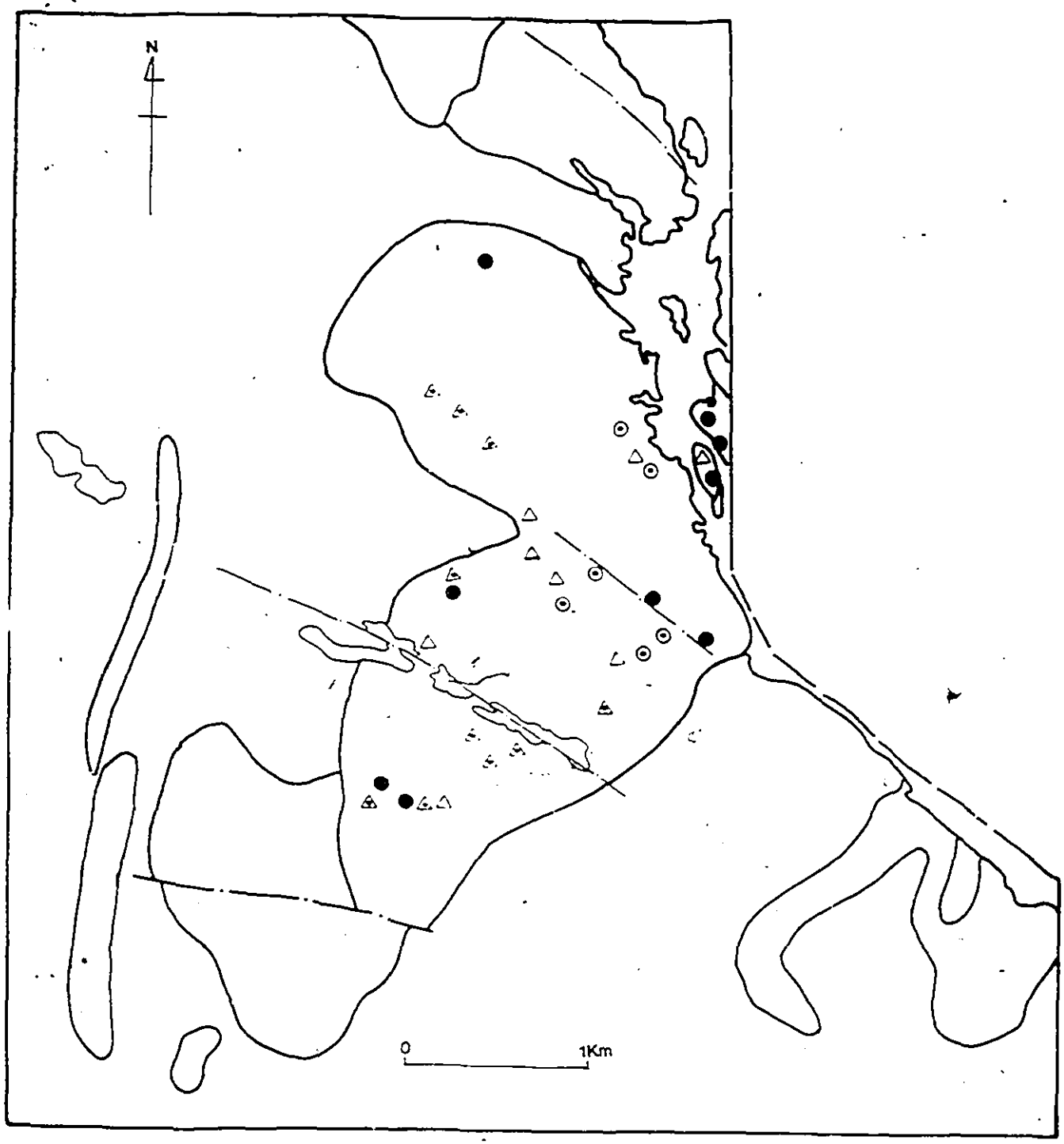

Fig. 2a Distribution of the four gabbro types.
⊙ - olivine gabbro
△ - leuco gabbro
● - pyroxene gabbro
◬ - hornblende gabbro

The following crystallization model is proposed for the pluton. Crystallization began by the formation and accumulation of euhedral magnesian olivine, closely followed by subhedral calcic plagioclase and some Fe-Ti oxide minerals, to give the olivine gabbros. The regular depletion of olivine and an increase in the crystallization of coarse plagioclase along with some pyroxenes and iron oxides, produced the leuco gabbro. Further crystallization proceeded with the continuous precipitation of Fe-Ti oxide minerals and plagioclase and the formation of large quantities of granular pyroxenes (enclosing smaller grains of olivine and plagioclase) to produce pyroxene gabbros. The final stage of crystallization was marked by a rise of water pressure with continuous precipitation of iron-oxide (ilmenite) and sodic plagioclase; pyroxenes now became less abundant due to a partial or complete recrystallization to amphiboles.

This proposed sequence is consistent with the progressive change in plagioclase toward a more sodic composition in the more differentiated rocks. It is also supported by textural constraints, such as subophitic texture and euhedral shapes of olivine and iron-oxide minerals in the early differentiate rocks. In the later rocks, particularly in the pyroxene gabbros, the pyroxene crystals become coarse granular enclosing olivine, plagioclase and iron oxide minerals.

The common occurrences of plagioclase-augite-olivine and plagioclase-orthopyroxene-augite orthocumulates suggest the crystallization

sequence of olivine, plagioclase, augite and orthopyroxene from parental tholeiitic magma.

The lack of hydrous phases and the early precipitation of Fe-Ti oxide minerals in the samples of the Chenaux gabbro indicate crystallization under conditions of low water pressure and relatively high oxygen fugacity. There is generally little evidence of elevated $P(H_2O)$ during much of the crystallization period. $P(H_2O)$ was apparently elevated during the last stage of crystallization, which presumably coincided with the recrystallization of the primary igneous assemblages to produce hydrous phases such as hornblende and biotite. It seems, therefore, that the initial water content of the magma was low and the pluton substantially consolidated before the introduction of significant amounts of water from external sources.

A quantitative statement as to the initial oxygen fugacity has not been possible due to a very low concentration of ulvospinel (less than 0.2%) in the magnetite. The early crystallization of some magnetite with magnesian olivine in these rocks is likely a result of relatively high $f(O_2)$ values. The melt, during fractional crystallization seems to have followed Bowen's trend in which at high $f(O_2)$, magnetite and magnesian olivine coprecipitate leaving a residual liquid enriched in silica.

Thus, an iron-enrichment trend was prevented, and most of the ferromagnesian minerals, particularly calcic pyroxene and olivine, became

magnesian rich as a result of the early precipitation of Fe-Ti oxides.

Table 5 - Representative Mineral Assemblages in Gabbros

	Olivine Gabbro		Anorthositic Gabbro		Pyroxene Gabbro		Hornblende Gabbro	
	1	2	1	2	1	2	1	2
Plagioclase	35	40	60	50	30	40	25	10
Olivine	15	20	5	<5	5	---	---	---
Calcic pyroxene	20	15	15	15	25	30	20	10
Orthopyroxene	10	15	---	10	15	10	trace	---
Hornblende	15	5	10	10	10	5	35	60
Iron-oxide	5	5	<5	5	10	10	10	5
Spinel	<5	trace	trace	trace	trace	trace	---	---
Biotite	---	---	trace	5	<5	5	5	trace
Garnet	---	---	---	5	---	---	---	---
Scapolite	---	---	trace	trace	---	trace	5	15
Epidote	---	---	---	---	trace	---	trace	trace
Pyrite	---	---	---	trace	trace	trace	trace	trace
Titanite	---	---	---	---	trace	trace	trace	trace
Rutile	trace	trace	trace	trace	trace	trace	trace	trace
Apatite	trace	---	trace	trace	trace	trace	---	---

Olivine Gabbro

The rock is characterized by relatively large quantities of euhedral to subhedral olivine (20%) together with augite, hypersthene, plagioclase, Fe-Ti oxides and rare hydrous mafic silicates indicating low water pressure during primary crystallization.

Olivine-bearing gabbros are found on the northeastern and central parts of the

body evidently representing the early phase in the crystallization sequence of the pluton.

The proportion of olivine decreases regularly with increasing differentiation; rocks bearing appreciable quantities of olivine (>15 percent) appear to be concentrated only on the pluton interior. This distribution suggests that the body exhibits a regular areal variation in rock types caused by differentiation, and further suggests that fractional crystallization has proceeded from the interior outwards to the pluton margins.

Textures in these rocks range from relict igneous (subophitic) to crystalloblastic reflecting the degree of recrystallization in response to metamorphic conditions.

Olivine is generally fresh and occurs, as large interstitial grains in granular samples, in reaction relationships with plagioclase surrounded by single or double rims of orthopyroxene and hornblende, as subhedral to anhedral crystals enclosed by pyroxene or plagioclase in poikilitic rocks, or rarely as large euhedral to subhedral crystal in cumulate textures occasionally enclosed by subophitic plagioclase laths (Fig. 3). Oxidized varieties have fractures filled with an opaque mineral.

Pyroxenes show a wide variation in mineral proportions and textures, being predominantly subhedral to anhedral equidimensional granoblastic with occasional

occurrence of subophitic crystals enclosing finer olivine, plagioclase and even Fe-Ti oxides. Subsolidus reactions between hypersthene and Fe-Ti oxide minerals developed remarkable intergrowths of orthopyroxene and iron-oxides. Replacement of clinopyroxene by fibrous amphibole is not uncommon. Some of these zones contain tourmaline and were possibly produced from a late magmatic fluid reacting with completely crystallized phases.

Plagioclase generally forms clear crystals with relict subophitic texture, but rarely it also shows an orthocumulate type of texture, i.e., cumulus plagioclase and intercumulus olivine and pyroxene. Sporadic alignment of platy plagioclase laths produce an igneous lamination in many places; this effect is more pronounced in the olivine gabbro than in the other varieties.

Zoning in plagioclase is very rare indicating slow cooling or perhaps metamorphic homogenization. Clouded plagioclase crystals contain some mafic silicates and tiny needle-like crystals, perhaps rutile. Fe-Ti oxides (magnetite and ilmenite) are present either as discrete crystals or connected grains with sharp, straight boundaries, and almost always contain biotite or/and hornblende rims.

a

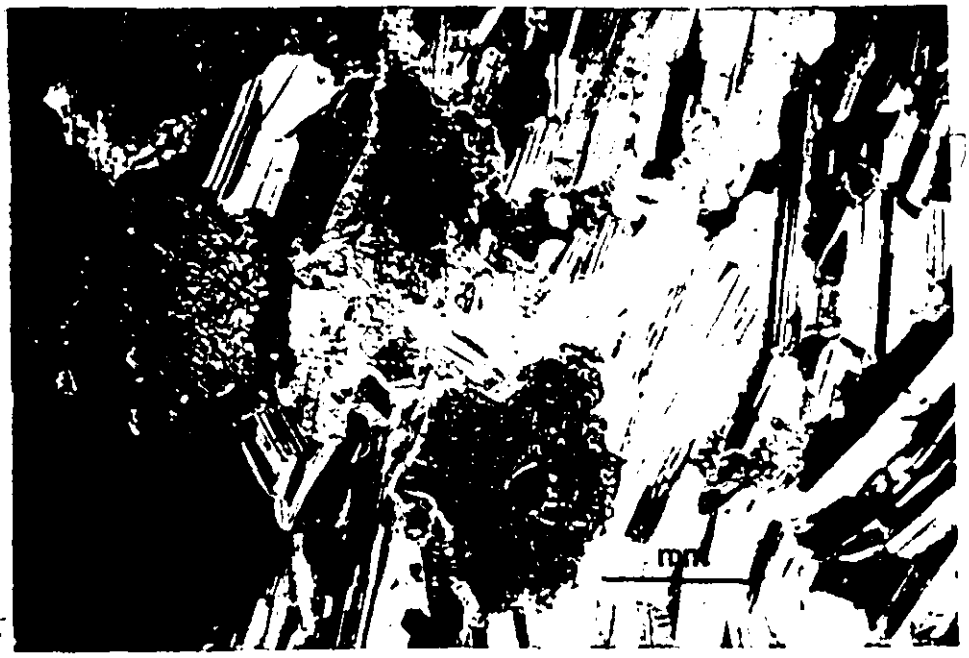

b

Fig. 3. Microtextural features of olivine:
a - granular grain with reaction rim of orthopyroxene and hornblende.
b - poikilitic texture; olivine and plogioclase within Ca proxene crystal.

Pyroxene Gabbro

This rock contains calcic pyroxene and lesser amounts of orthopyroxene making up about 50 percent, and plagioclase with minor olivine, Fe-Ti oxides and in places amphibole and biotite. Spinel, titanite and carbonate are also present.

Pyroxenes typically occur as large discrete granular and poikilitic crystals occasionally enclosing plagioclase, Fe-Ti oxides, and olivine crystals. Where olivine is present, the rock may show subophitic texture. Plagioclase occurs as subhedral to euhedral laths and most of the crystals are clouded with abundant oriented needles of opaque inclusions. Olivine is rare, apparently having altered largely and completely to pyroxene during metamorphism. This is indicated by traces of corroded olivine cores in the pyroxene-plagioclase microstructures now rimmed by hornblende spinel intergrowth (Fig. 4). Fe-Ti oxides are more abundant than in olivine gabbro, and these minerals are characteristically rimmed by green to brown hornblende or less commonly by red-brown biotite.

These widely diverse mineral assemblages and textures in the pyroxene gabbro samples may not necessarily reflect different temperatures and pressures, but instead indicate recrystallization under different water pressures.

Reaction microstructures are not as common as in the olivine gabbro; however, reaction rims around Fe-Ti oxides and to some extent pyroxene are widespread in these rocks. Vermicularly intergrown hypersthene and Fe-Ti oxide are also present. Superimposed on the pre-existing textures and mineralogy are

local alteration zones in which hydrous minerals such as green hornblende and brown biotite partially or completely replace pyroxenes. Here, plagioclase laths are sericitized and show ragged and serrate margins as opposed to the primary sharp contacts and with subhedral to anhedral crystal form.

Fig. 4. Hornblende (h) replacing calcic pyroxene (p)

Leuco Gabbro

These rocks are dominantly composed of plagioclase (up to 60%), augite, hypersthene, with minor olivine and Fe-Ti oxides. Garnet, biotite and amphibole are present locally in various proportions.

Plagioclase is invariably the most abundant, sometimes to the extent of forming virtually a monomineralic cumulus phase with interstitial minerals. No evidence of zoning is observed and the crystal is commonly clouded by tiny opaque inclusions (Fig. 5). Sericitization and to some extent scapolitization has developed randomly. Pyroxenes range in texture from interlocked equant cumulus to coarse crystalloblastic discrete crystals, mainly enclosing larger oxidized euhedral olivine, Fe-Ti oxides, and plagioclase.

Pyroxenes are mainly fresh, but some show partial or complete recrystallization, to amphibole with minor isolated biotite flakes. At an advanced stage of recrystallization, the pyroxenes break down and form a fine-grained mosaic mass that is difficult to identify. Most of the olivines in these rocks are found enclosed poikilitically within the pyroxenes. These olivine grains have margins outlined by opaques, surrounded by pleochroic hypersthene. Discrete olivine crystals, though rare, commonly exhibit consecutive reaction rims of orthopyroxene and hornblende. Fe-Ti oxides are present with their characteristic reaction rims of hornblende and rarely biotite. These oxides mostly have sharp contacts with adjacent plagioclase or pyroxene crystals; elsewhere, the interfacial contact

boundary becomes more diffuse with the presence of additional phases as the reaction proceeds. Poikiloblastic garnet forms crystals up to 2 cm in diameter that are easily recognizable in hand specimens. It seems that there are at least two garnet varieties in the leucogabbros. The first one forms a very coarse porphyroblastic crystal embedded within plagioclase; the second variety is associated to and is continuous with the development of pyroxene-plagioclase reaction microstructures.

Observed reaction relations in these rocks include olivine to orthopyroxene, augite to orthopyroxene, and orthopyroxene and augite to green hornblende intergrown with fine grained spinel. Optically similar hornblende to that of reaction rims commonly forms thin zones and patches along clinopyroxene cleavage and parting planes.

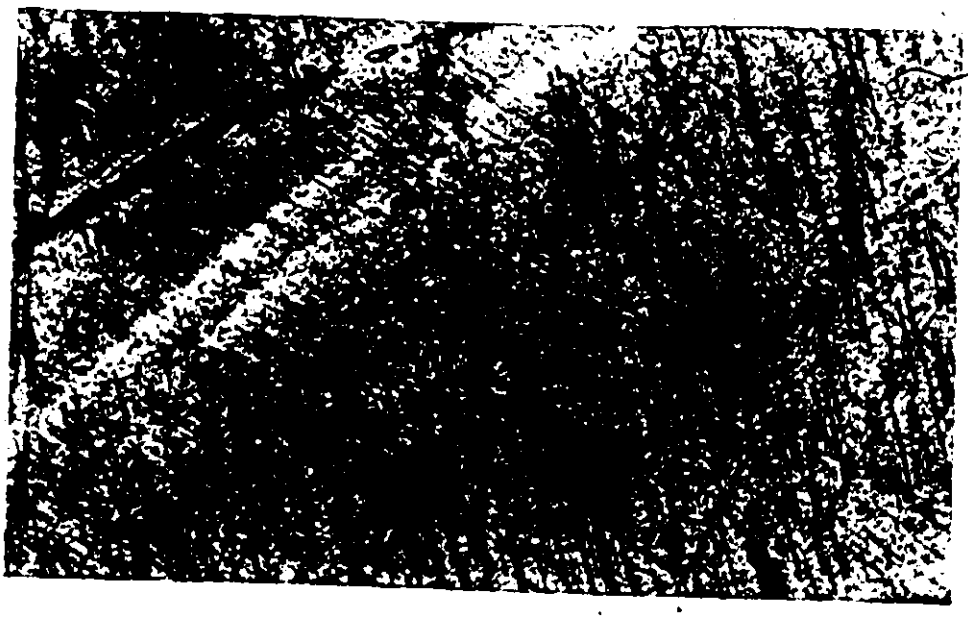

Fig. 5. Cumulus plagioclase clouded by aligned tiny opaque crystals.

Hornblende Gabbro

This rock is characterized by abundant light green hornblende that has presumably crystallized directly from the melt and also recrystallized from pyroxenes. The rock is made up essentially of hornblende, Fe-Ti oxides and plagioclase which is altered commonly to sericite or scapolite. Composition ranges from pyroxene-hornblende gabbro to a rock very rich in prismatic hornblende (>70%). Biotite, titanite and epidote are also present.

Hornblende shows a wide range of textural and compositional variations. Most of the crystals are long prismatic and poikilitic, some are fibrous and form irregular boundaries with the adjacent plagioclase (Fig. 6). At places, relict calcic pyroxene exists in the central part of the hornblende grains. In general, no other reaction relations are developed among the mafic phases. Plagioclase is mainly altered to sericite and scapolite; where fresh, it shows igneous texture with no or very little clouding by opaque inclusions. Large concentrations of Fe-Ti oxides occur either as discrete crystals or clusters without the reaction rim seen commonly in the other gabbroic rocks. In one thin section, ilmenite is rimmed by titanite. Biotite is abundant where there is high opaque concentration; flakes may form independent plates or be intergrown with hornblende.

Fig. 6. Subhedral and poikilitic hornblende crystals with traces of calcic pyroxene
h = hornblende
cpx = calcic pyroxene
s = scapolite

Late Plutons, Dikes and Veins

Granite

One poorly-exposed, small granite body was mapped within the gabbro, south of the Muskrat fault (Fig. 2). The granite is apparently undeformed and unmetamorphosed and was evidently intruded into the gabbro; however, it could be a large inclusion. The rock is massive, and homogeneous pink granite, mainly medium grained, with rare occurrences of xenoliths of a gabbroic rock that may be

amphibolite/metagabbro or Chenaux gabbro. The granite is composed predominantly of subhedral plagioclase, microcline, quartz and traces of biotite.

Aside from this small granitic body, the western end of the Chenaux gabbroic pluton is marked by granitic to granodioritic rocks closely associated with the gabbro, forming a sort of hybridized rock. This is possibly a granophyre but the preferred interpretation is that it is an earlier granitic phase engulfed by the gabbro, forming a sort of hybridized rock.

Mafic Dikes

These rocks are very common in the gabbro and also in the adjacent marbles. They are mainly encountered near contacts and good exposures are found northeast of Garden Lake (Fig. 2).

Mafic dikes are highly variable in size; the width ranges from 0.30 m to about 200 m. The rocks are usually uniform in composition and in grain size throughout their entire length. They are dark green, fine grained, occasionally grading to medium grained gabbros. Characteristically they show ophitic to subophitic texture and consist mainly of hornblende, plagioclase, and olivine with rare garnet, titanite biotite and scapolite. Traces of calcic pyroxene are present in the recrystallized hornblende.

Pyroxenite Dike

A pyroxenite dyke was seen on the southern part of the pluton along the road cut of Highway 17, intruding the gabbro. The rock is massive, medium grained, homogeneous and composed entirely of diopside.

Pegmatite

Pegmatite veins bearing tourmaline have been encountered at different localities in the area mapped. Where found in the marbles, they are rimmed by restricted zones of skarn, rich in diopside, amphibole, garnet, and magnetite. Where they cut gabbro, reaction zones rich in tourmaline may be present.

The pegmatite dikes are composed mainly of microcline, plagioclase, and quartz with rare biotite and muscovite. They are variable in orientation and irregular in size and shape. East of Storyland, close to the Ottawa River (Fig. 2), two east-trending large hornblende-rich pegmatite bodies (about 60 m long and 15 m wide) are widely developed.

Aplite

Aplite, pink and commonly jointed, is found within the gabbro as small and lenticular bodies generally less than a few metres long and a metre wide. These rocks are fine-grained and consist of plagioclase, orthoclase, quartz, muscovite, and biotite. They possibly represent a phase comagmatic or cogenetic with the

pegmatites.

One highly sheared aplite dyke dominated by alkali feldspar is mapped near Chenaux Dam within the sheared and mylonitized gabbro.

Quartz Veins

Quartz veins are not widely developed in the marble but small-scale veining is common within the gneisses. In the gabbro, quartz veins about half a meter wide are present in places. Maximum quartz-vein concentrations are found in the sheared gabbros, running parallel to the mylonitic foliation. These veins are highly sheared and boudinaged; they may be large scale tension gash fillings, formed during shearing (Fig. 7). Quartz veins are well exposed in road cuts near Chenaux Dam.

Fig. 7. Sheared and boudinaged quartz veins near Chenaux Dam. Scale is 30 cm. long.

Chapter IV

CHEMICAL COMPOSITION

Twenty-five representative samples from the four gabbroic rock groups and eight samples from the country rock amphibolites have been analyzed by standard XRF techniques. Analytical procedures and precision are given in Appendix A. FeO was determined by titration. Analyses of the gabbro and the amphibolite are listed in Table 6 and 7 respectively. Localities of the samples analyzed are shown on Fig. 8.

The analyzed gabbro specimens represent all observed varieties, including rocks from the contact as well as the central portion of the Chenaux body. Mineral proportions within the gabbro are diverse, and the concentration range for major elements is also considerable. The overall variations within the body are systematic. Rocks from the east are olivine-bearing and can be distinguished from the rocks on the west and on the south by the absence of hornblende, biotite and epidote. The compositional differences are attributed to primary variations in the whole-rock chemistry, and also to minor addition or removal of matter during recrystallization.

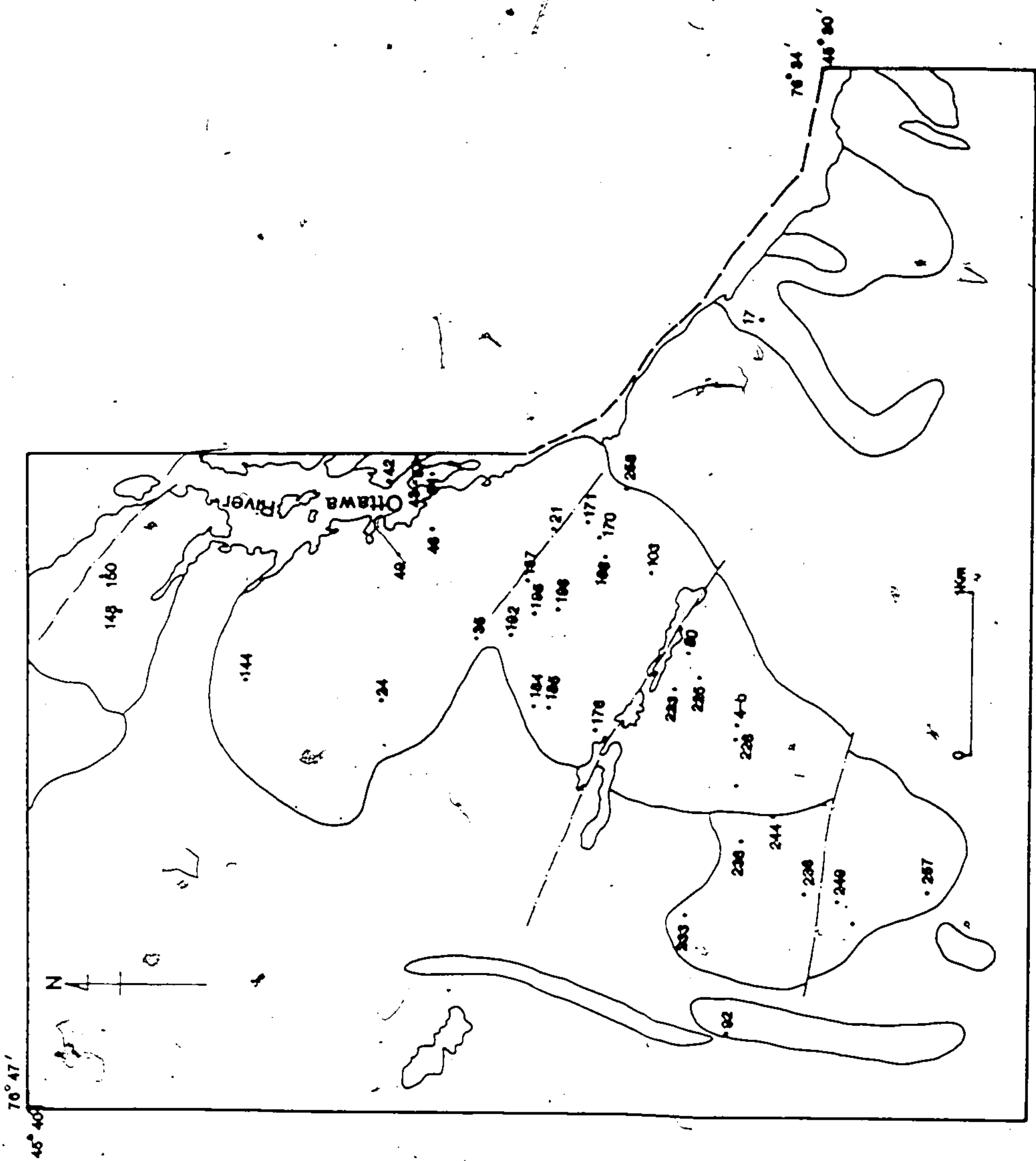
Ottawa River
N
1Km
76°47′
45°40′
76°34′
45°50′

Chemical variations across the body are assessed through plots of K_2O, MgO and Zr versus various other major and trace elements. In general, very few inter elemental relations were observed (Fig. 9). Most of the plots show either an exponential or a saw-tooth pattern with systematic rise and fall in element concentrations as the crystallization proceeds (Fig. 10). The maximum apparently indicates a point where the titanium oxide joins the liquidus, especially when TiO_2 is greater than 0.5 percent.

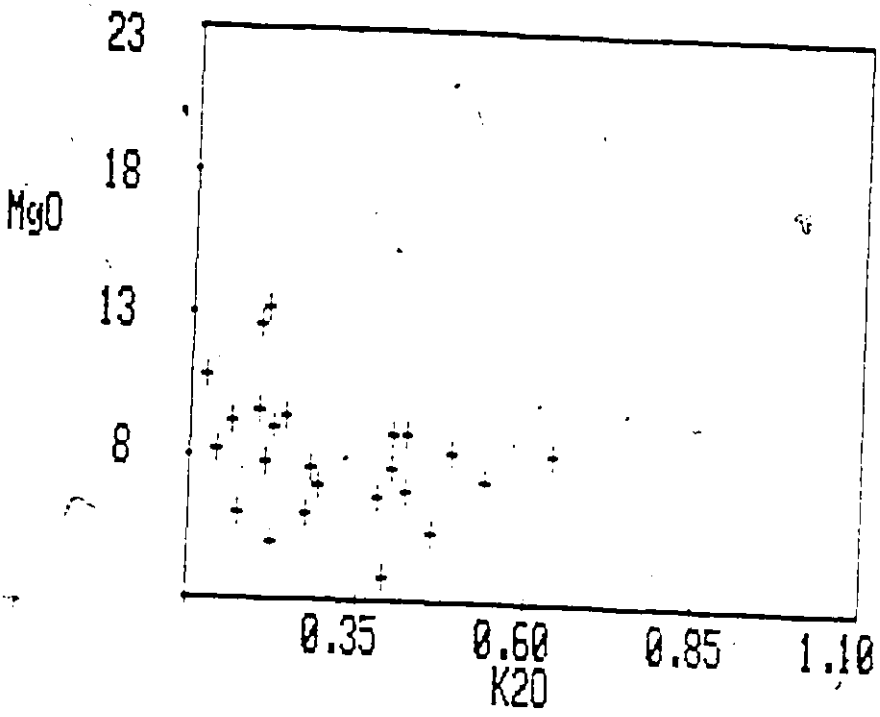

Fig. 9. Plot of MgO against K_2O (weight %), Chenaux gabbro.

The rise and fall pattern does not seem to have resulted from a periodic or a successive invasion of the chamber, because igneous layering is not a prominent feature of this body and topographically the highest portion of the pluton is predominantly underlain by rocks of early differentiates.

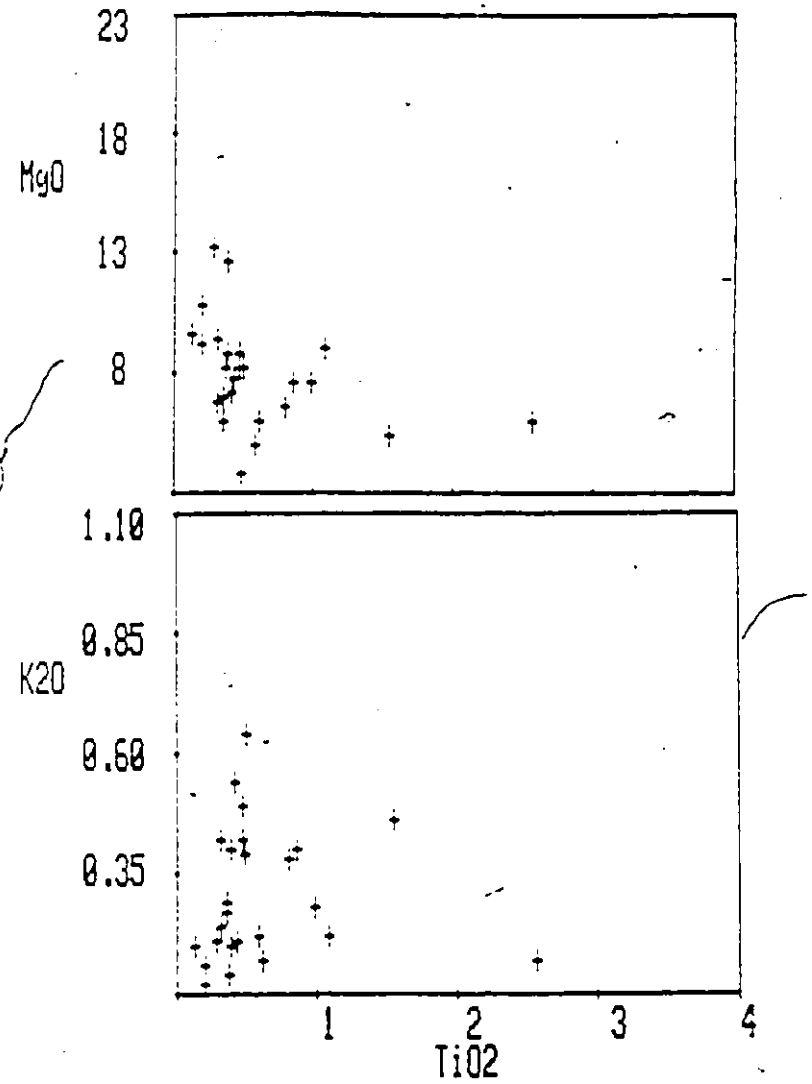

Fig. 10. Plot of MgO and K_2O against TiO_2 (weight %), Chenaux gabbro.

The possibility that different stratigraphic levels of the pluton may have crystallized from different batches of magma successively invading the chamber cannot be excluded. However, such a complex model does not seem to be necessary for this pluton.

A plot of TiO_2 versus Y and Zr (Fig. 11) shows a linear trend perhaps indicating magmatic fractionation.

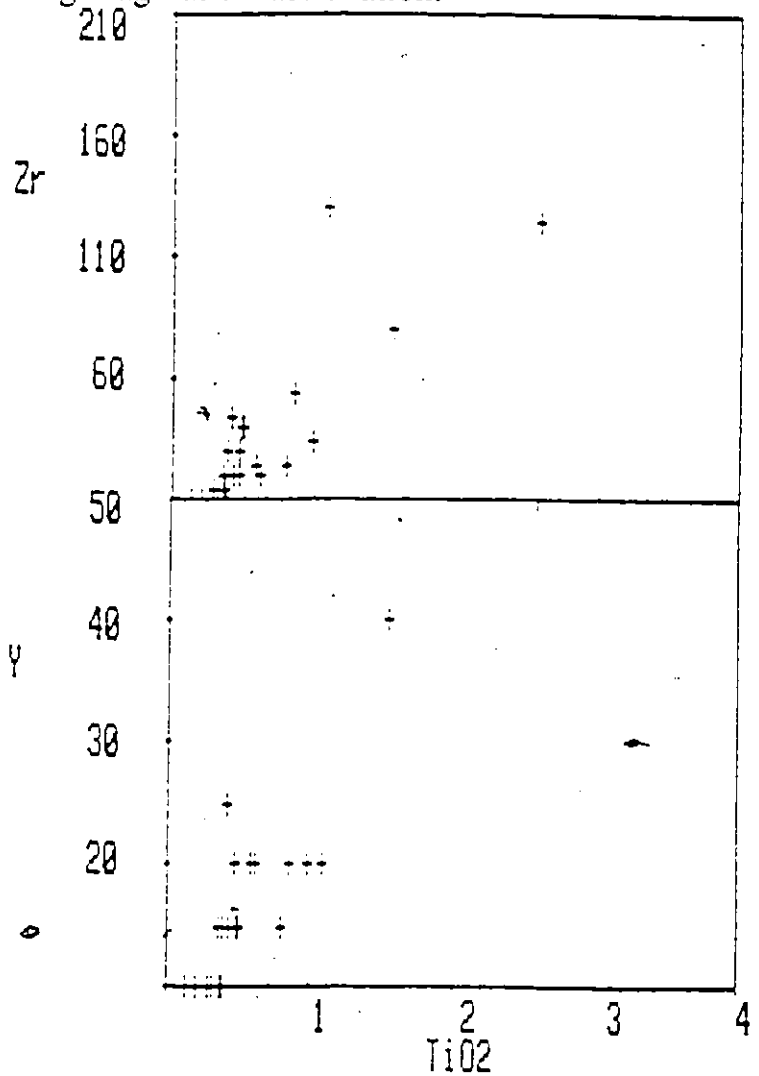

Fig. 11. Plot of Zr and Y (ppm) against TiO_2 (weight %), Chenaux Gabbro.

FeO and MgO show the highest degree of variation, varying from 14 to 4 weight percent indicating the degree and the trend of fractionation. FeO and MgO behave as a coherent group, correlating strongly to each other over most of the field of variation (Fig. 12).

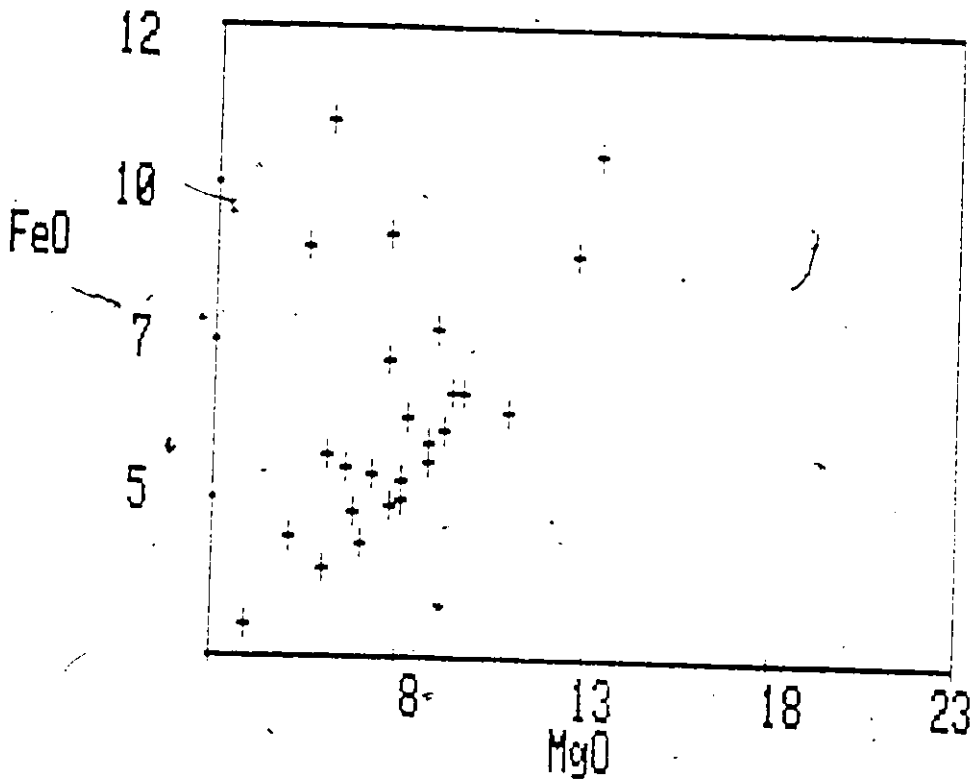

Fig. 12. Plot of FeO against MgO, (weight %) Chenaux gabbro.

The highest alumina concentration is found in the leuco gabbros, and lower values are noted in the pyroxene and hornblende gabbros reflecting the proportion of plagioclase relative to pyroxene and hornblende. The Al_2O_3 versus Sr plot shows no trend, but a typical clustered pattern (Fig. 13). The great majority of the rocks are less variable for CaO. Concentrations of Na_2O and K_2O are rather low and uniform; however, there is slight enrichment from olivine to hornblende gabbros.

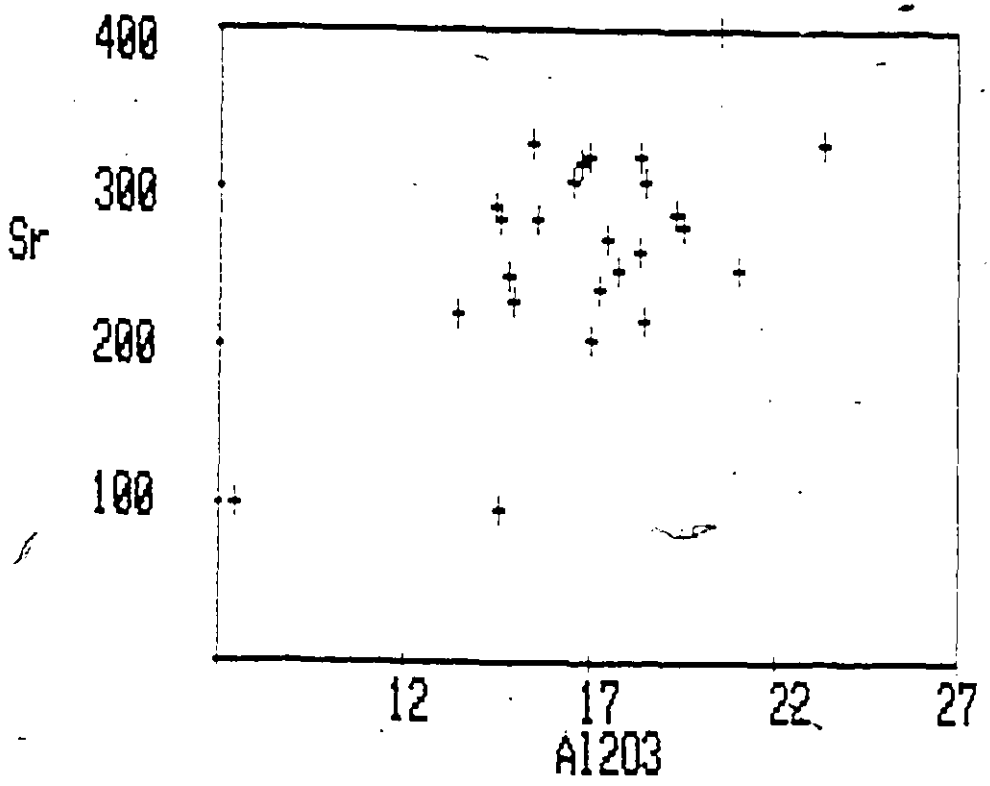

Fig. 13. Plot of Sr (ppm) against Al_2O_3 (weight %), Chenaux gabbro.

The rocks on the AFM plot (Fig. 14) do not follow the usual calc-alkaline trend, but proceed on a course of iron-enrichment distinguished by the increase of Na_2O and K_2O concentrations from olivine gabbro to hornblende gabbro. In these rocks, more distinct iron enrichment was evidently prevented by the early precipitation of Fe-Ti oxide minerals. On the same plot, the rocks fall within the non-cumulate arc gabbro and diorite composition field of Beard (1986).

In the Al_2O_3-CaO-MgO diagram (Fig. 15), the rocks do not show a discrete trend, but cluster away from magnesium-rich peridotitic composition. The Chenaux melt, when it arrived at the present level of exposure, evidently had crystals of augite, plagioclase and locally olivine, intimating a low-pressure eutectic-like composition, which is common for basaltic rocks in general (Yoder, 1976). The melt, therefore, was not primary, but had some history of fractional crystallization and differentiation prior to its emplacement. The calcium and alumina enrichment relative to magnesium indicates that calcic pyroxene and plagioclase as the two main phases that controlled the differentiation.

An attempt was made to assess plagioclase and pyroxene fractionation by the use of Cartesian diagrams of Pearce (1969), on which the axes are represented by ratios of two elements. Al_2O_3 is chosen here as a denominator since it is generally considered to be relatively less mobile. Most of the ratio plot diagrams (Fig. 16) show scatter, possibly the result of complex differentiation behaviour, but a distinct

trend is present in the Ca-Si plot, consistent with plagioclase and pyroxene as the two major phases that controlled the differentiation.

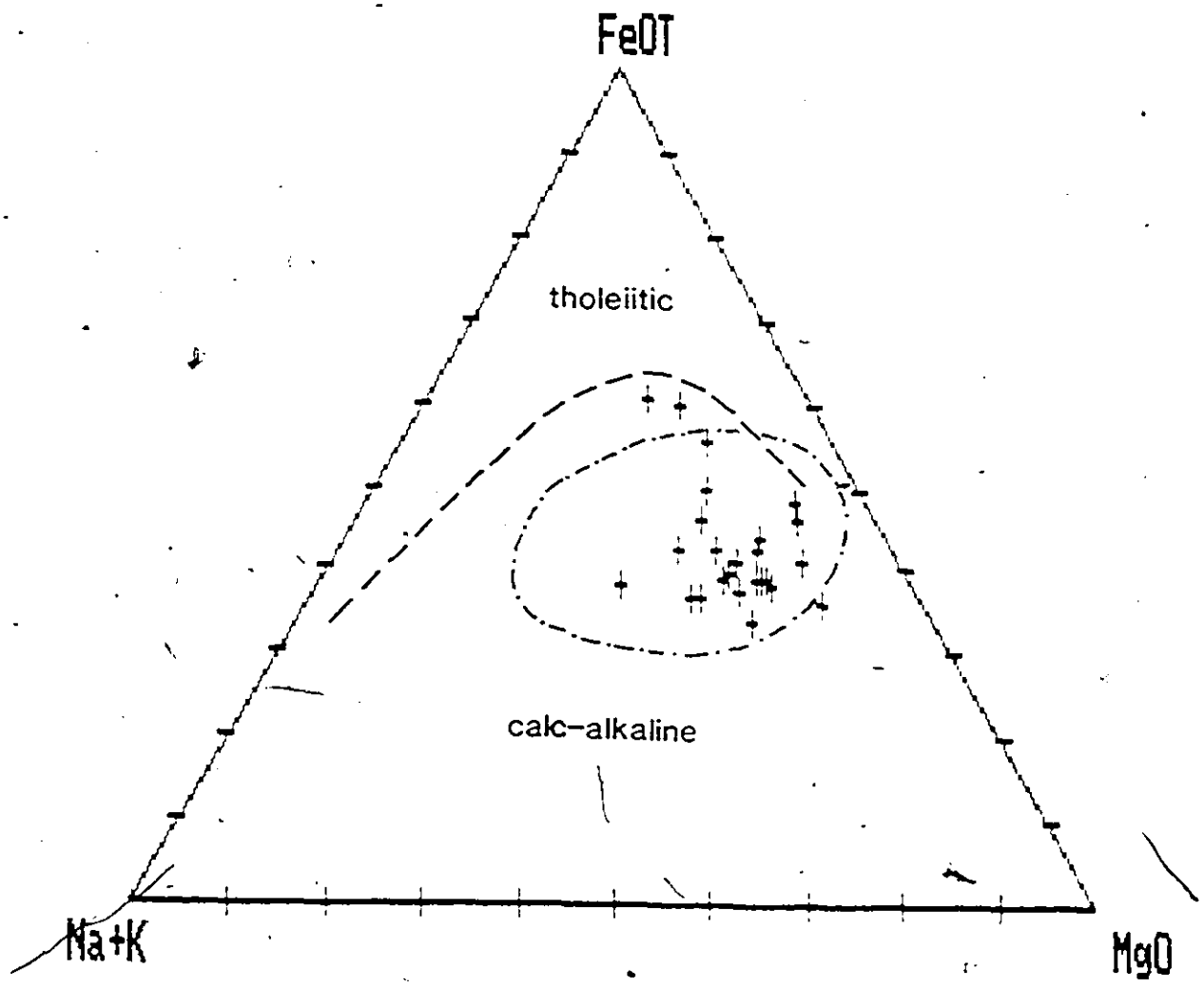

Fig.14. AFM diagram, showing data from the Chenaux gabbro. Circled area indicates non-cumulate gabbro-diorite composition field of Beard (1986); tholeiitic and calc-alkaline fields are after Irvine and Baragar (1971).

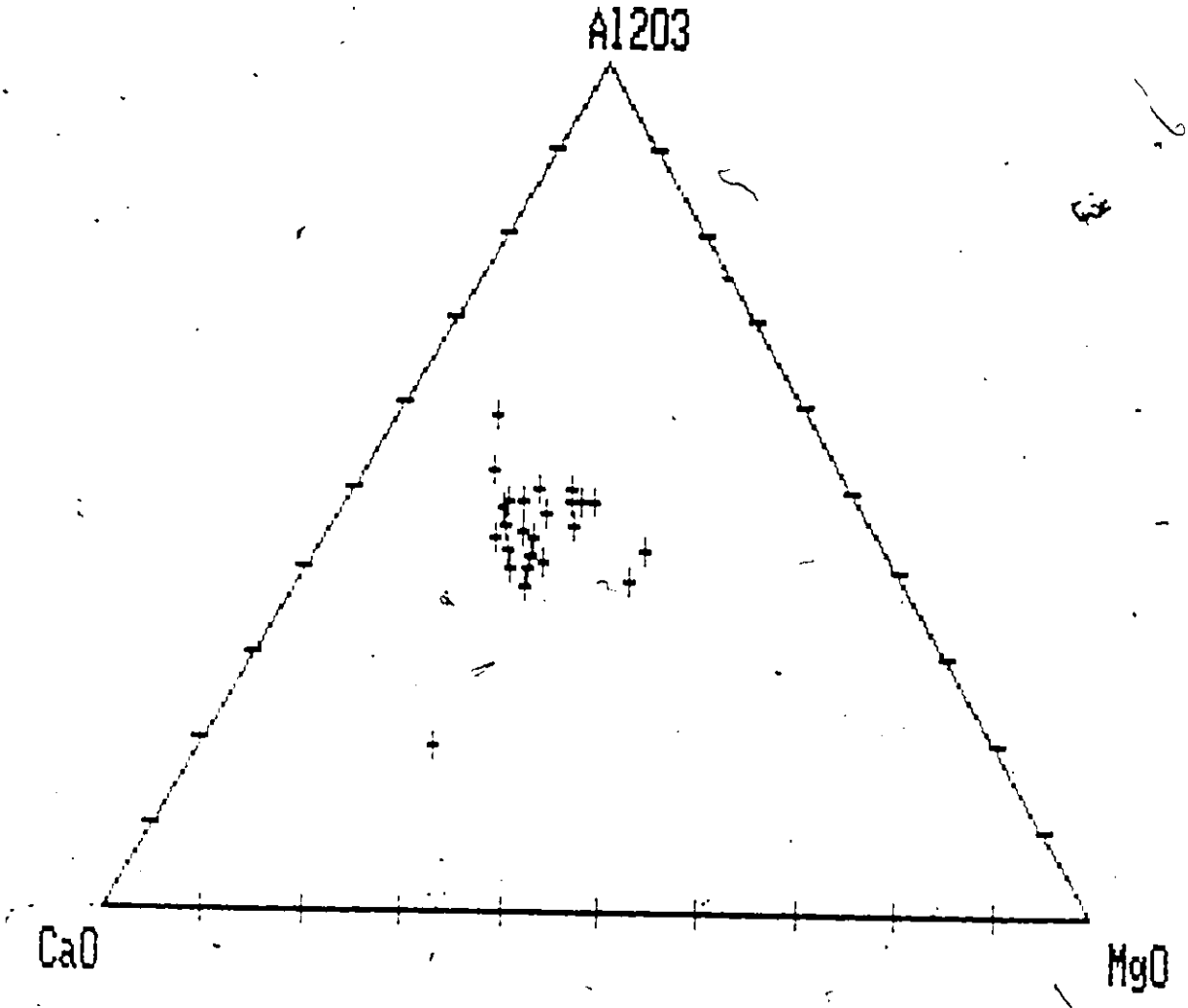

Fig. 15. Plot of data for the Chenaux gabbro in the Al_2O_3-Cao-MgO diagram.

The areal distribution of MgO, FeO, CaO and Na2O + K_2O within the pluton are shown in Figure 17. Composition classes are plotted rather than raw data, in order to distinguish possible chemical variations. It is possible to see a weak trend of depletion of MgO from the center towards the edge of the pluton. Total alkalies have their higher values around the flank of the body. The highest values of Na_2O + K_2O coincide with the lowest Mg/(Mg+Fe) ratio (Fig. 18), particularly in the western part of the pluton. Mg/(Mg + Fe) is generally high in the center, where olivine-bearing rocks are abundant. These chemical features indicate that the direction of differentiation is evidently towards the west. Field evidence and gravity data (Chapter IV) support this view. A westward differentiation trend is also shown by the change in rock types, in which olivine-free gabbros become predominant, sometimes intermingled with granitic rocks near the western flank of the gabbro.

The XRF analyses of eight rock samples from the amphibolite are listed in Table 7. The analyses indicate that all members of this unit have a normal basalt composition, and plot on the tholeiitic field on the AFM diagram (Fig. 19). The rocks are distinguished from the Chenaux gabbro by their lower MgO and total alkalies and by higher TiO_2 and P_2O_5 contents.

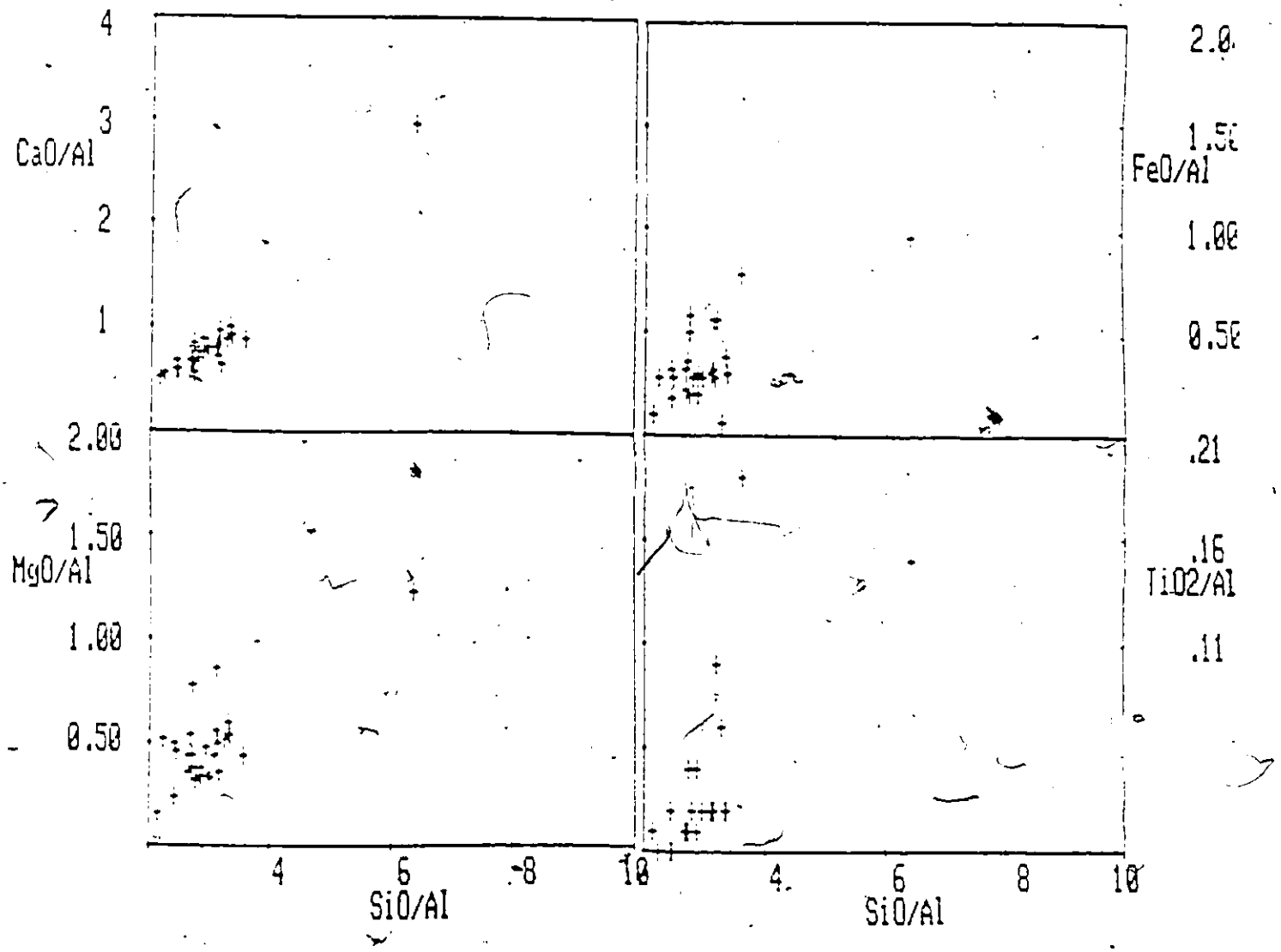

Fig. 16. Pearce-type weight ratio plots.

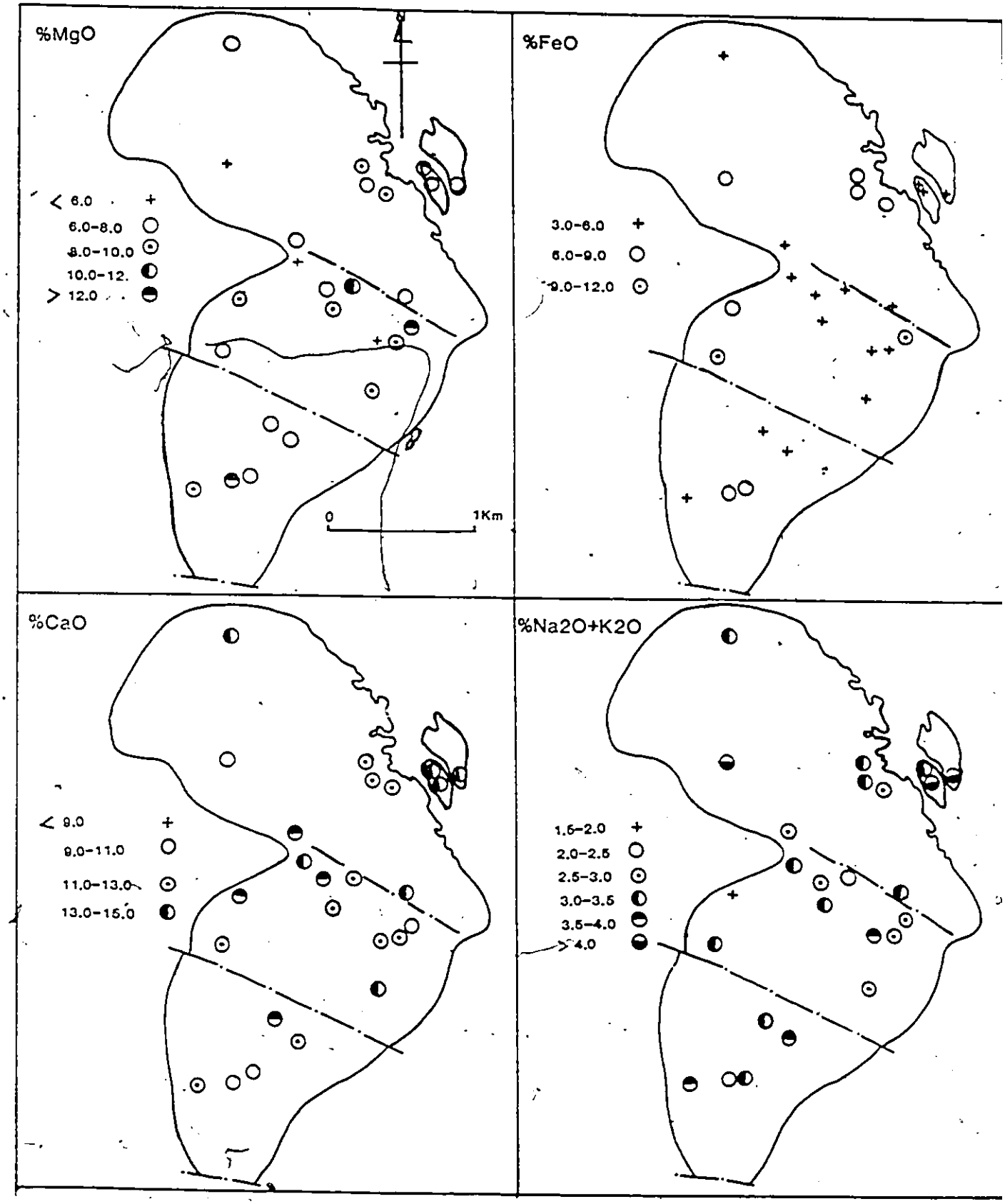

Fig. 17. Areal distribution within the Chenaux gabbro of percent MgO, CaO, FeO and $K_2O + Na_2O$.

On a discrimination plot of TiO_2-MnO-P_2O_5 diagram (Fig. 20), the amphibolites cluster on the mid-ocean-ridge-basalt field. This same trend is also shown on FeO- Al_2O_3-MgO discrimination diagram (Fig. 21) where the rocks fall in the ocean ridge field reflecting a chemistry compatible with an oceanic or marginal basin environment.

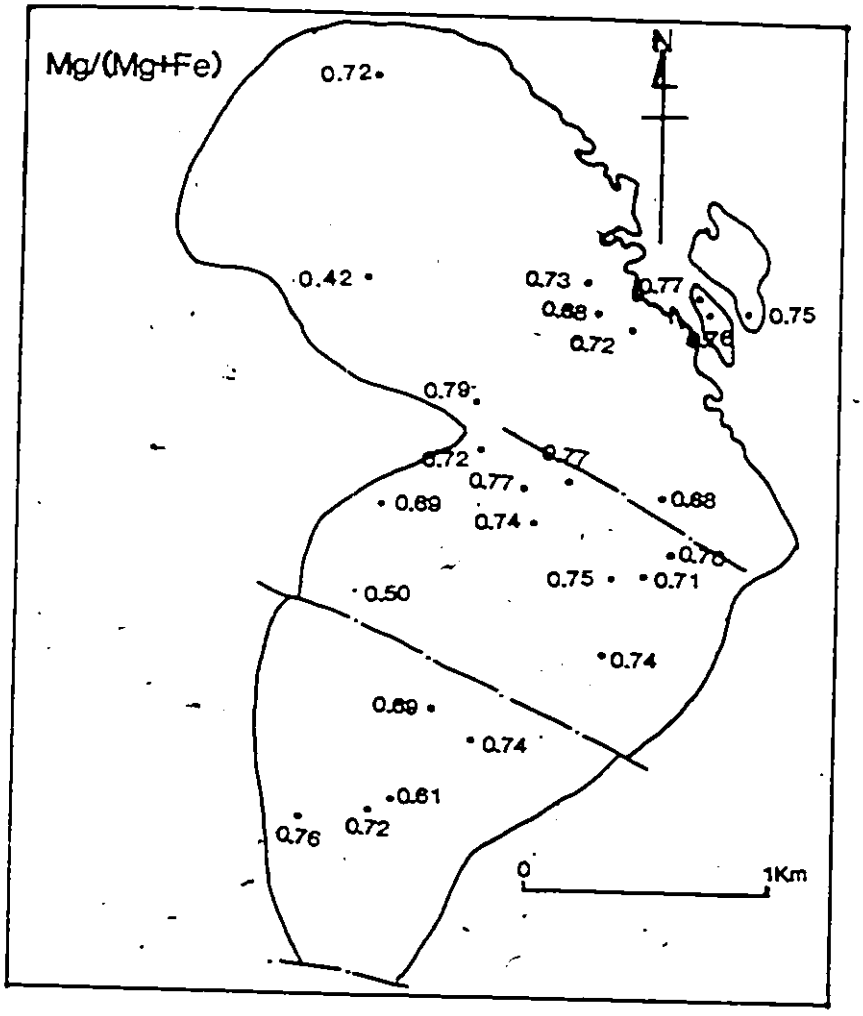

Fig. 18. Distribution of Mg/(Mg +Fe) in the gabbros.

Within the mafic plutonic belt in the western margin of the Central Metasedimentary Belt, there are several gabbro, diorite, granodiorite, granite and syenite suites of plutonic rocks together with associated volcanics. However, it is not clear whether the mafic plutons are generated independently as roots of volcanic centres or to have a genetic link with the associated granitoids. Easton (1986) demonstrated that there is a systematic variation in temporal relations among volcanism (1250 ± 90 Ma), mafic intrusions (1240 Ma) and syenitic suites (1220 - 1250 Ma) in the Central Metasedimentary Belt of Ontario.

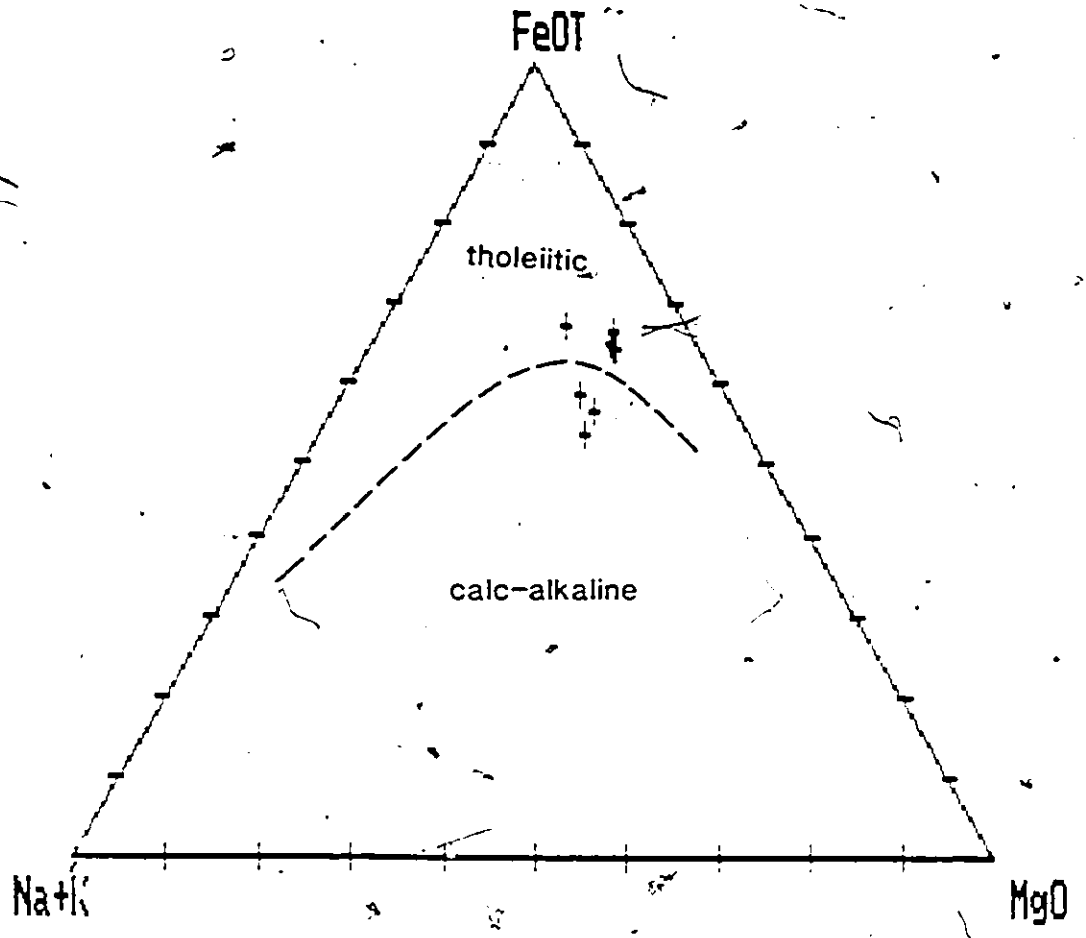

Fig. 19. AFM diagram for the amphibolite.

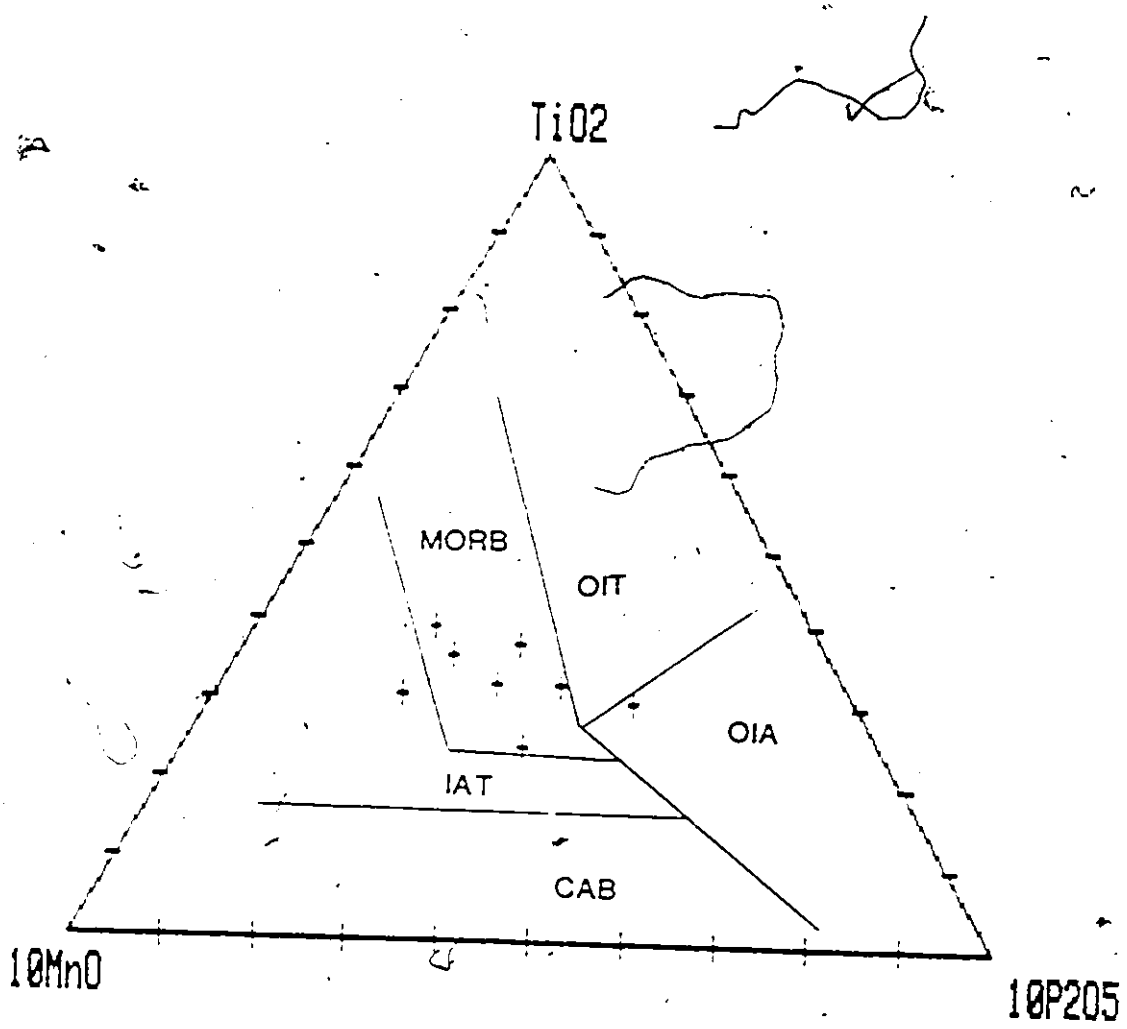

Fig. 20. TiO_2 - MnO - P_2O_5 discrimination diagram after Mullen (1983). OIT, ocean-island tholeiites; OIA, ocean-island alkali basalts; MORB, mid-ocean ridge basalts; IAT, island-arc tholeiites; CAB, calc-alkaline basalts.

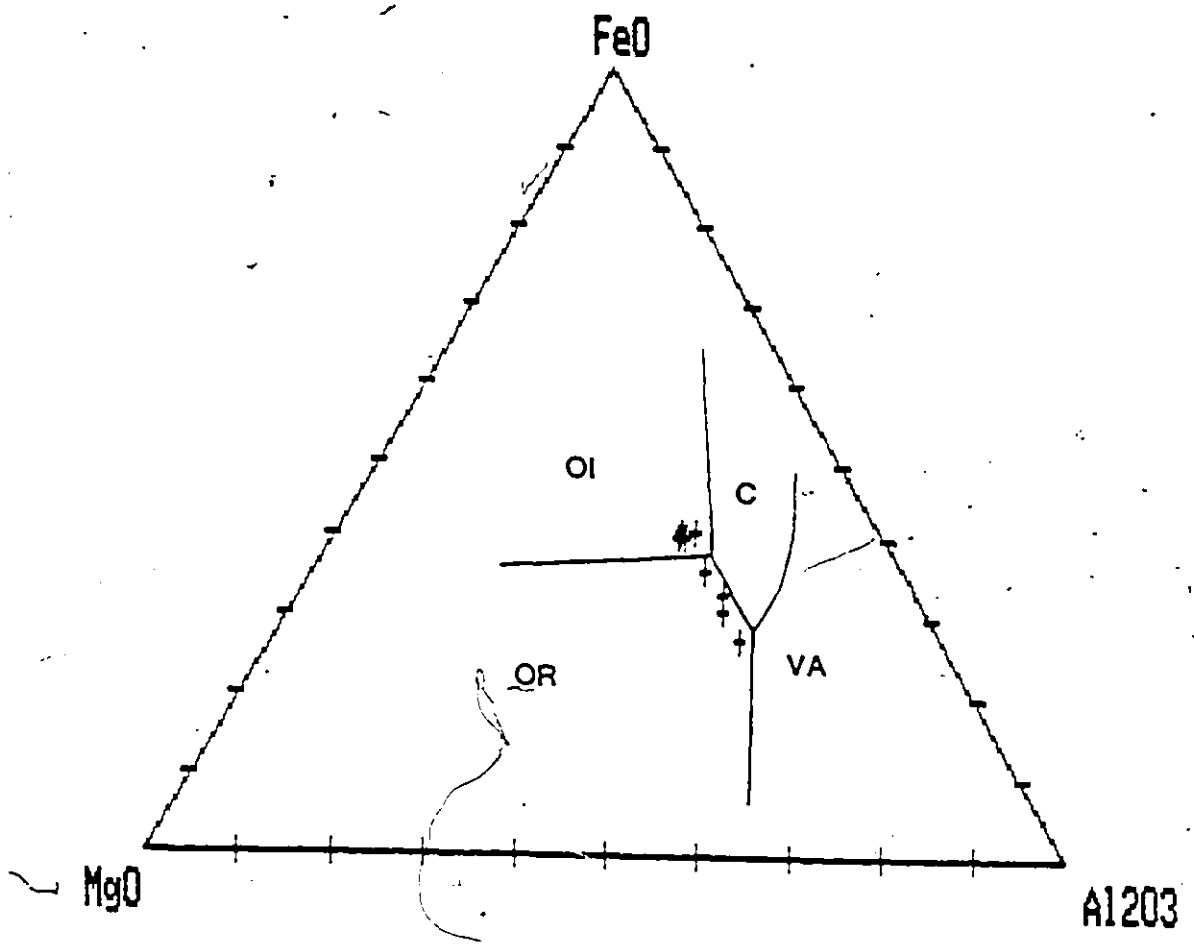

Fig. 21. FeO - MgO - Al_2O_3 discrimination diagram after Pearce et al. (1977). OI, ocean-island basalts; C, continental basalts: OR, ocean-ridge and-floor basalts; VA, volcanic-arc rocks.

The association of the Chenaux intrusion with amphibolities and granitoids can be useful in understanding the nature of the magma source and the tectonic settings in which these rocks were formed. The gabbros and the amphibolites discussed above are compositionally continuous in terms of whole-rock chemistry and can be considered as a differentiated series.

Modelling the lithological variations observed from the amphibolites, gabbros and granitoids in the area will help to establish a proper tectonic setting and genetic relationships; if any, of these rock groups.

Chapter V

MINERAL CHEMISTRY

Mineral analyses of ten representative samples from the gabbros were obtained in the McGill University Microprobe Laboratory using a CAMECA RSX.11M instrument. Synthetic and natural standards were employed. FeO in one hornblende was measured by titration; in pyroxenes, an assumption of FeO^{2+}/FeO (expressed as total iron) equals 0.88 was used to estimate Fe^{2+} : Fe^{3+} (Kretz et al. 1989). Analyses are presented in Table.8. Analytical methods and precision are given in Appendix B.

Olivine

Olivine is relatively restricted and occurs only in the central part of the pluton. The composition of the melt perhaps was not appropriate for olivine to form in abundance, or it might have formed, but settled to the lower unexposed portion of the intrusion. However, the limited crystallization of olivine does not seem to have been controlled by a reaction relationship between olivine crystals and the melt, because there is much less orthopyroxene than calcic pyroxene in these rocks as a whole.

Olivines, where present, occur as large euhedral crystals in reaction microstructures with orthopyroxene and hornblende/spinel intergrowth rims, and

also as subhedral to euhedral crystals enclosed by pyroxenes. Usually the crystals are fresh but replaced by magnetite and iddingsite along internal partings are also frequent. The measured composition ranges from Fo_{74-78}. Individual grains of olivine are mainly compositionally homogeneous with slight variations. These variations are controlled by the bulk-rock composition (Fig. 22). This figure also indicates that all the minerals (calcic pyroxene, orthopyroxene, and hornblende) are more Mg-rich than the rock, except one orthopyroxene sample. This is because the ratio of Mg/(Mg + Fe) in the rocks is influenced by the amount of magnetite present in the rock samples. Average microprobe analyses are listed in Table 8A (p.93).

Olivine shows systematic variation in composition with the co-existing orthopyroxene suggesting a close approach to equilibrium between the two minerals (Figure 23).

The partition co-efficient for the distribution of Mg and Fe between co-existing olivine and orthopyroxene ($K_D \doteq ((X_{Mg}/X_{Fe})_{olivine} \cdot (X_{Fe}/X_{Mg})_{opx})$ averages 0.80 in the olivine gabbro samples. According to Medaris (1969), Mg and Fe partitioning between olivine and orthopyroxene is not sensitive to temperature over the range 700° to 1300°. The experimental results of Williams (1971) indicate the temperature dependence of Fe and Mg partitioning between olivine and orthopyroxene. However, temperature extimates were not possible for several

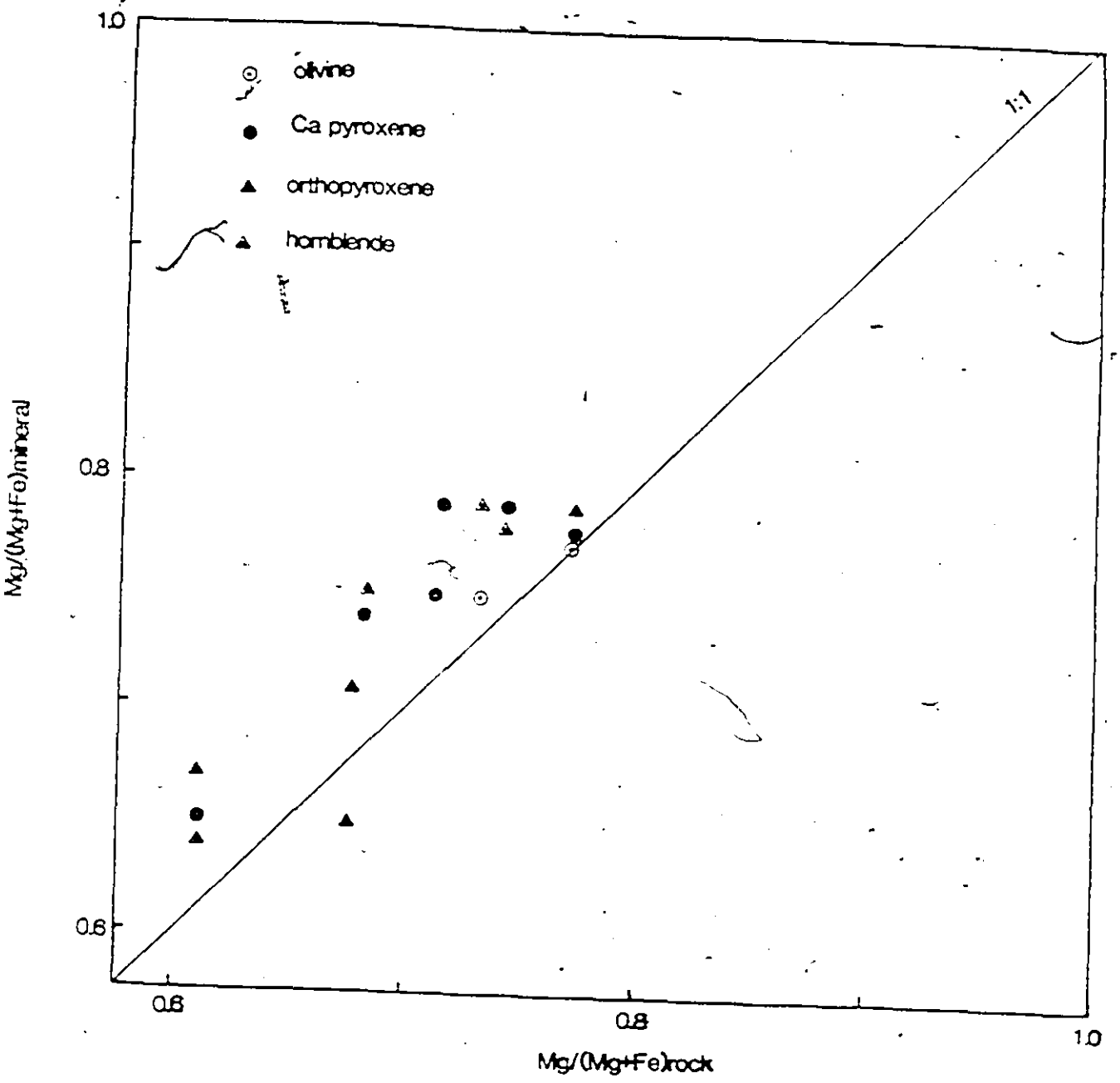

Fig. 22. Relationship of bulk rock chemistry to the constituting minerals.

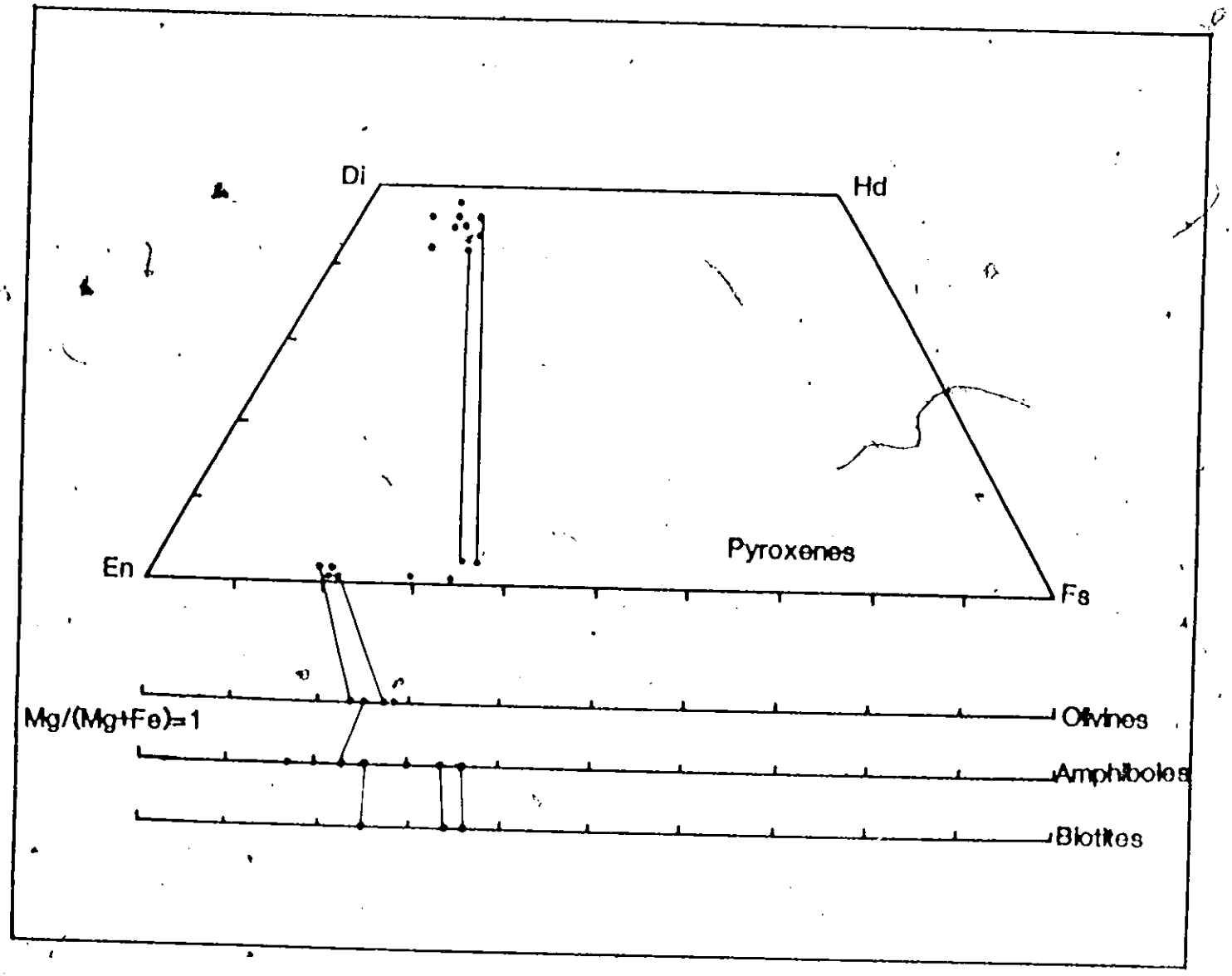

Fig.23. Pyroxene quadrilateral with compositions of ferromagnesian silicates in gabbros.

fayalite-enstatite and forsterite-ferrosilite pairs using William's curve.

Plagioclase

Plagioclase is invariably the most abundant phase, sometimes to the extent of forming virtually monomineralic aggregates. The volume percent of plagioclase varies among gabbro samples, being highest within the leucocratic varieties. In most rocks the abundance ranges from 40 to 60 percent.

Plagioclase occurs as subhedral to euhedral subophitic twinned and unzoned tabular crystals enclosed by pyroxene or olivine. It also forms larger more equant cumulate grains of compound plagioclase megacrysts, particularly in the leuco gabbros.

Individual crystals are very rarely zoned. Homogeneous crystals are very common, with very minor variations in their anorthite content from core to rim. Such homogenization can be due to slow cooling or to metamorphic recrystallization. The measured compositional range for plagioclase in all gabbroic rocks analyzed is An_{57-76}. Plagioclase in any one specimen has a more restricted compositional range which varies with the Fe and Mg content of the coexisting mafic minerals. For example, olivine gabbro (sample 157) which has the most magnesian mafic phases, contains Ca-rich plagioclase of composition An_{75}; hornblende gabbro (sample 103), containing the most Fe-rich mafic phases, has

plagioclase composition of An_{57}. The K_2O content of plagioclase, expressed as mole percent orthoclase, is extremely low, but increases very slightly with increasing albite component. Microprobe analyses are listed in Table 8B (p.94).

Some plagioclase crystals are clouded with abundant oriented needles of opaque inclusions. Grain boundaries among the plagioclase crystals are mostly sharp. However, corroded and embayed grain boundaries are equally common where reaction microstructures develop between plagioclase and adjacent mafic phases. Plagioclase in hornblende gabbro is partially or wholly altered to scapolite, and to some extent to sericite, epidote and calcite.

Pyroxenes

Orthopyroxene and clinopyroxene occur as both igneous and metamorphic phases, clinopyroxenes (subophitically intergrown with plagioclase) being more common as a primary phase. In contrast to the igneous pyroxenes, metamorphic crystals occur as smaller grains or clusters of grains, but in many instances they display a radial orientation about a reactant phase such as olivine or another pyroxene.

Metamorphic orthopyroxene is most commonly developed in rims about olivine grains and occasionally about primary igneous clinopyroxene. Most of the

metamorphic clinopyroxene is present as rims surrounding metamorphic orthopyroxene.

Clinopyroxene

Clinopyroxene is the most abundant mafic phase in the gabbroic samples and is usually colorless or pale with no pleochroism. It occurs either as large subophitic crystals enclosing plagioclase or as equidimentional granular grains. Hypidiomorphic and poikilitic grains are also common. Recrystallization of clinopyroxene to green hornblende is very patchy in the olivine gabbros; however, the hornblende gabbros show more or less complete recrystallization with a slight iron-enrichment in the hornblende. Cleavage and parting planes of many crystals are lined with opaque minerals. The opaque mineral may be either exsolved iron oxide or a late magmatic reaction product.

Microprobe analyses of augite are listed in Table 8C (p.96). The Ca:Mg:Fe ratios of augite in various gabbroic rocks are plotted in the pyroxene quadrilateral (Fig. 23). The compositions (which show a great variation even within a single slide) plot mainly in the augite field, near the diopside-salite boundary. Some zoned varieties show a systematic increase in Fe, Ti and Ca from the center to the edge of the crystals, coupled with a decrease in Mg. This trend, of increasing Fe to Mg in augite crystals towards the edge, was also reported by Kretz (1985) in the Grenville swarm of gabbro dikes indicating that the augite was in equilibrium with the melt as

the temperature declined. Several clinopyroxene analyses indicate that their Mg/(Mg + Fe) ratio is slightly higher than that of the coexisting orthopyroxene (Fig. 23).

Orthopyroxene

Orthopyroxene occurs generally as discrete subhedral to anhedral small crystals and as a reaction rims around olivine. It is slightly pleochroic from pale reddish to pale brown. Optical zoning is rare in orthopyroxene; some crystals show a magnesium-rich core, with systematic enrichment in iron taking place from core to rim; these variations do not exceed two percent.

The composition of the orthopyroxene in a given sample is not highly variable. Conspicuous differences may be seen between the discrete crystals and those developed in reaction rims about olivines and clinopyroxenes. The former variety has high iron, in the range of 20 to 24 percent FeO and slightly lower magnesium, up to 22 percent MgO. The iron content in the orthopyroxene in reaction rims is in the range of 14 to 15 percent FeO. The alumina abundance everywhere is rather low, ranging from 0.80 to 2.10 weight percent Al_2O_3. This variation is neither systematic nor controlled by coexisting mineral phases. Calcium is relatively high in the discrete igneous crystals (1.35 to 1.5 weight percent CaO); whereas those from reaction rims have much lower concentration

(0.08 to 0.70 weight percent CaO). Low alumina and calcium contents in the orthopyroxenes were considered by Evans (1977) to be a characteristic feature of orthopyroxenes in the granulite facies. Microprobe analyses of orthopyroxene is listed in Table 8D (p.99).

The Fe-Mg distribution coefficient for coexisting orthopyroxenes and clinopyroxenes ($K_D = (X/1 - X)_{opx} \cdot (1 - X/X)_{cpx}$) averages 1.8.

The pyroxene geothermometer of Kretz (1982) was used to estimate the temperature of equilibration of coexisting augite and orthopyroxene from the olivine gabbro. The temperature calculated using the transfer equation for two pyroxene pairs are 820 and 825°C. The calculated temperature is lower than crystallization temperature estimated for other gabbroic bodies (Morse et. al, 1980 and Loney and Himmelberg, 1983), except for very late stages of crystallization. These data, may indicate that the solidus of the Chenaux intrusion was depressed relative to other gabbroic intrusions probably due to water migration towards the upper portion of the chamber. However, the unexposed lower part of the pluton could have crystallized before the more differentiated roof rocks under higher temperature conditions, possibly as a result of crystal settling. On the other hand, the limited range of calculated temperatures might instead represent subsolidus equilibration of the two pyroxenes during the slow cooling of the intrusion.

Pressure under which the Chenaux gabbro was emplaced and crystallized was calculated for an orthopyroxene-garnet pair in a sample of leuco gabbro using the orthopyroxene-garnet equilibrium of Wood (1974). The calculation yielded a geologically unreasonable pressure of 24 kb using a minimum temperature of 640°C. This extremely high value indicates an absence of equilibration between the garnet and orthopyroxene in leuco gabbro.

Hornblende

Hornblende in these gabbroic rocks can be grouped into at least two varieties.

reaction microstructure

This group includes hornblendes developed as metamorphic reaction rims about primary magmatic minerals in magnesium-rich rocks. These are mostly intergrown with fine spinels and their composition depends on the reactant phases about which they develop.

A plot of (Na + K) against Al^{IV} (Deer, et. al., 1980), Fig. 24, indicates that all are hornblendes grading toward Tschermakite. Microprobe analyses of representative samples are given in Table 8E (p.101).

The hornblende analyses are exceedingly aluminous, Al_2O_3 ranges from 15 to 29 weight percent, though most values are less than 20. Higher values of alumina

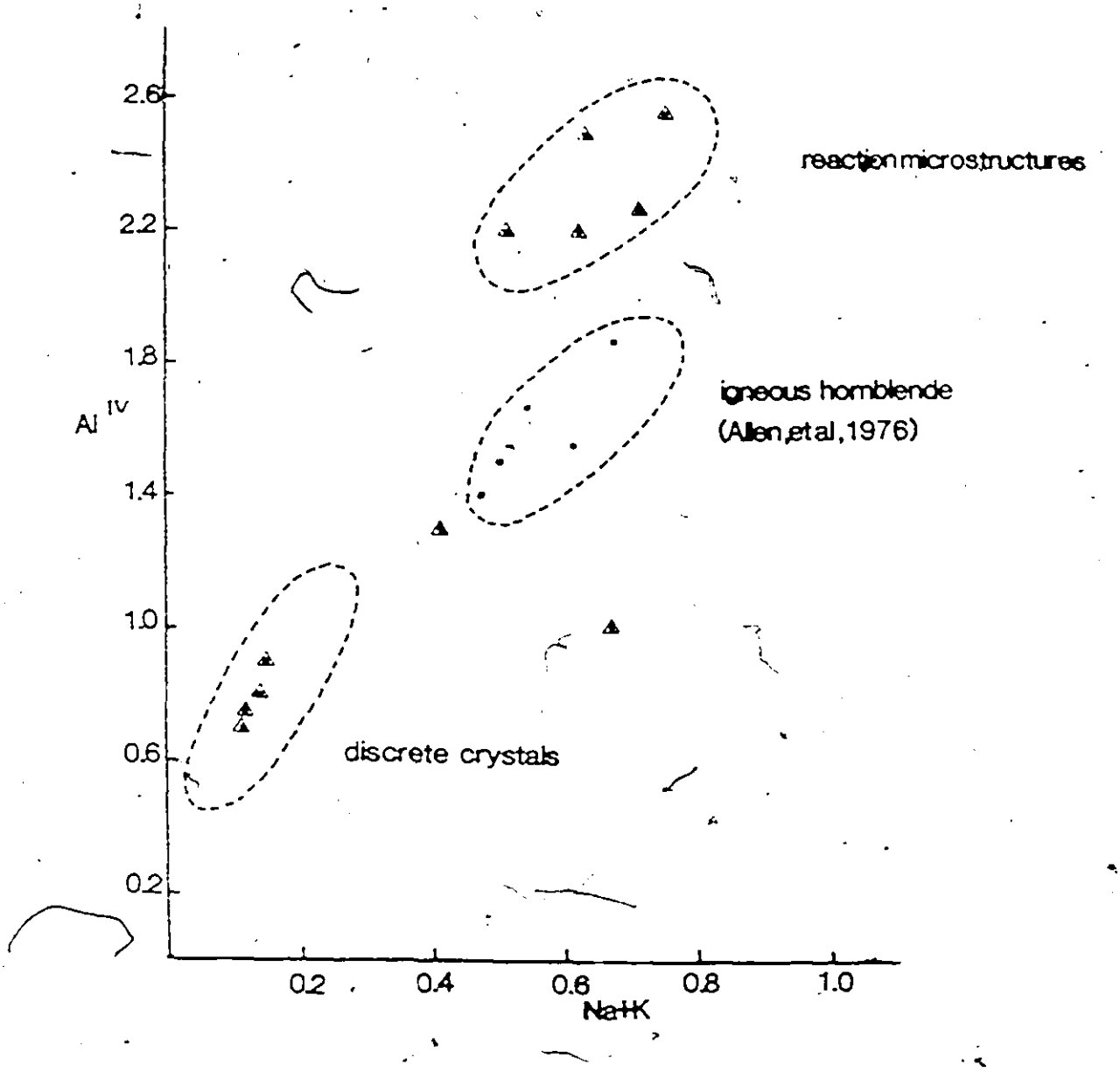

Fig. 24. Plot of Al vs. Na + K in amphiboles. Triangles denote hornblendes from Chenaux gabbro and dots denote hornblende from Kilauea olivine tholeiite (Allen et al., 1976).

result from the commonly intergrown fine spinel crystals. The intergrowth of spinel with hornblende is at various proportions; hence, correction for alumina has not been possible. CaO concentration is relatively uniform, being 11 weight percent. Na_2O ranges from 1.35 to 2.5 weight percent and K_2O and TiO_2 are generally low. Mg/(Mg + Fe) ratios range from 0.75 to 0.83, higher than those of coexisting olivines and pyroxenes.

The Fe-Mg distribution coefficients for three calcic hornblende and the coexisting olivine, where $K_D = (Fe/(Fe + Mg)/Mg/(Fe + Mg)_{olivine}$ $(Mg/(Fe + Mg)/Fe/(Fe + Mg)_{hbd}$, equals 1.40, which is close to the 1.44 obtained experimentally by Helz (1973) at 930°C. This temperature is much higher than the metamorphic temperature of the region, which is probably in the order of 650 (Turner, 1981).

discrete crystals

Hornblende of the second group occurs as subhedral brownish-green crystal and is found predominantly in the olivine-free (more highly differentiated) gabbros. It occurs as poikilitic grains and pseudomorphs, evidently formed by the replacement of pyroxenes, and to some extent of plagioclase. Relict patches of pyroxenes may be present. Some granoblastic crystals seem to have grown from plagioclase. Traces of albite twinning may be observed within some incipiently

developed crystals. Microprobe analyses are given in Table 8E (p.101).

Calcic hornblende analyses plot between tremolite and hornblende forming a linear trend, on a (Na + K) Vs Al^{iv} diagram (Fig. 24), within the composition field of metamorphic amphiboles, as defined by Jamieson (1981). Compared to the first variety, amphiboles of the second group contain much less alumina. Al_2O_3 content ranges from 4.5 to 5.5. weight percent, increasing with an increase in the total alkali content. The CaO concentration is almost similar. Generally they have lower concentrations of Na, K, Ti, and Al^{iv} which, according to Jamieson (1981), is a characteristic feature of low temperature metamorphic amphiboles. Mg/(Mg + Fe) ratio is almost similar, averaging 0.80.

In addition to the two major amphibole groups, there are very localized occurences of a late amphibole which occurs as a network of veins. These thin veins in places contain tourmaline.

Biotite

Biotite, in the gabbroic rocks, is highly pleochroic (from light to deep reddish-brown) and is commonly present in the more differentiated rocks. It occurs either as subidioblastic lath or xenoblastic crystals, occasionally forming patches in hornblende and rarely poikiloblastically enclosing crystals of hornblende. Mostly, it appears to be secondary in origin, having formed from hornblende and

Fe-Ti oxides and rarely from garnet. Biotite also occurs as a reaction rim around Fe-Ti oxides. The rimming is usually incomplete, and is often represented by one or two individual flakes.

The composition of biotite, as determined in the three gabbro samples (Table 8F-p.104), is highly variable with regard to Fe, Mg, Ca, and Ti. The Mg/Mg + Fe^{+} ratio of boitite is lower than olivine and pyroxenes and is similar to that of amphiboles in which it coexists together (Fig. 23). At present, no inference can be made from the available microprobe data on the relative proportion of Fe^{2+} and Fe^{3+}.

Harry and Pauk (1979) indicated that variations in total iron reflect progressive change in the oxidation state of iron during crystallization. Studies by Eugster and Wones (1962) and Speer (1981) have shown conclusively that the composition of biotite in igneous rocks depends mainly on the oxygen fugacity that prevails during crystallization. Hence, the observed variation in Fe may reflect a variation in oxidation state of the melt. Alternatively, the biotite may be a metamorphic mineral, with an Fe:Mg ratio determined by that of the reactant minerals.

CaO concentrations of biotite are higher in the pyroxene gabbro, compared to the leuco gabbro. Iron content in leuco gabbro samples averages 14.5 weight percent and 10 weight percent in the pyroxene gabbro. The other constituent

oxides show fairly similar composition. Na_2O is characteristically low, in the range of 0.30 weight percent. Sodium content in biotite decreases with increasing of Fe/(Fe + Mg) ratio, because in the highly differentiated rocks, sodium is incorporated into plagioclase and hornblende rather than biotite (Harry and Paul, 1979).

Magnetite & Ilmenite

The Fe-Ti oxide minerals occur in all rocks either as discrete crystals or inter-connected grains with sharp and straight boundaries. A magnetite-ilmenite pair analyzed ($Mt_{99.87}$ $Usp_{0.13}$ and Ilm_{94} Hm_6) has undergone subsolidus re-equilibration and does not define an oxygen fugacity or temperature of crystallization.

Separate grains of ilmenite and magnetite occur in some rocks, and in one rock, ilmenite occurs intergrown with magnetite as clustered granules. Such textures were evidently formed by an exsolution-oxidation reaction, as proposed by Buddington and Lindsley (1964). They occur prominantly in the most fractionated rocks reflecting more extensive subsolidus reaction, promoted possibly by fluids. Buddington and Lindsley also indicated that the coexisting magnetite-ilmenite pair, if primary, is useful in estimating $f(O_2)$ and temperature, provided the rocks cooled quickly. In gabbroic rocks, which have cooled slowly, these two phases, for the

most part are the result of subsolidus oxidation, and therefore can only indicate the temperature of cessation of exsolution rather than temperature of crystallization (Haggerty, 1974).

Analyses of magnetite and ilmenite are listed in Table 8G (p.105). Both ilmenite and magnetite contain minor elements such as Mn, Na, Si, Al, Mg, K and Ca in very low concentrations. Mg, Mn and Ca have an effect on the $f(O_2)$-T stability range of Fe-Ti oxides (Lindsley, 1963). MnO is higher (0.86 weight percent) in the ilmenite compared to magnetite. Thus, for coexisting ilmenite-magnetite pairs, Mn is strongly partitioned into the ilmenite regardless of whether the ilmenite is primary or resulted from an oxidation-exsolution reaction (Neuman, 1974).

Scapolite

Scapolitization has affected both the gabbroic body and the country-rock amphibolite to the south. Scapolite is restricted mainly to the hornblende gabbro, although it does occur in the other gabbro units, but to a lesser extent. In the hornblende gabbros, single plagioclase laths are replaced partially or completely by a number of small Ca-rich scapolite crystals (meionite) identified by their high birefringence (Kerr, 1977). Most plagioclase is at least marginally affected by the process, although relatively fresh plagioclase is locally preserved.

Analyses of scapolite are shown in Table 8H (p.106). The scapolite is distinctly rich in calcium (15.2 weight percent) and Na concentration averages 4.6 weight percent. The Na/(Na + Ca) ratio is about 0.77.

The distribution of Na and Ca between scapolite and plagioclase was used to estimate temperatures, using the Goldsmith and Newton (1977) method. An extrapolation of the Na/(Na + Ca) ratios on the plagioclase-scapolite diagram gave a temperature of 800°C.

Garnet

Garnet occurs as large discrete cluster of grains mainly in the pyroxene and leuco gabbros. In places, it forms prominent poikiloblastic grains within plagioclase and rarely around pyroxene-hornblende reaction zones. It is not clear whether the garnet was formed as a result of metamorphic reactions or as part of the igneous assemblage. Although garnet has been considered as a high pressure phase, when present in metamorphosed igneous rocks, it can also form at moderate pressure by the reaction: olivine and plagioclase = garnet (Craig, 1982). In the Adirondack meta-igneous rocks, garnet generally crystallized by replacement of an alumina-rich phases such as plagioclase or symplectites of clinopyroxene-spinel (Whitney and McLelland, 1973, McLelland and Whitney, 1980).

The analysis of a garnet porphyroblast in leuco gabbro is listed in Table 8I (p.107). The single crystal that was analyzed is homogeneous. The average

composition (ten points, from core to rim within a single crystal) is almandine (61), pyrope (20), spessartine (4), grossularite (10) and andradite (4 percent).

Chapter VI

GRAVITY SURVEY

Introduction

A gravity survey across the Chenaux gabbro and part of the marbles was conducted in order to supplement the observed field relationships between these two rock types. The survey, which takes advantage of the strong contrast in density between the gabbro and surrounding rocks, was aimed to delineate the gabbro boundary, but most importantly to aid in evaluating the attitude of the contacts in the subsurface, and to allow an estimate to be made of the depth of the body.

Two traverses in a northwest-southeast direction and about 3.5 km apart were chosen across the marbles and gabbroic body. One traverse follows Highway 17, the other follows parallel secondary roads. A total of 100 gravity stations were established along the two profiles. Additional anomaly values were obtained from the Geological Survey of Canada, Geophysical Data Center. Measurements were taken at 500-meter intervals using a standard model Worden gravimeter No. W807, which has sensitivity of 0.3 milligals per scale division. Elevations were determined with two altimeters, and drift corrections were made by reoccupancy of a base station each hour. Dry and wet bulb temperatures were also recorded. All stations were tied to gravity station 9468-64 at the Renfrew Police Station, which is part of the Canadian gravity standardization network. Simple Bouguer anomalies

were calculated using an IBM-compatible Fortran version of a gravity reduction program, at the Geophysics Division, Geological Survey of Canada.

Seventy-four representative samples of fresh rock were selected within the gabbro and the host rocks for density measurement (Table 9).

TABLE 9. SUMMARY OF ROCK DENSITIES

	Gabbro - Amphibolite	Country rocks (excluding biotite-hornblende-garnet gneiss)
Average	3.023	2.699
Range	2.855 - 3.300	2.602 - 2.770
Standard Deviation	0.1636	0.0557
Number of Samples	54	20

Results and Interpretations

The simple Bouguer gravity anomaly contour map with the gabbroic body superimposed is produced at a scale of 1:34,400 (Fig. 25). The gabbro body shows a considerable mass excess in comparison with the marble host rocks and the strongest positive gravity anomaly is located on the central part of the pluton. Gravity values decrease toward the margins of the gabbro. The decrease towards the contact from the central gravity high of -8 mgal ranged from -26 mgal on the west to about -18 mgal on the eastern contact. The configuration of the anomaly

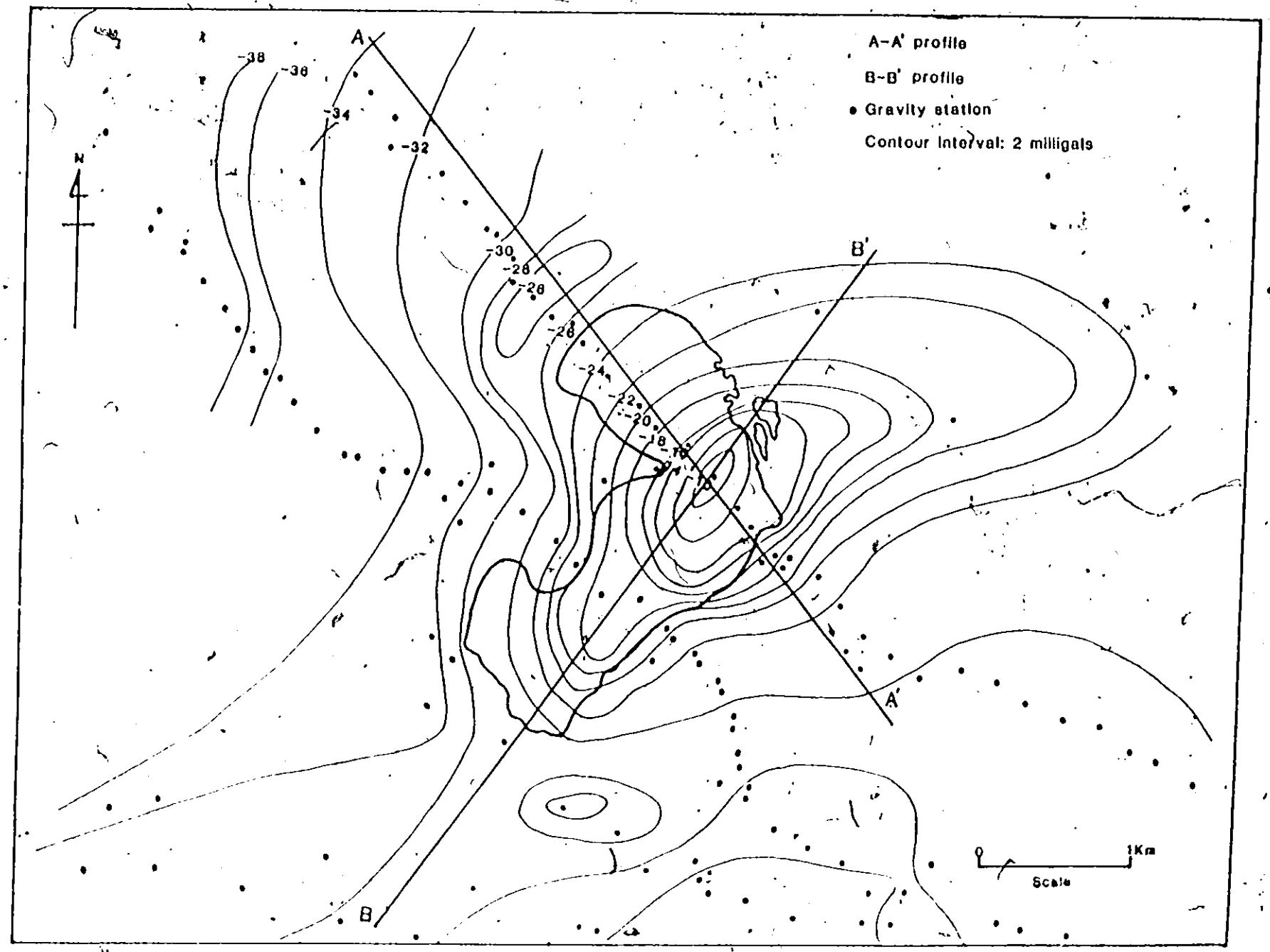

Fig.25. Simple Bouguer anomaly over the Chenaux gabbro

is largely conformable with the gabbro contact towards NW and SE, but on the NE the isogal contours initially follow the gabbro outline, but away from the contact toward Quebec, the gradient becomes less steep. Relationships in the southern part of the pluton, where the gabbro is in contact with amphibolite, are not clear due to similar densities of the two rock types.

Gravity models were done along two profile lines (A-A' and B-B'; Fig. 26a and 26b) using Margrav 2 modelling program (Broome, 1986). The aim of the modelling is to evaluate quantitatively the depth and the general form of the pluton beneath the surface.

Observed Bouguer values from the gravity map were plotted along A-A' in Fig. 26a and B-B' in Fig. 26b. The small regional gradient in both profiles was removed by keeping the center of the body constant, at the intersection of the two profiles. The regional gradient is not related to near-surface bodies such as the Chenaux pluton, but rather is controlled by large features deep in the crust. The corrected values from each profile together with the geological constraints such as the position and nature of the contact, and density contrasts between the two rock units were used in constructing the model. Figures 26a and 26b show reasonably close fits of observed and calculated anomalies along A-A' and B-B', respectively. The possibility of getting a different result if a higher density is assigned to the gabbro cannot be ruled out. However, the mushroom-like form will persist even though the depth of the model would decrease.

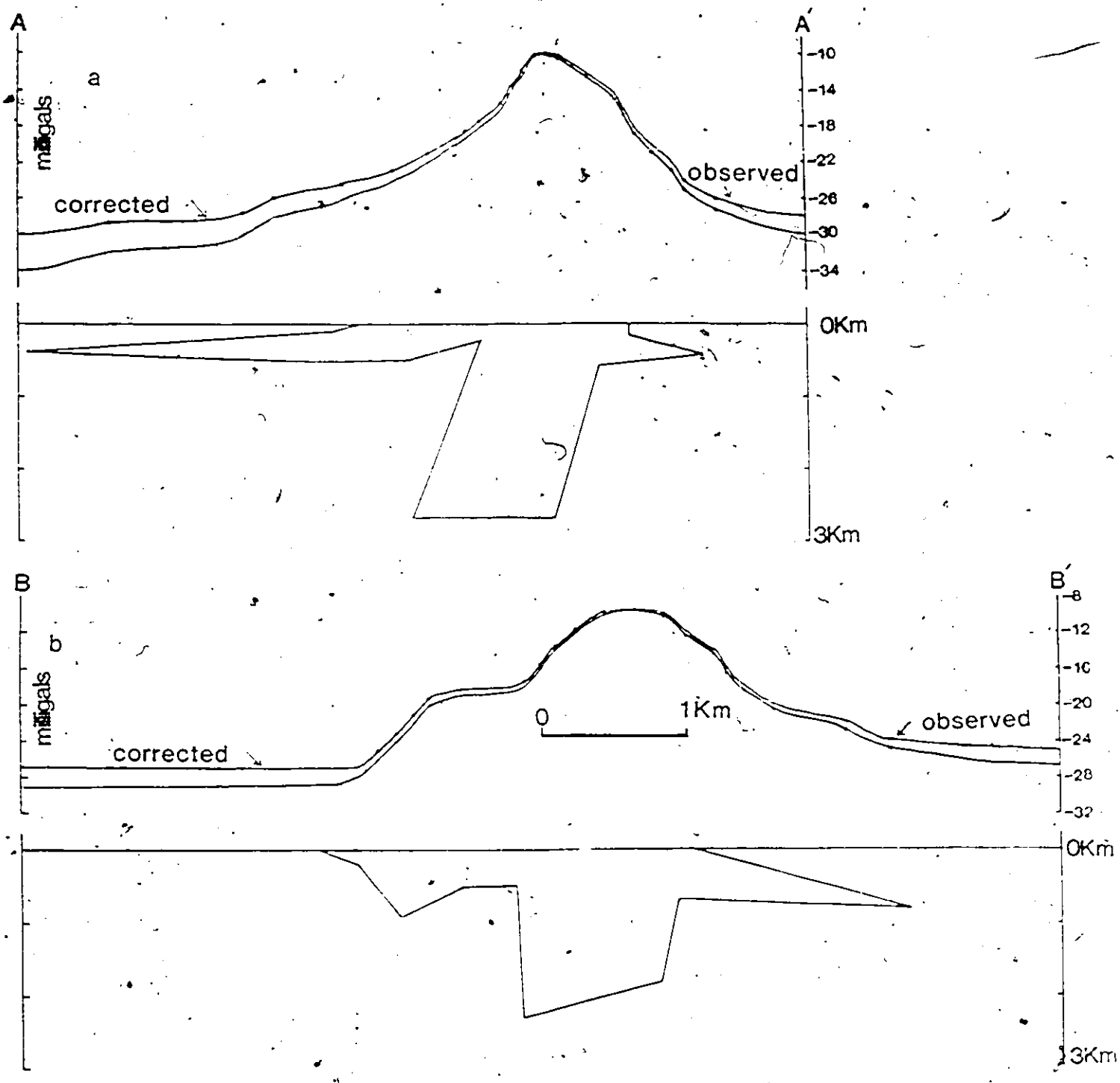

Fig. 26a. Gravity profile and model along traverse A-A'
Fig. 26b. Gravity profile and model along traverse B-B'
Dots are calculated gravity.

According to Figure 26a, the main body is plug-like and inclined steeply toward the northwest. Moreover, the body shows an asymmetrical mushroom-like cross section, in which the western part spreads laterally about 3 km beneath the marble. The maximum depth in this model is 2.7 km. The NE - SW profile, shown in Fig. 26b, further attests to the mushrooming pattern of the body spreading laterally on both sides of the central mass. Here also the maximum depth is the same with that observed along the A-A' profile. The strong positive gravity anomaly at the centre of the body could be explained by a high density core of ultramafic rocks at depth in the Chenaux gabbro. Surface geology, however, offers no evidence to support the existence of such an ultramafic body.

The highest gravity anomaly was measured on the east central part of the body that coincides with the abundance of olivine gabbros. The anomally declines from -8 mgal on the center to -26 mgal toward the western portion of the pluton. Based on these facts, it is porposed that the gabbroic melt, when it arrived at the present level of exposure, through its vertical feeder, precipitated olivine, which was partially removed by gravity settling. Later, the residual melt enriched in Ca, Al and total alkalies migrated westward and continued to differentiate during lateral flow.

In summary, gravity data across the Chenaux gabbro yield a distinct positive anomaly. The gabbro is mushroom-like and is inclined steeply toward the

northwest. This assymmetric mushroom-like gabbroic mass dips outward and spreads laterally beneath the host marble; the lateral spread is prominent toward the west. The maximum depth of the Chenaux pluton is approximately 2.7 km below the surface.

Chapter VII

STRUCTURAL GEOLOGY

All rock types of the area have undergone episodes of deformation which have produced foliations, folds and shear zones. Generally, the rocks are characterized by northerly trending structures which were produced as a result of the Grenvillian Orogeny. There are some indications as to the polyphase and also non-uniform nature of the deformation.

In the marbles, mineral foliation is mostly parallel to the compositional layering. Layering and mineral aggregate foliations trend northwesterly around the western part of the pluton swinging to the northeast, east of the pluton. This deviation is attributed to folding related with the intrusive activity. Dip of foliation ranges from 30 to 70° and dip direction is invariably easterly.

Contacts are characterized by small to large scale disharmonic folds oriented in various directions. In places, contacts are also marked by mylonite or protomylonitic rocks of either the marble or both the marble and the gabbro. Mylonitized gabbro locally grades to a brecciated variety indicating ductile/brittle deformations in contact zones. A sheared contact is well exposed below Chenaux Dam. Here, within the sheared zone, there is a continuous outcrop of pegmatoidal hornblende-rich rock. Within the marbles, isolated north trending anastomosing shears one centimeter to three meters wide occur. These shears have abrupt

boundaries and are marked by aligned micas. A folded and detached gabbro dyke is seen within a few meters of the contact. The fold is isoclinal and has a northwest trending axis, plunging at a moderate angle.

Gneissosity and mineral aggregate foliation in the gneisses are generally oriented in a northeasterly direction. Dip of foliation ranges from shallow to moderate and dip directions are to the southeast and northwest. Granitic gneisses bear the imprint of a greater amount of strain and locally they show highly stretched and detached layers. In places, five to ten metre-wide high strain zones form protomylonitic layers with abundant porphyroblasts of K-feldspar. Biotite-muscovite gneiss shows at least two generations of folds. F_1 folds are isoclinal and have a northwest or northeast trend with a plunge angle ranging from horizontal to about 5°. The axial planes of the folds dip toward the northwest. F_2 folds developed as recumbent folds with near-horizontal axial planes. Lineations are rather shallow, plunging typically to the north-northeast.

In the gabbro, deformation is highly variable; in places, it looks massive, elsewhere it shows good tectonic foliation or layering. Small-scale isolated thin shears occur within the body.

The northeastern part of the gabbro is marked by a zone of intensely sheared rocks which have strong planar fabric. Mylonitic foliation runs submeridionally being inclined vertical to moderately to the east and to the west.

Porphyroclasts of plagioclase and recrystallized calcic pyroxene show distinct sigmoidal asymmetry with "tail" of finer material on both sides of the tail. Due to the poor exposure of a foliation surface with a well defined lineation, stretching direction has not been confirmed with a reliable degree of certainty. This part of the pluton also contains the maximum concentrations of quartz veins formed by the filling of tension fractures.

Ductile deformation is also noted in one of the aplite dykes intruding the gabbro. The dyke is sheared together with the host gabbro and transformed to mylonite or ultramylonite. Mylonite foliation trends northwesterly and dips moderately southwest, with down-dip lineation. The foliation is defined by alternating very fine grained layers with quartz-rich ribbons. The quartz grains in these quartz ribbons are aligned at an angle to the fine grained layer indicating a C-S fabric. The shear fabric in this dyke suggests a northeasterly movement direction. The time of the ductile deformation is not documented.

Another prominent geological feature of the region is a series of northwest trending linear features crossing all the rock units that are evidently faults. Muskrat fault traverses the central part of the gabbro, along Colingham and Catherine lakes, and divides the body into two blocks (Fig. 2). Topographically the southern block is evidently downthrown. Steep escarpments exist on the flanks of Colingham and Catherine lakes which presumably rest upon fault breccia and gouge. These faults are part of the Ottawa rift structure (Lumbers, 1982).

Chapter VIII

METAMORPHISM

The marbles and gneisses, which host the gabbro, contain metamorphic mineral assemblages indicative of middle amphibolite facies.

Marbles at the lowest grade observed contain tremolite and diopside, but closer to the contact zone they locally contain forsterite; wollastonite or brucite were not found.

The mafic gneiss units are composed primarily of plagioclase and green hornblende with subordinate biotite, garnet, quartz and iron oxide. Granitic gneisses are mainly biotite-bearing; locally they contain sillimanite. Pelitic gneisses on the east contain muscovite, biotite, plagioclase, K-feldspar, quartz and local garnet, intimating middle amphibolite facies.

The metamorphic effect on the gabbroic assemblage is largely confined to partial or complete recrystallization of plagioclase, calcic pyroxene, orthopyroxene and more importantly the development of reaction rims and zones about crystals of olivine, pyroxene and Fe-Ti oxides in most of the units.

The pluton shows diverse mineral assemblages and textures and is situated above the garnet isograd and below sillimanite-K-feldspar isograd. Textures range from relict igneous subophitic to crystalloblastic varieties, with intermediate stages being locally preserved. The difference in the degree of recrystallization

appears to depend on the availability of water rather than temperature, because gabbroic specimens with contrasting textures and mineralogy are intimately associated in the field; all types are intermingled within a limited area.

Primary plagioclase in the gabbros occurs as coarse and often twinned crystals. Recrystallized plagioclase developed clear edges (free of inclusions) against adjacent plagioclase, and in the advanced stage of recrystallization they form untwinned granoblastic crystals.

The various microstructures in the gabbros represent the partial readjustment of the igneous assemblages that were unstable during subsequent pressure-temperature conditions. Thin section observations suggest that these microstructures formed by isochemical metamorphic recrystallization in the solid state promoted by diffusion of H_2O to the reaction sites. Moreover, through mass balance calculations of the reactant and product phases, it was possible to define the chemical changes related to a series of metamorphic reactions, to be described below. Generally, the crystallization of hornblende in these rocks required the accession of iron and magnesium from olivine and pyroxenes and calcium, aluminum and silicon from plagioclase.

Thus, amphibolization in gabbro is marked by the internal replacement of both primary and seconday pyroxenes by hornblende, with an introduction of considerable amounts of H_2O. Temporal relationships between the reaction

microstructures developed about olivine, pyroxenes and Fe-Ti oxides and the onset of amphibolitization has not been resolved. However, the late-stage olivine-free gabbros exhibit no reaction microstructures but frequently show heavy amphibolitization.

Figure 27 gives a general estimate of the pressure and temperature conditions of the various equilibrium assemblages in the study area. The postulated path represents prograde metamorphism. The postulated sequence of events with regard to the Chenaux gabbro is shallow intrusion, cooling and consolidation, and burial to the maximum pressure-temperature conditions. The olivine-plagioclase reaction microstructures indicate that the assemblages passed through the pyroxene-spinel field. If garnet was formed by recrystalliztion of primary igneous minerals, the path can be extended to the garnet-calcic pyroxene field.

The gabbro body was emplaced into regionally deformed and metamorphosed Grenville Supergroup rocks that were deposited in the interval 1.3 to 1.2 Ga (1980), Moore and Thompson. Field mapping demonstrates that the intrusion was emplaced before the onset or at least at the earlier stage of a deformation that prevailed before peak metamorphism. Since regional metamorphism appears to postdate the most intense deformation, it is likely that the reaction microstructures have formed during a prograde regional metamorphism, along a path shown in Fig. 27.

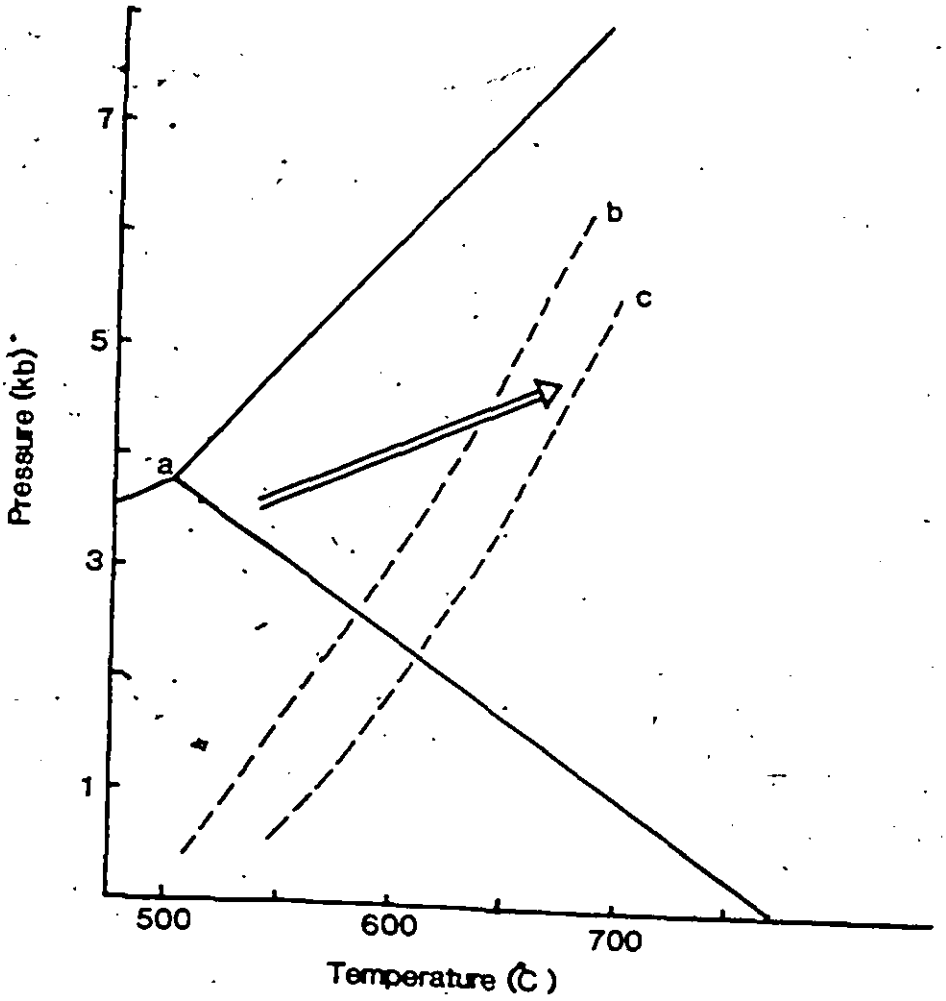

Fig. 27. Temperature-pressure diagram showing a possible path of increasing metamorphic grade.

a - aluminosilicate triple point (Hodges et al. 1982).
b - tremolite + dolomite = forsterite + calcite (Metz, 1976).
c - muscovite + quartz = K-feldspar + aluminosilicate (Kerrick, 1972).

Mineral Reactions

The metamorphic effect on the pre-existing gabbroic assemblages is largely confined to partial or complete recrystallization of plagioclase, clinopyroxene and orthopyroxene and more prominently to the development of reaction zones and rims about crystals of olivine, pyroxene and Fe-Ti oxides.

Spectacular reaction microstructures are commonly developed in the various gabbroic units as a result of near-isochemical metamorphic reaction in the solid state, promoted by diffusion of H_2O and possibly other constituents to the reaction sites. Such microstructures can help in understanding the compositional changes related to metamorphic reactions and also provide clues as to the origin of component ions in the newly developed minerals; whether they are extracted from the pre-existing igneous minerals or introduced from elsewhere to the reaction site.

Reactions between olivine and plagioclase, pyroxenes and plagioclase, and Fe-Ti oxides and plagioclase, produced microstructures in mafic and ultramafic rocks similar to those described by Stormer (1969), Griffin (1973), Emslie (1983), Davidson and Grant (1986), Kretz (1989) and others. Theories on the origin of such microstructures can be reduced to two categories. The first theory (Mason, 1967 and Griffin and Heier, 1973), assumes intrusion at depth followed by subsolidus reaction of olivine, pyroxene and Fe-Ti oxide minerals with

plagioclase (and perhaps interstitial fluid) during cooling from magmatic temperature to ambient metamorphic temperature at high pressure. The second theory which has been more favoured (Frodesen, 1968, Stormer, 1969, Whitney and McLelland, 1973) assumes high level intrusion, burial by tectonic stacking and metamorphism after consolidation with partial or complete readjustment of the igneous assemblages during subsequent elevation of temperature and pressure conditions.

Regarding the origin of the various reaction microstructures in the Chenaux gabbro, prograde regional amphibolite facies metamorphism, shortly after or perhaps contemporaneous with the final stage of the intrusion is here favoured, based on petrographic and microprobe data. Introduced water is a very important factor during the recrystallization, since basic rocks contain very little water, insufficient for most metamorphic reactions to take place (Reynolds and Frederickson, 1962). The varying amount of water supplied during metamorphism had a strong effect on which of the processes took place, either the development of reaction microstructures on a small scale or amphibolitization on a larger scale.

Depending on the amount of water supplied during metamorphism, the reactions stopped at different stages. For example, in olivine microstructures, olivine at places is completely rimmed; elsewhere, reaction zones just started to form with incomplete or totally without hornblende. Such variability in the

development of hornblende certainly reflects a slow and variable supply of water. It is also possible to follow step by step the metamorphism from the reaction-microstructure-forming stage in olivine gabbros through the stages where the replacement of calcic pyroxene is gradually increasing in pyroxene gabbros.

Olivine-Plagioclase Microstructures

Reaction microstructure related to olivine is very common and occurs between texturally igneous olivine and plagioclase. The reaction zone may consist of narrow, double and sometimes triple silicate layers separating olivine from plagioclase (Fig. 28). Typically it consists of corroded olivine surrounded by a continuous rim of colorless to pale brown hypersthene, which is in turn partially or wholly rimmed by a fine intergrowth of radially-oriented brown to colorless hornblende or a fine intergrowth of hornblende and spinel. The central olivine sometimes decreases in size, and in places the olivine core completely disappears, as a result of inward growth of hypersthene to replace the core. A reaction relationship between olivine and calcic pyroxene is not observed.

In the Chenaux gabbro, garnet was not produced by the metamorphic reaction between plagioclase and olivine. Experimental work of Green and Hibberson (1970) indicates that the absence of garnet within such reaction zones depends on the initial composition of olivine. According to the experiments,

Fig. 28. Olivine - plagioclase microstructure. The inner rim (about olivine) consists of orthopyroxene, and the outer rim of a hornblende-spinel intergrowth.

sufficiently fayalitic olivine is required to develop garnet directly from plagioclase and olivine with increasing pressure prior to the formation of pyroxene and spinel.

In the Adirondack metagabbros, however, the pyroxene-spinel stability field has not been eliminated for olivine composition up to about 45% Fa at least, (Whitney and McLelland, 1973). The composition of olivine in the Chenaux olivine gabbro is more magnesian, ranging from Fa_{22} - Fa_{26}, not sufficiently fayalitic to favour the development of garnet around olivine microstructures.

Pyroxene-Plagioclase Microstructures

This microstructure includes both calcic pyroxene and orthopyroxene as cores, followed outward by a continuous rim of green hornblende (Fig. 29). The typical variety consists of central calcic pyroxene followed by colorless orthopyroxene and an outermost, wider hornblende rim. Rarely, the hornblende rim consists of an actinolite-cummingtonite admixture, together with individual flakes of brown biotite and occasional garnet crystals. It is not clear whether the garnet is a product of the pyroxene -----> amphibole reaction.

Textural evidence indicates that garnets in these rocks occurs in at least two different modes. Firstly, it occurs as crudely defined outermost reaction rims around pyroxene-hornblende reaction zones being continuous with and broadly

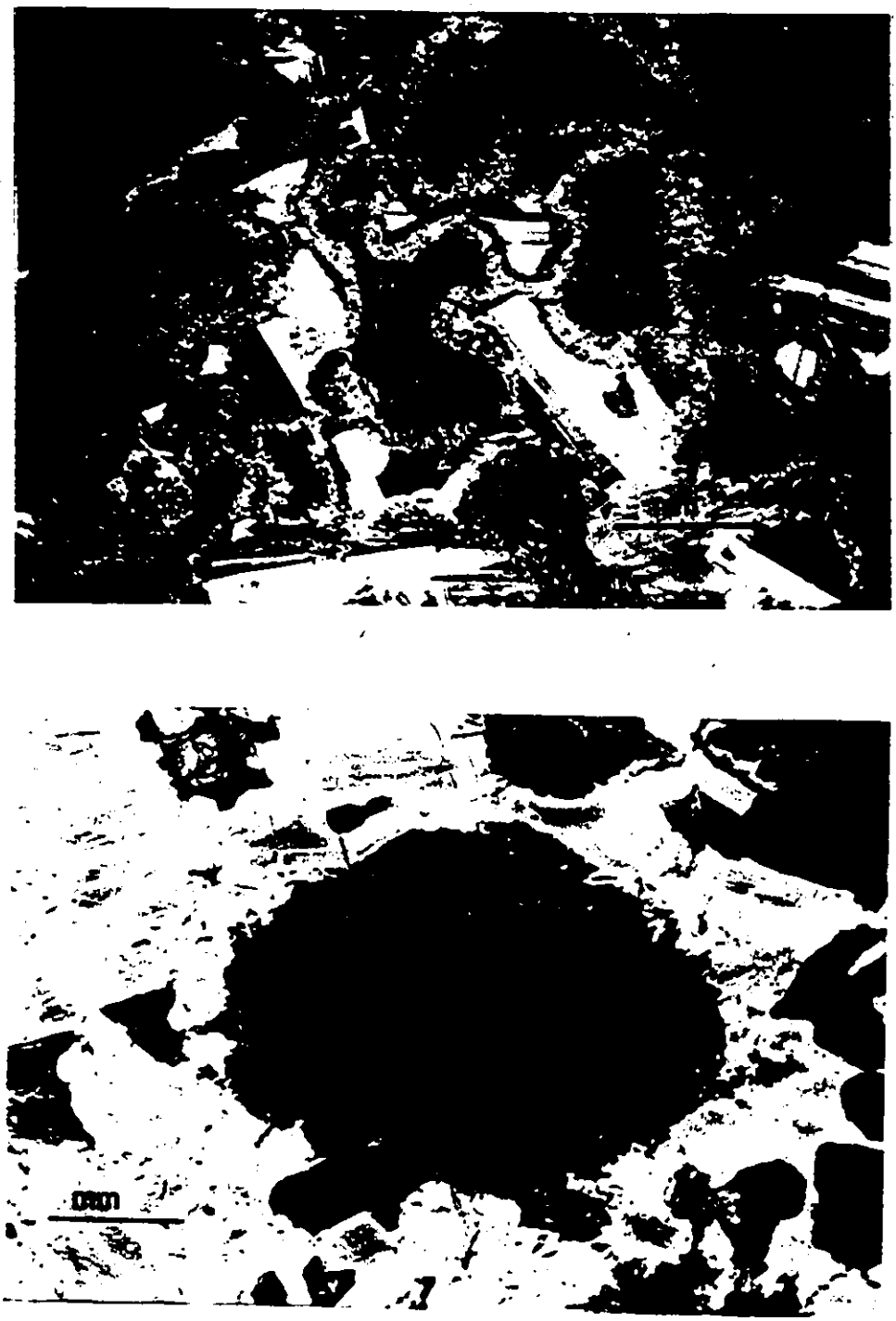

Fig. 29. Pyroxene-plagioclase microstructure.

synchronous with the reaction microstructures. Secondly, it occurs as fine clusters at plagioclase-pyroxene interfaces, and sometimes as very coarse prophyroblastic or xenoblastic crystals completely surrounded by plagioclase. Kretz (1989) proposed a reaction assuming an initial olivine as a primary source of Fe and Mg (supposedly consumed at the earlier stage) to react with plagioclase (mainly the anorthite component) to hornblende and garnet:

$$\text{Olivine} + \text{Ab} + \text{An} + \text{Or} + H_2O \text{ -----> } \text{Hornblende} + \text{Garnet}$$

<u>Fe-Ti Oxide-Plagioclase Microstructure</u>

These microstructures consist of an oxide core surrounded by green hornblende (Fig. 30). Occasional flakes of red brown biotite occur in close proximity to the oxide phase. Garnet is not present. The central oxide is commonly magnetite, sometimes with ilmenite. The hornblende is green aluminous hornblende with a similar composition to that described above. It deeply embays the surrounding phases, usually plagioclase and occasionally orthopyroxene. Where the hornblende replaces plagioclase, fine green spinel crystals are developed as radiating intergrowths on the outer rim. These hornblendes can be distinguished from the discrete hornblende crystals by their aluminous nature and high TiO_2 content (Chapter V).

Fig. 30. Fe-Ti oxide-plagioclase microstructure.

Fe-Ti oxides and plagioclase cannot by themselves give the appropriate hornblende composition observed in these rocks. This is particularly apparent for hornblende developed around Fe-Ti oxide cores that originally existed as isolated interstitial grains between plagioclase laths. This textural evidence calls for additional components, notably Mg, to be introduced from the local environment to the reaction site. Mg was possibly derived from nearby orthopyroxene. The interface between the Fe-Ti oxide and the surrounding hornblende rim is in most cases irregular, implying that the iron oxide was consumed and provided the Fe required for the production of hornblende.

Mass Balance Calculation

Table 10 shows analyses of olivine, orthopyroxene, hornblende + spinel and plagioclase obtained at one site in the olivine-plagioclase microstructure.

Olivine is unzoned, orthopyroxene is slightly aluminous and the hornblende analysis shows high Al due to the presence of intergrown spinel. Plagioclase is slightly zoned. A single plagioclase crystal adjacent to the reaction zone shows An_{74}, with anorthite content increasing to An_{77} toward the core. A small increase in MgO/(MgO + FeO) ratio from olivine (0.65) across orthopyroxene (0.70) to hornblende + spinel (0.72) is indicated. The hornblende-spinel ratio is in the order of 5:1.

Table 10 Microprobe Analyses of the Minerals in an Olivine-Plagioclase Microstructure

	Olivine	Orthopyroxene	Hornblende + Spinel	Plagioclase
FeO	21.7	14.0	8.5	0.26
MnO	0.27	0.28	0.11	0.02
Na_2O	0.02	0.01	2.2	2.88
SiO_2	38.3	55.3	40.1	49.9
F	0.02	0.12	0.05	0.02
Al_2O_3	0.02	1.0	19.1	31.4
MgO	39.9	28.8	15.7	0.41
K_2O	0.01	0.02	0.32	0.05
CaO	0.02	0.21	11.0	14.8
TiO_2	0.0	0.06	0.84	0.01
Sum	100.26	99.80	98.02	99.75

*All Fe expressed as FeO.

Based on these analyses, a balanced equation is obtained by assuming both fayalite and forsterite, and anorthite and albite components to have participated in the reaction separately, to form hornblende + spinel and orthopyroxene. The presumed reaction is:

$$a(Mg_2\,SiO_4) + b(Fe_2\,SiO_4) + c(CaAl_2\,Si_2O_8) + d(Na\,Al\,Si_3O_8) =$$

1.0(hornblende + spinel) + f(orthopyroxene)

	Forsterite	Fayalite	Anorthite	Albite	Hornblende + Spinel	Orthopyroxene	
	a	b	c	d	1.0	f	
Na				d	0.59		(1)
Ca			c		1.63		(2)
Mg	2a				3.24	0.77f	(3)
Fe		2b			0.99	0.21f	(4)
Al			2c	d	3.11	0.02f ≈ 0	(5)
Si	a	b	2c	3d	5.56	0.99f	(6)

Na: d = 0.59

Ca: c = 1.63

Mg: 2a = 3.24 + 0.77f

a = 1.62 + 0.34f

Fe: 2b = 0.99 + 0.21f

b = 0.50 + 0.10f

Al: 2c + d = 3.11

3.8 ~ 3.1

Si: a + b + 2c + 3d = 5.56 + 0.99f

1.62 + 0.34f + 0.50 + 0.10f + 3.2 + 1.7 = 5.56 + 0.99f

f = 2.65

Mg: a = 1.62 + 0.34f

a = 2.5

Fe: b = 0.5 + .10f

b = 0.76

Check:

	Reactant	Product
Na	0.59	0.59
Ca	1.63	1.63
Mg	5.0	4.6
Fe	1.5	1.4
Al	3.8	3.1
Si	7.9	7.3

The nearly-balanced equation is:

$$2.5\ Mg_2SiO_4 + 0.67\ Fe_2SiO_4 + 1.63\ CaAl_2Si_2O_3 + 0.59\ NaAlSi_3O_3$$

olivine Fo_{77} An_{73}

$$+ [H_2O, Ti, K, F ---]$$

$$= 1.0\ Ca_{1.63}Na_{0.59}Mg_{3.24}Fe_{0.99}Al_{3.11}Si_{5.56}O_{22}(OH)_2 +$$

(hornblende + spinel)

$$1.75\ Mg_{0.77}Fe_{0.21}Al_{0.02}Si_{0.99}O_3$$

orthopyroxene

The equation evidently indicates that Mg and Fe from olivine entered orthopyroxene, hornblende and spinel and Ca, Na and Al from plagioclase entered hornblende. Water does not appear in the reactants, and migrated to the reaction sites. H_2O was possibly necessary to facilitate the diffusion of the elements and for the production of hornblende.

Components such as K, Ti and F which do not appear in the reactant phases were certainly introduced to the reaction site from the nearby minerals or from beyond the reaction site by diffusion. K was possibly derived from contained biotite and perhaps from the minor orthoclase component of the plagioclase. Ti was apparently derived from the invariably present Fe-Ti oxide minerals and F from beyond the reaction zone perhaps as part of the fluid phase.

Kretz (1989) argued against the presence of an intergranular fluid at the reaction sites prior to the metamorphic recrystallization and supported the idea of diffusion of H, K, Ti, etc. to the reaction site from the nearby environs or from elsewhere. In the same work, it was also indicated that the various possible species of the H phases to be either H_2O, H_3O+, OH or HF. The view of an introduced fluid phase is in line with the various textural evidence observed in the olivine-gabbros. In these rocks, at places olivine is completely reacted; elsewhere, reaction zones have just started to form with incomplete or totally without hornblende rims. Such inconsistency in the development of hornblende reflects variation in the relative ease in the mobility of constituent ions, and more importantly the diffusion rate of H species either from the local environment or from elsewhere to the reaction site.

Chapter IX

SUMMARY AND CONCLUSIONS

Several late to post-metamorphic gabbro plutons occur in a belt trending northeasterly along the boundary zone of the Central Metasedimentary Belt and Central Gneiss Belt of the Grenville Province.

The Chenaux gabbro intrusion is part of a chain of mafic plutons along the western margin of the Central Metasedimentary Belt. The pluton has an elbow-like shape, dominated by four rock types and intruded into marbles and gneisses of the Grenville Supergroup.

On the evidence of field data and gravity measurements, the intrusion appears to be a plug-like body with steeply dipping contacts that may converge inward at relatively shallow depth; the pluton may extend only 2.7 km into the subsurface.

The intrusion represents a single differentiated body or a cyclic unit in a larger poorly exposed intrusion consisting of olivine gabbro, leuco gabbro, pyroxene gabbro and hornblende gabbro. This succession possibly represents advancing stages of crystal fractionation and differentiation of a parent magma.

The rocks principally consist of plagioclase, olivine, augite, orthopyroxene, hornblende and Fe-Ti oxides and exhibit textures that range from relict igneous varieties to crystalloblastic types that appear to represent equilibrium assemblages.

The common occurrences of plagioclase-augite-olivine and plagioclase-orthopyroxene-augite orthocumulates suggest the crystallization sequence of olivine, plagioclase, augite and orthopyroxene from parent tholeiitic magma.

Compositional variation of phases is small, with progressive change in the Mg/(Mg + Fe) ratio of coexisting ferromagnesian minerals and with plagioclase varying from An_{76} to An_{57}.

It was not possible to determine the initial liquid composition, due to the absence of recognizable chilled border rocks or layered sequences that would reflect the liquid path of crystallization. In the MgO - CaO - Al_2O_3 diagram (Fig. 15), the rocks form a cluster away from Mg-rich peridotitic composition, and represent relatively evolved melts which had some history of fractional crystallization and differentiation before emplacement. The Al_2O_3 and CaO enrichment also indicates that calcic pyroxene and plagioclase as the two main phases that controlled the differentiation.

The lack of hydrous phases and the early precipitation of Fe-Ti oxide minerals indicate crystallization under conditions of low water pressure and relatively high oxygen fugacity. A quantitative statement as to the initial oxygen fugacity was not possible to determine due to a very low concentration of ulvospinel in the magnetite. Due to the presence of magnetite and absence of quartz in

forsterite-bearing rocks, it is reasonable to place the level of $f(O_2)$ above the magnetite-fayalite buffer.

The areal distribution of MgO and total alkalies (Fig. 17) and the distribution of olivine within the pluton (used as differentiation indices) suggest that fractional crystallization has proceeded from the interior outwards to the western margin of the pluton. This interpretation is supported by the finding that the highest gravity anomaly coincides with the greatest olivine abundance, in the central part of the pluton, declining continuously toward the west.

Layering ascribed to a primary igneous origin has been observed in a few localities; generally it is very rare. More common are patchy segregations of markedly different grain size and/or different phases. The implication of this lack of layering is that convection was either very slow or not periodic during igneous cooling.

The northeastern part of the pluton is marked by a zone of mylonite. Near this sheared boundary, the gabbros are mostly recrystallized to amphibolite and contain abundant quartz vein boudins. The shear fabric in an aplite dyke which intrudes the gabbro suggests a northeasterly movement direction of the upper block.

The shearing, even though mainly restricted to a contact zone, is unlikely to have been induced during emplacement of the gabbro melt. More likely it took place in a continuous high-strain zone that bounds the mafic plutonic belt against

adjacent lithotectonic domains or subdomains within the Central Metasedimentary Belt.

The age of the ductile deformation and also the age of the gabbro pluton are not known. Since the aplite dykes which intrude the gabbro have been affected by the shearing, the time of the ductile deformation is certainly later than gabbro intrusion and possibly synchronous with pegmatite emplacement. Since the Chenaux intrusion is emplaced into country rocks of Middle Proterozoic age (Lumbers, 1982), constraint is placed on its lower age limit at 1.3 Ga.

No distinct contact aureole is present in the marbles as would be expected as a result of high temperature of the intrusion. The absence of contact index minerals in the marbles partly indicates that the temperature of the intrusion was not high enough to crystallize minerals like periclase or wollastonite which indicate higher temperature conditions. In one thin section, calcite and quartz are present together. This information indicates low temperature, probably tectonic emplacement, but may also reflect lack of suitable reactants in wallrock and/or lack of fluid ingress from the pluton.

The pyroxene geothermometer indicates a temperature of equilibration of the pluton at about 820°C. This fact is in agreement with the contention of low temperature conditions during emplacement and the general absence of contact metamorphic minerals in the marble. It appears that topographically lower portions of the pluton have crystallized under higher temperature conditions

relative to the more differentiated roof rocks; this is possibly the result of crystal settling and water migration to the top of the chamber, lowering the liquidus temperatures in the more evolved upper portion. The presence of abundant marble xenoliths around Storyland and Highway 17 indicates that the presently exposed part of the pluton is the apical part which is barely unroofed by erosion.

Metamorphism in these rocks involved a series of hydration reactions, forming mineral assemblages characteristic of lower temperatures than those of the parent, allowing hornblende and epidote to develop at the expense of pyroxenes and olivines, and the crystallization of more sodic plagioclase. Textures range from relict igneous subophitic to crystalloblastic. Some of the gabbro specimens are completely recrystallized to amphibolite, while others preserve relict igneous textures and have mineral assemblages nearly identical to unmetamorphosed gabbro. Such textural and mineralogical variations appear to result not so much from local variations of temperature and pressure, but on diverse ingress of water during metamorphism.

Spectacular reaction microstructures between olivine and plagioclase, pyroxenes and plagioclase, and Fe-Ti oxide and plagioclase are commonly developed in olivine and pyroxene gabbros as a result of near-isochemical metamorphic reaction in the solid state, promoted by diffusion of H_2O and possibly other constituents to the reaction sites. Such microstructures can help in

understanding the compositional changes related to metamorphic reactions and also provide clues as to the origin of component ions in the newly developed minerals; whether they are extracted from the pre-existing igneous minerals or introduced from elsewhere to the reaction site.

A satisfactorily balanced reaction equation for the olivine microstructures is obtained through mass balance calculations. The equation shows the rearrangement of atoms or ions during metamorphism and also identifies elements (F, K, Ti...) which migrated to the reaction sites. A two way diffusion across the original interface between olivine and plagioclase is indicated; the diffusion of iron and magnesium to the plagioclase, and silicon with a little aluminum and calcium to the olivine, explains the chemical composition of the microstructures. The formation of amphibole from plagioclase indicates that water must be introduced from elsewhere to the reaction site, apparently carrying with it certain elements such as Cl, F, K and Ti.

Prograde regional amphibolite facies metamorphic, shortly after or perhaps contemporaneous with the final stage of the intrusion is here favoured, for the origin of the various reaction microstructures in the Chenaux gabbro.

Scapolite is common in various regional metamorphic settings and since the Ca-rich scapolite of the study area is closely related with the amphibolitized rocks; scapolitization of plagioclase is considered to be related temporally to the regional metamorphism that affected the region.

The association of the Chenaux gabbro with granitoids and amphibolites is used to assess the nature of the magma source and the tectonic environment in which the rocks were formed.

The amphibolites on the AFM composition diagram follow a tholeiitic trend of differentiation. The gabbros show a calc-alkaline trend which coincides also with the composition of non-cumulate arc gabbros and diorites. The chemical composition of the amphibolites is best accounted for by an oceanic or marginal basin environment.

REFERENCES

Allen, J.C., Boettcher, A.L. and Marland, G. 1975.
Amphiboles in Andesite and Basalt: Stability as a Function of P-T-f(O_2), American Mineralogist, Volume 60, pages 1064-1085.

Baer, A.J., Poole, W.H., and Sanford, B.V., 1977.
Riviére Gatineau: Geological Survey of Canada Map 1334A.

Beard, J.S., 1986.
Characteristic Mineralogy of Arc-Related Cumulate Gabbros: Implications for the Tectonic Setting of Gabbroic Plutons and for Andesite Geneses. Geology Volume 14, pages 848-851.

Britton, J.M., 1979.
Late-Tectonic Syenite and Granite Plutons of the Grenville Province of Southwest Quebec and Southeast Ontario, In Current Research, Part B: GSC paper 79-1B, pages 163-166.

Broome, J., 1986.
An Interactive Magnetics and Gravity Modelling Programme for IBM-Compatible Microcomputers, Magrav 2. GSC open file 1334.

Buddington, A.F., and Lindsley, D.H., 1964.
Iron-Titanium Oxide Minerals and Synthetic Equivalents. Journal of Petrology, 5, pages 310-57.

Craig, A.J. and Essene, E.J., 1982.
The Formation of Garnet in Olivine-Bearing Metagabbros from the Adirondacks, Contributions to Mineralogy and Petrology 81, pages 240-251.

Davidson, A. and Grant, S.M., 1986.
Reconnaissance Geology of Western and Cental Algonquin Park and Detailed Study of Coronitic Olivine Metagabbro, Central Gneiss Belt, Grenville Province of Ontario; in Current Research, Part B, Geological Survey of Canada, paper 86-1B, pages 837-48.

Davidson, A., 1986.
New Interpretations in the Southwestern Grenville Province - in the Grenville Province, ed. by J.M. Moore, A. Davidson and A.J. Baer, Geological Association of Canada, Special Paper 31, pages 59-74.

Deer, W.A., Howie, R.A., and Zussman, J., 1966.
An Introduction to the Rock Forming Minerals, Longman's, London.

DeJongh, W.K., 1975.
Table of Influence Coefficients. Unpublished Report for Philip's Application Laboratory, Endhoven, Holland.

Easton, R.M., 1986.
Geochemistry of the Grenville Province, In the Grenville Province, Edited by J.M. Moore, A. Davidson and A.J. Baer, Geological Association of Canada Special Paper 31, pages 127-173

Emslie, R.F., 1983
The Coronitic Michael Gabbros, Labrador. Assessment of Grenvillian Metamorphism in Northeastern Grenville Province; in Current Research, Part A, Geological Survey of Canada, Paper 83-1A, pages 139-145.

Eugster, H.P. and Wones, D.R., 1962.
Stability Relations of the Ferruginuous Biotite, Annite, Journal of Petrology 3, pages 82-125.

Evans, B.W., 1977.
Metamorphism of Alpine Peridotite and Serpentinite. Annual Review of Earth and Planetary Science, 5, pages 397-447.

Ferry, J.M. and Spear, F.S., 1978.
Experimental Calibration of the Partitioning of Fe and Mg Between Biotite and Garnet, Contributions to Mineralogy and Petrology, 66, pages 113-117.

Frodesen, S., 1968.
Coronas Around Olivine in a Small Gabbro Intrusion, Bambles Area, South Norway, Oslo. Norsk Geologisk Tidsskrift, Volume 48, pages 201-206.

Goldsmith, J.R. and Newton, R.C., 1977.
Scapolite-Plagioclase Stability Relations at High Pressures and Temperatures in the System $NaAlSi_3O_80CaAl_2Si_2O_8$-$CaCO_3$-$CaSO_4$, American Mineralogist,Volume 62, pages 1063-1081.

Green, D.H. and Hibberson, W., 1970.
The Instability of Plagioclase in Peridotite at High Pressures, Lithos, 3, pages 209-221.

Griffin, W.L. and Heier, K.S., 1973.
Petrological Implications of Some Corona Structures, Lithos, 6, pages 315-35.

Haggerty, S.E., 1976.
Opaque Mineral oxides in Terrestrial Igneous Rocks. MSA. Review in Mineralogy, Oxide Minerals, Volume 3, pages Hg101-277.

Harry, Y.M., Jr. and Paul, G.N., Jr., 1979.
Mineralogy and Petrology of the Dutchman's Creek Gabbroic Intrusion, South Carolina. American Mineralogist, Volume 64, pages 531-545.

Helz, R.T., 1973.
Phase Relations of Basalts in Their Melting Range at $P(H_2O) = 5$ kb as a Function of Oxygen Fugacity; I. Mafic Phases, Journal of Petrology, 14, pages 249-302.

Hodges, K.V. and Spear, F.S., 1982.
Geothermometry, Geobarometry and the Al_2SiO_5 Triple Point at Mt. Moosilauke, New Hampshire, American Mineralogist, Volume 67, pages 1118-1134.

Irvine, T.N. and Baragar, W.R.A., 1971.
A Guide to the Chemical Classification of the Common Volcanic Rocks. Canadian Journal of Earth Sciences, Vol. 8, Number 5, pages 523-548.

Jamieson, R.A., 1981.
Metamorphism During Ophiolite Emplacement - The Petrology of the St. Anthony Complex, Journal of Petrology, 22, pages 397-449.

Katz, M., 1969.
Geology of Saint-Patrice Lake and Protage-du-Fort Areas, Quebec Department of Natural Resources, Quebec, P.Q., Preliminary Report 578.

Kerr, P.F., 1977.
Optical Mineralogy, Fouth Edition, McGraw Hill Inc.

Kerrick, D.M., 1972.
Experimental Determination of Muscovite + Quartz Stability with $P(H_2O) < P_{total}$, American Journal of Science, Volume 272, pages 946-958.

Kretz, R., 1982.
Transfer and Exchange Equilibria in a Portion of the Pyroxene Quadrilateral as Deduced from Natural and Experimental Data. Geochimica et Cosmochimica Acta, 46, pages 411-421.

Kretz, R., Hartree, R., Garrett, D. and Cermignani, C., 1985.
Petrology of the Grenville Swarm of Gabbro Dikes, Canadian Precambrian Shield. Canadian Journal of Earth Sciences, 22, pages 53-71.

Kretz, R., Jones, P., and Hartree, R., 1989.
Grenville Metagabbro Complexes of the Otter Lake Area, Quebec, Canadian Journal of Earth Sciences, 26, pages 215-230.

Lindsley, D.H., 1963.
Fe-Ti Oxides in Rocks as Thermometers and Oxygen Barometers. Carnegie Institute of Washington, Year Book 62, pages 60-66.

Loney, R.A. and Himmelberg, G.R., 1983.
Structure and Petrology of the La Perouse Gabbro Intrusion, Fairweather Range, Southeastern Alaska. Journal of Petrology, Volume 24, Part 4, pages 377-423.

Lumbers, S.B., 1982.
Renfrew County Area. Ontario Geological Survey, Report 212.

Mason, R., 1969.
Electron-Probe Microanalysis of Coronas in a Tractolite from Sulitjelma, Norway. Mineralogical Magazine 36, pages 504-514.

McLelland, J.M. and Whitney, P.R., 1980.
A generalized Garnet-Forming Reaction for Metaigneous Rocks in the Adirondacks. Contributions to Mineralogy and Petrology, 72, pages 111-122.

Medaris, L.G., 1969.
Partitioning of Fe^{++} and Mg^{++} between Coexisting Synthetic Olivine and Orthopyroxene. American Journal of Science, 267, pages 945-968.

Metz, P., 1976.
Experimental Investigation of the Metamorphism of Siliceous Dolomites, III. Equilibrium Data for the Reaction: 1 Tremolite + 11 Dolomite = 8 Forsterite + 13 Calcite + 9 CO_2 + 1 H_2O for the Total Pressure of 3,000 and 5,000 Bars. Contribution to Mineralogy and Petrology, 58, pages 137-148.

Moore, J.M., Jr. and Thompson, P.H., 1980.
The Flinton Group, A Late Precambrian Metasedimentary Succession in the Grenville Province of Eastern Ontario, Canadian Journal of Earth Sciences, Volume 17, pages 1685-1707.

Morse, S.A., Lindsley, D.H. and Williams, R.J., 1980.
Concerning Intensive Parameters in the Skaergaard Intrusion. American Journal of Science, 280-A, pages 159-170.

Mullen, E., 1983.
$MnO/TiO_2/P_2O_5$: A Major Element Discriminant of Basaltic Rocks of Ocean Environment and its Implications for Petrognesis. Earth and Planetary Science Letters, 65, pages 41-58.

Neuman, E.R., 1974.
The Distribution of Mn^{2+} and Fe^{2+} Between Ilmenites and Magnetites in Igneous Rocks. American Journal of Science, 274, pages 1074-1088.

Pearce, T.H., 1968.
A Contribution to the Theory of Variation Diagrams. Contribution to Mineralogy and Petrology, 19, pages 142-157.

Pearce, T.H., Gorman, B.E. and Birkett, T.C., 1977.
The Relationship Between Major Element Chemistry and Tectonic Environment of Basic and Intermediate Volcanic Rocks. Earth and Planetary Science Letters, 36, pages 121-132.

Potts, P.J., Tindle, G., and Isaacs, M.C., 1983.
On the Precision of Electron Microprobe Data: A new Test of Homogeneity of Mineral Standards. The American Mineralogist, volume 68, pages 1237-1242.

Quinn, H.A., 1951.
Renfrew Map-Area, Renfrew and Lanark Counties, Ontario, Geological Survey of Canada, paper 51-27, 79p.

Reynolds, R.C. and Fredrickson, A.F., 1962.
Corona Development Concept. Geological Society of America, Bulletin 73, pages 59-71.

Silver, L.T. and Lumbers, S.B., 1966.
Geochronoligic Studies in the Bancroft-Madoc Area of the Grenville Province, Ontario, Canada; Abstract, p.15;6 in Geological Society of America, Special Publication No. 87.

Speer, J.A., 1984.
Micas in Igneous Rocks. MSA, Review in Mineralogy, Micas, Ed. Bailey, S.W., Volume 13, pages 299-356.

Stormer, I.C., 1969.
Basic Plutonic Intrusions of the Risor-Sondeled Area, South Norway. The Original Lithologies and Their Metamorphism, Norsk Geologisk Tidsskrift, Volume 49, pages 403-431.

Turner, F.J., 1981.
Metamorphic Petrology. Mineralogical, Field, and Tectonic Aspects, Second Edition; McGraw-Hill, pages 416-470.

Whitney, P.R. and McLelland, J.M., 1973.
Origin of Coronas in Metagabbros of the Adirondack Mts. New York. Contributions to Mineralogy and Petrology, 39, pages 81-98.

Williams, R.J., 1971.
Reaction Constants in the System Fe-Mg-SiO_2-O at 1 ATM Between 900° and 1300°C: Experimental Results. American Journal of Science, Volume 270, pages 334-360.

Wood, B.J., 1974.
The Solubility of Alumina in Orthopyroxene Coexisting with Garnet. Contributions to Mineralogy and Petrology, 46, pages 1-15.

Wynne-Edwards, H.R., 1972.
The Grenville Province; in Variation in Tectonic Styles in Canada, ed R.A. Price and R.J.W. Douglas, Geological Association of Canada, Special Paper 11, pages 263-334.

Yoder, H.S., Jr., 1976.
Generation of Basaltic Magma. National Academy of Sciences, Washington, D.C.

APPENDIX A

WHOLE ROCK ANALYSES

Rock analyses were carried out on a Philips PW 1410/20 AHP automated X-ray fluorescence unit at the Geochemistry Laboratory, University of Ottawa. The determinations were made on fused disc using Cr radiation and the technique of alpha coefficients described by DeJongh (1975).

Analytical precision is expressed in terms of a coefficient of variation (c) defined as c = (S/W)100, where w is weight percent (wt %) of element oxide or parts per million (ppm) of element and s is standard deviation in the same units. Estimated values of c, based on replicate determinations, are as follows: 0.8 (SiO_2, TiO_2, Al_2O_3, FeO, CaO) 1.2 (K_2O), 2.0 (MgO), 2.5 (Na_2O), 4.0 (MnO), 10 (trace elements).

Table 6 Chemical Analyses of Chenaux Gabbros

	1 (171)	2 (46)	3 (157)	4 (49)	5 (196)	6 (170)
SiO_2	46.1	46.3	47.0	47.1	48.1	49.1
TiO_2	0.28	0.32	0.20	0.13	0.20	0.37
Al_2O_3	17.0	17.2	21.0	19.3	19.5	18.4
Fe_2O_3	0.10	2.7	0.90	0.10	1.50	1.70
FeO	10.0	6.2	5.9	6.2	5.6	5.8
MnO	0.16	0.15	0.11	0.11	0.12	0.13
MgO	13.3	9.4	10.9	9.7	9.2	8.2
CaO	9.7	11.6	11.5	11.3	11.8	12.6
Na_2O	2.61	2.65	2.06	2.83	2.93	2.55
K_2O	0.21	0.24	0.12	0.20	0.16	0.14
P_2O_5						
SUM	99.46	96.76	99.69	96.97	99.11	98.99
Ba	105	65	80	75	85	95
Cr	130	400	230	275	250	420
Zr	15	15	10	10	10	15
Sr	205	235	250	285	275	215
Y	10	10	10	10	10	10
$X=Mg/(Mg+Fe^{2+})$	0.70	0.72	0.77	0.73	0.74	0.71

	7	8	9	10	11	12	13	14	15
	(228)	(4.6)	(47)	(35)	(195)	(192)	(168)	(176)	(43)
SiO_2	45.1	47.3	48.5	48.8	49.3	49.6	49.8	47.9	48.7
TiO_2	0.39	0.86	0.98	0.43	0.35	0.58	0.48	2.57	0.50
Al_2O_3	14.6	17.4	14.9	15.6	18.3	20.5	23.3	13.4	14.6
Fe_2O_3	3.4	3.9	3.6	1.9	0.90	1.9	1.8	2.1	2.9
FeO	8.4	8.7	6.7	4.4	3.8	3.9	2.5	10.5	4.5
MnO	0.20	0.19	0.17	0.12	0.10	0.11	0.08	0.20	0.14
MgO	12.7	7.7	7.7	7.8	7.0	5.1	3.9	6.1	8.1
CaO	10.6	9.9	12.9	15.0	15.1	13.9	12.7	13.2	13.6
Na_2O	2.13	2.73	3.23	2.52	2.54	2.99	3.38	2.95	2.69
K_2O	0.20	0.40	0.28	0.21	0.29	0.22	0.39	0.17	0.64
P_2O_5		0.11	0.02			0.02		0.24	
SUM	97.72	99.19	98.98	96.78	97.68	98.82	98.33	98.33	96.37
Ba	170	170	75	105	140	210	110	10	210
Cr	180	30	60	170	250	220	320	40	180
Zr	10	55	35	20	20	25	40	125	40
Sr	95	270	230	280	260	400	330	220	280
Y	15	20	20	15	15	20	15	50	15
X	0.72	0.61	0.68	0.79	0.77	0.72	0.75	0.50	0.77

	16	17	18	19	20	21	22	23	24	25
	(21)	(57)	(144)	(24)	(184)	(61)	(242)	(223)	(103)	(225)
SiO_2	50.5	50.5	50.8	46.7	47.3	47.5	47.8	48.4	49.0	49.2
TiO_2	0.61	0.35	0.42	1.54	1.09	0.47	0.39	0.80	0.47	0.31
Al_2O_3	18.3	17.7	16.5	14.7	7.4	14.4	15.4	16.9	16.7	18.4
Fe_2O_3	2.2	1.8	1.4	5.2	1.7	2.1	1.6	1.7	1.6	1.4
FeO	5.2	3.4	4.9	8.5	7.2	5.4	5.1	5.0	4.8	4.3
MnO	0.13	0.11	0.11	0.21	0.13	0.14	0.14	0.12	0.11	0.11
MgO	6.1	6.0	7.3	5.5	9.0	8.8	8.8	6.6	8.1	6.8
CaO	13.9	13.2	13.4	9.4	22.1	14.7	13.3	15.1	13.5	13.0
Na_2O	2.9	3.36	2.83	3.56	1.26	3.45	3.33	2.72	2.14	3.39
K_2O	0.17	0.27	0.54	0.46	0.22	0.42	0.40	0.38	0.49	0.42
P_2O_5	nd	nd	nd	0.20	nd	0.03	0.02	nd	nd	nd
SUM	100.01	96.69	98.20	96.07	97.4	97.41	96.28	97.72	96.91	97.28
Ba	100	145	320	465	35	610	410	150	125	150
Cr	215	150	250	25	30	150	280	160	545	145
Zr	20	15	45	80	130	20	30	25	30	10
Sr	320	250	305	245	100	290	330	320	315	305
Y	20	15	25	40	20	20	10	15	20	10
X	0.75	0.75	0.72	0.42	0.69	0.76	0.76	0.69	0.74	0.74

Table 7 Chemical Analyses of Amphibolites

	1	2	3	4	5	6	7	8
	(238)	(185)	(258)	(249)	(236)	(244)	(257)	(233)
SiO_2	44.2	44.5	45.1	49.4	43.7	45.0	45.5	47.6
TiO_2	3.0	2.3	2.3	1.2	2.5	2.41	2.2	1.2
Al_2O_3	12.4	12.8	13.0	15.7	12.8	12.7	13.4	14.4
Fe_2O_3	4.2	2.2	1.8	3.2	9.1	1.9	2.9	2.7
FeO	13.5	13.5	13.7	8.4	9.3	13.9	11.2	9.6
MnO	0.24	0.20	0.26	0.19	0.29	0.25	0.21	.19
MgO	7.4	7.2	6.8	6.8	5.8	7.4	6.8	6.7
CaO	10.7	10.2	11.5	9.7	9.1	12.0	12.2	10.4
Na_2O	2.20	2.28	2.07	3.26	3.12	2.58	3.99	3.13
K_2O	0.26	0.26	0.30	0.97	0.72	0.52	.19	.44
P_2O_5	0.45	0.18	0.15	0.08	0.23	0.12	.25	.18
SUM	98.55	95.62	96.98	98.90	96.66	98.18	98.34	96.54
Ba	110	nd	nd	200	530	nd	15	125
Cr	180	75	225	110	nd	220	200	35
Zr	110	45	70	130	130	50	55	90
Sr	160	220	160	230	250	185	165	230
Y	60	40	45	40	50	60	30	30
$X=Mg/(Mg+Fe^{2+})$	0.49	0.49	0.47	0.59	0.52	0.49	0.53	0.56

APPENDIX B

MINERAL ANALYSES

Analytical Methods and Precision

Mineral analysis was obtained by use of a CAMECA CAMEBAX Micro system at McGill University, and their MBXCOR Micro software package.

Operating conditions were as follows: accelerating voltage 15.0 kV, current 10nA, beam width 5 μm, counting time 25 s. Natural and synthetic minerals were used as standards.

Regarding microprobe mineral analyses, Potts et al. (1983) expressed precision in terms of K, defined as: $K = S/W^{1/2}$ and they found K fell in the range of 0.03-0.04. With the later value, $c = 4/W^{1/2}$, and for different values of w, the corresponding values of c (in parentheses) are as follows: 50(1/2), 10 (1), 4 (2), 1 (4), and 0.16 (10). Mineral analyses are listed in Table 8.

TABLE 8A. MICROPROBE ANALYSES OF OLIVINE

	1 (157)	2 (157)	3 (49)	4 (49)
SiO_2	38.3	39.46	39.67	38.72
TiO_2	---	0.02	---	0.01
Al_2O_3	0.02	---	---	---
FeO	21.74	20.35	22.75	23.37
MnO	0.27	0.33	0.29	0.27
MgO	39.88	39.25	38.2	38.15
CaO	0.02	0.02	0.01	---
K_2O	0.01	0.02	---	---
Na_2O	0.02	0.01	---	0.02
TOTAL	100.28	99.48	100.92	100.57
$X=Mg/(Mg+Fe^{2+})$	0.77	0.78	0.75	0.75
Nº of Analyses	3	3	1	1

TABLE 8B. MICROPROBE ANALYSES OF PLAGIOCLASE

	1 (21)	2 (170)	3 (196)	4 (4-b)	5 (157)
SiO_2	53.2	50.72	50.78	51.62	49.88
TiO_2	0.02	0.06	0.04	0.06	0.01
Al_2O_3	29.41	29.8	31.02	30.98	31.36
FeO	0.15	0.15	0.02	0.05	0.26
MnO	0.01	---	---	0.03	0.02
MgO	0.02	0.04	---	---	0.41
CaO	12.48	12.73	14.38	13.61	14.80
Na_2O	4.31	4.85	3.43	3.73	2.88
K_2O	0.09	0.65	0.06	0.01	0.05
TOTAL	99.75	99.02	99.74	100.10	99.69
an/an+ab	0.62	0.60	0.70	0.67	0.74
Nº of Analyses	3	1	1	1	3

	6 (49)	7 (4-b)	8 (103)	9 (103)	10 (196)	11 (4-b)
SiO_2	50.6	51.5	52.26	53.32	50.88	54.50
TiO_2	0.04	0.04	---	0.01	0.04	0.03
Al_2O_3	30.85	30.8	30.10	29.09	30.07	28.79
FeO	0.08	0.19	0.07	0.06	0.10	0.11
MnO	0.05	0.01	0.03	0.02	---	0.01
MgO	---	0.01	0.01	---	---	0.01
CaO	13.81	14.40	12.96	12.21	13.51	11.91
Na_2O	3.86	3.44	3.85	4.45	3.97	4.67
K_2O	0.04	0.02	0.06	0.05	0.05	0.08
TOTAL	99.45	100.15	99.35	99.34	98.62	100.14
an/an+ab	0.67	0.70	0.65	0.60	0.65	0.59
N° of Analyses	1	3	1	5	1	4

TABLE 8C. MICROPROBE ANALYSES OF AUGITE

	1 (21)	2 (21)	3 (170)	4 (196)
SiO_2	51.1	51.59	51.96	51.05
TiO_2	0.60	0.65	0.48	0.68
Al_2O_3	3.45	3.53	2.96	3.50
Fe_2O_3	1.18	1.31	1.01	1.14
FeO	7.66	8.62	6.63	7.46
MnO	0.20	0.26	0.22	0.19
MgO	13.94	14.93	14.35	14.77
CaO	21.42	19.79	21.45	20.96
Na_2O	0.46	0.38	0.46	0.56
K_2O	---	0.01	0.02	0.02
TOTAL	100.01	101.07	99.54	100.33
$X=Mg/(Mg+Fe_{2+})$	0.76	0.75	0.79	0.79
Nº of Analyses	3	3	4	3

	5 (49)	6 (49)	7 (21)	8 (196)
SiO_2	53.25	52.87	52.48	51.08
TiO_2	0.48	0.35	0.4	0.69
Al_2O_3	3.05	3.21	2.25	3.55
Fe_2O_3	0.78	0.93	1.19	0.98
FeO	5.12	6.13	6.09	6.45
MnO	0.17	0.15	0.25	0.21
MgO	15.6	15.9	13.67	14.79
CaO	21.82	19.65	21.75	21.15
Na_2O	0.38	0.51	0.41	0.49
K_2O	0.01	0.04	0.02	0.01
TOTAL	100.66	99.74	98.51	99.40
X	0.85	0.85	0.81	0.80
N° of Analyses	3	3	3	3

	9 (21)	10 (21)	11 (4-b)
SiO_2	51.46	51.57	46.1
TiO_2	0.46	1.74	0.46
Al_2O_3	2.6	3.25	11.28
Fe_2O_3	1.31	1.2	1.85
FeO	8.59	7.89	12.12
MnO	0.24	0.21	0.60
MgO	14.09	14.66	12.61
CaO	20.81	20.47	11.92
Na_2O	0.40	0.37	1.3
K_2O	0.02	---	0.65
TOTAL	99.98	101.36	98.89
X	0.74	0.75	0.65
Nº of Analyses	1	3	2

TABLE 8D. MICROPROBE ANALYSES OF HYPERSTHENE

	1 (21)	2 (4-b)	3 (157)	4 (157)	5 (157)
SiO_2	54.08	58.44	53.35	54.66	53.37
TiO_2	0.16	---	0.02	0.15	0.19
Al_2O_3	1.49	1.25	0.81	2.1	2.1
Fe_2O_3	2.67	3.03	1.93	1.88	1.95
FeO	17.52	19.91	12.65	12.35	12.8
MnO	0.52	0.51	0.32	0.38	0.29
MgO	24.14	22.03	29.47	28.19	28.11
CaO	0.68	0.17	0.08	0.68	0.41
Na_2O	0.06	0.03	0.01	0.02	0.01
K_2O	---	---	0.01	0.01	0.01
TOTAL	101.32	100.37	98.63	100.42	99.24
X	0.71	0.66	0.80	0.80	0.79
Nº of Analyses	1	1	3	1	6

	6 (157)	7 (49)	8 (49)	9 (21)	10 (21)	11 (21)
SiO_2	55.33	56.31	55.36	53.44	53.03	53.24
TiO_2	0.06	0.03	0.01	0.31	0.31	0.28
Al_2O_3	0.99	1.07	0.91	1.28	1.32	1.31
Fe_2O_3	1.85	1.99	2.07	3.23	3.20	3.1
FeO	12.25	13.11	13.61	21.21	21.05	20.39
MnO	0.28	0.36	0.27	0.60	0.53	0.52
MgO	28.83	27.74	28.36	20.94	21.64	21.49
CaO	0.21	0.08	0.09	1.49	1.35	1.37
Na_2O	0.01	0.01	0.01	0.02	0.02	0.03
K_2O	0.02	0.01	0.01	0.01	---	---
TOTAL	99.83	100.71	100.70	102.53	102.45	101.73
X	0.80	0.79	0.79	0.64	0.65	0.65
Nº of Analyses	5	5	2	2	3	5

TABLE 8E. MICROPROBE ANALYSES OF AMPHIBOLE

	1 (21)	2 (170)	3 (4-b)	4 (157)	5 (157)
SiO_2	43.12	39.04	40.59	40.13	40.91
TiO_2	0.90	0.45	0.05	0.94	0.90
Al_2O_3	15.08	19.11	17.53	19.05	15.75
Fe_2O_3	3.0	3.5	4.5	2.60	2.60
FeO	7.7	8.0	10.6	6.10	5.90
MnO	0.17	0.12	0.18	0.11	0.08
MgO	13.22	13.44	10.85	15.68	15.46
CaO	11.70	11.18	10.20	10.95	11.69
Na_2O	1.82	2.38	2.31	2.18	0.26
K_2O	0.74	0.59	0.43	0.32	0.58
TOTAL	97.64	97.96	97.32	98.11	94.15
$X=Mg/Mg+Fe^{2+}$	0.75	0.75	0.64	0.83	0.83
N° of Analyses	4	4	5	5	3

	6 (157)	7 (49)	8 (4-b)	9 (103)	10 (103)
SiO_2	36.07	42.24	47.36	50.92	52.51
TiO_2	0.08	0.06	0.06	0.26	0.27
Al_2O_3	29.38	21.94	10.49	5.29	4.69
Fe_2O_3	2.40	2.3	4.7	3.5	3.4
FeO	5.80	5.1	11.1	7.9	7.6
MnO	0.11	0.10	0.19	0.17	0.18
MgO	11.85	10.84	14.15	16.27	16.5
CaO	10.91	13.08	8.89	12.34	12.2
Na_2O	1.59	1.76	1.35	0.51	0.39
K_2O	0.22	0.26	0.30	0.09	0.08
TOTAL	98.56	97.71	98.63	97.26	97.83
X	0.78	0.79	0.70	0.78	0.80
Nº of Analyses	5	4	5	2	3

	11 (103)	12 (103)	13 (4-b)
SiO_2	53.02	52.1	41.97
TiO_2	0.19	0.23	0.31
Al_2O_3	4.45	5.01	15.05
Fe_2O_3	3.2	3.4	6.0
FeO	7.5	7.8	13.8
MnO	0.17	0.17	0.20
MgO	16.54	16.26	8.11
CaO	12.06	12.27	11.09
Na_2O	0.40	0.45	1.75
K_2O	0.08	0.09	0.98
TOTAL	97.65	97.81	99.35
X	0.80	0.78	0.51
Nº of Analyses	5	4	1

TABLE 8F. MICROPROBE ANALYSES OF BIOTITE

	1 (21)	2 (4-b)	3 (4-b)
SiO_2	36.69	37.62	36.97
TiO_2	2.15	1.28	2.44
Al_2O_3	17.02	17.68	17.73
FeO	10.0	14.74	14.44
MnO	0.03	0.02	0.02
MgO	17.87	16.01	14.96
CaO	1.18	0.01	0.007
Na_2O	0.31	0.30	0.32
K_2O	8.49	8.92	9.26
TOTAL	95.89	96.7	96.24
X=Mg/(Mg+Fe)	0.76	0.67	0.65
Nº of Analyses	2	5	7

Total iron expressed as FeO.

TABLE 8G. MICROPROBE ANALYSES OF MAGNETITE AND ILMENITE

	1 (21)	2 (170)	3 (196)	4 (21)
SiO_2	0.07	0.34	0.18	0.02
TiO_2	0.06	0.31	0.16	51.59
Al_2O_3	0.26	0.29	0.35	0.03
Fe_2O_3	68.12	66.90	67.29	3.47
FeO	30.87	30.71	30.63	42.86
MnO	0.03	---	---	0.86
MgO	0.02	0.08	0.10	1.50
CaO	0.04	0.03	0.31	---
Na_2O	0.01	0.11	0.07	---
K_2O	0.01	0.03	0.02	---
TOTAL	99.59	98.81	99.10	100.39

TABLE 8H. MICROPROBE ANALYSES OF SCAPOLITE

	1 (103)	2 (103)	3 (103)
SiO_2	49.08	49.24	48.56
TiO_2	---	---	---
Al_2O_3	25.36	25.48	25.37
FeO	0.02	0.08	0.04
MnO	0.09	0.04	---
MgO	---	---	---
CaO	15.01	15.48	15.12
Na_2O	4.64	4.42	4.64
K_2O	0.24	0.27	0.25
OH	2.04	2.06	2.03
TOTAL	96.57	97.17	96.10

TABLE 8L MICRORROBE ANALYSES OF GARNET

	1 (4-6)	2 (4-b)	3 (4-b)
SiO_2	38.37	38.53	38.02
FeO	27.22	27.59	27.46
Fe_2O_3	1.50	2.10	1.68
Al_2O_3	20.44	20.17	20.48
CaO	5.06	4.98	5.14
MgO	5.10	5.02	5.61
MnO	1.79	1.92	1.60
TOTAL	99.48	100.32	99.98

According to Figure 26a, the main body is plug-like and inclined steeply toward the northwest. Moreover, the body shows an asymmetrical mushroom-like cross section, in which the western part spreads laterally about 3 km beneath the marble. The maximum depth in this model is 2.7 km. The NE - SW profile, shown in Fig. 26b, further attests to the mushrooming pattern of the body spreading laterally on both sides of the central mass. Here also the maximum depth is the same with that observed along the A-A' profile. The strong positive gravity anomaly at the centre of the body could be explained by a high density core of ultramafic rocks at depth in the Chenaux gabbro. Surface geology, however, offers no evidence to support the existence of such an ultramafic body.

The highest gravity anomaly was measured on the east central part of the body that coincides with the abundance of olivine gabbros. The anomally declines from -8 mgal on the center to -26 mgal toward the western portion of the pluton. Based on these facts, it is porposed that the gabbroic melt, when it arrived at the present level of exposure, through its vertical feeder, precipitated olivine, which was partially removed by gravity settling. Later, the residual melt enriched in Ca, Al and total alkalies migrated westward and continued to differentiate during lateral flow.

In summary, gravity data across the Chenaux gabbro yield a distinct positive anomaly. The gabbro is mushroom-like and is inclined steeply toward the